INTERACTIONS OF B16F1 MURINE MELANOMA CELLS WITH THE HEPATIC MICROVASCULATURE OF C56BL/6 MICE IN LIVER METASTASIS

by

SANDRA E. SCHERBARTH

A Thesis

Submitted to the School of Graduate Studies

in Partial Fulfilment of the Requirements

for the Degree

Masters of Science

University of Manitoba

ISBN 0-612-16267-2

Canada

Name

Dissertation Abstracts International and *Masters Abstracts International* are arranged by broad, general subject categories. Please select the one subject which most nearly describes the content of your dissertation or thesis. Enter the corresponding four-digit code in the spaces provided.

PATHOLOGY

SUBJECT TERM

0571

SUBJECT CODE

UMI

Subject Categories

THE HUMANITIES AND SOCIAL SCIENCES

COMMUNICATIONS AND THE ARTS

Architecture 0729
Art History 0377
Cinema 0900
Dance 0378
Fine Arts 0357
Information Science 0723
Journalism 0391
Library Science 0399
Mass Communications 0708
Music 0413
Speech Communication 0459
Theater 0465

EDUCATION

General 0515
Administration 0514
Adult and Continuing 0516
Agricultural 0517
Art 0273
Bilingual and Multicultural 0282
Business 0688
Community College 0275
Curriculum and Instruction 0727
Early Childhood 0518
Elementary 0524
Finance 0277
Guidance and Counseling 0519
Health 0680
Higher 0745
History of 0520
Home Economics 0278
Industrial 0521
Language and Literature 0279
Mathematics 0280
Music 0522
Philosophy of 0998
Physical 0523
Psychology 0525
Reading 0535
Religious 0527
Sciences 0714
Secondary 0533
Social Sciences 0534
Sociology of 0340
Special 0529
Teacher Training 0530
Technology 0710
Tests and Measurements 0288
Vocational 0747

LANGUAGE, LITERATURE AND LINGUISTICS

Language
- General 0679
- Ancient 0289
- Linguistics 0290
- Modern 0291

Literature
- General 0401
- Classical 0294
- Comparative 0295
- Medieval 0297
- Modern 0298
- African 0316
- American 0591
- Asian 0305
- Canadian (English) 0352
- Canadian (French) 0355
- English 0593
- Germanic 0311
- Latin American 0312
- Middle Eastern 0315
- Romance 0313
- Slavic and East European 0314

PHILOSOPHY, RELIGION AND THEOLOGY

Philosophy 0422
Religion
- General 0318
- Biblical Studies 0321
- Clergy 0319
- History of 0320
- Philosophy of 0322

Theology 0469

SOCIAL SCIENCES

American Studies 0323
Anthropology
- Archaeology 0324
- Cultural 0326
- Physical 0327

Business Administration
- General 0310
- Accounting 0272
- Banking 0770
- Management 0454
- Marketing 0338

Canadian Studies 0385
Economics
- General 0501
- Agricultural 0503
- Commerce-Business 0505
- Finance 0508
- History 0509
- Labor 0510
- Theory 0511

Folklore 0358
Geography 0366
Gerontology 0351
History
- General 0578
- Ancient 0579
- Medieval 0581
- Modern 0582
- Black 0328
- African 0331
- Asia, Australia and Oceania 0332
- Canadian 0334
- European 0335
- Latin American 0336
- Middle Eastern 0333
- United States 0337

History of Science 0585
Law 0398
Political Science
- General 0615
- International Law and Relations 0616
- Public Administration 0617

Recreation 0814
Social Work 0452
Sociology
- General 0626
- Criminology and Penology 0627
- Demography 0938
- Ethnic and Racial Studies 0631
- Individual and Family Studies 0628
- Industrial and Labor Relations 0629
- Public and Social Welfare 0630
- Social Structure and Development 0700
- Theory and Methods 0344

Transportation 0709
Urban and Regional Planning 0999
Women's Studies 0453

THE SCIENCES AND ENGINEERING

BIOLOGICAL SCIENCES

Agriculture
- General 0473
- Agronomy 0285
- Animal Culture and Nutrition 0475
- Animal Pathology 0476
- Food Science and Technology 0359
- Forestry and Wildlife 0478
- Plant Culture 0479
- Plant Pathology 0480
- Plant Physiology 0817
- Range Management 0777
- Wood Technology 0746

Biology
- General 0306
- Anatomy 0287
- Biostatistics 0308
- Botany 0309
- Cell 0379
- Ecology 0329
- Entomology 0353
- Genetics 0369
- Limnology 0793
- Microbiology 0410
- Molecular 0307
- Neuroscience 0317
- Oceanography 0416
- Physiology 0433
- Radiation 0821
- Veterinary Science 0778
- Zoology 0472

Biophysics
- General 0786
- Medical 0760

EARTH SCIENCES

Biogeochemistry 0425
Geochemistry 0996
Geodesy 0370
Geology 0372
Geophysics 0373
Hydrology 0388
Mineralogy 0411
Paleobotany 0345
Paleoecology 0426
Paleontology 0418
Paleozoology 0985
Palynology 0427
Physical Geography 0368
Physical Oceanography 0415

HEALTH AND ENVIRONMENTAL SCIENCES

Environmental Sciences 0768
Health Sciences
- General 0566
- Audiology 0300
- Chemotherapy 0992
- Dentistry 0567
- Education 0350
- Hospital Management 0769
- Human Development 0758
- Immunology 0982
- Medicine and Surgery 0564
- Mental Health 0347
- Nursing 0569
- Nutrition 0570
- Obstetrics and Gynecology 0380
- Occupational Health and Therapy 0354
- Ophthalmology 0381
- Pathology 0571
- Pharmacology 0419
- Pharmacy 0572
- Physical Therapy 0382
- Public Health 0573
- Radiology 0574
- Recreation 0575
- Speech Pathology 0460
- Toxicology 0383

Home Economics 0386

PHYSICAL SCIENCES

Pure Sciences
Chemistry
- General 0485
- Agricultural 0749
- Analytical 0486
- Biochemistry 0487
- Inorganic 0488
- Nuclear 0738
- Organic 0490
- Pharmaceutical 0491
- Physical 0494
- Polymer 0495
- Radiation 0754

Mathematics 0405
Physics
- General 0605
- Acoustics 0986
- Astronomy and Astrophysics 0606
- Atmospheric Science 0608
- Atomic 0748
- Electronics and Electricity 0607
- Elementary Particles and High Energy 0798
- Fluid and Plasma 0759
- Molecular 0609
- Nuclear 0610
- Optics 0752
- Radiation 0756
- Solid State 0611

Statistics 0463

Applied Sciences
Applied Mechanics 0346
Computer Science 0984
Engineering
- General 0537
- Aerospace 0538
- Agricultural 0539
- Automotive 0540
- Biomedical 0541
- Chemical 0542
- Civil 0543
- Electronics and Electrical 0544
- Heat and Thermodynamics 0348
- Hydraulic 0545
- Industrial 0546
- Marine 0547
- Materials Science 0794
- Mechanical 0548
- Metallurgy 0743
- Mining 0551
- Nuclear 0552
- Packaging 0549
- Petroleum 0765
- Sanitary and Municipal 0554
- System Science 0790

Geotechnology 0428
Operations Research 0796
Plastics Technology 0795
Textile Technology 0994

PSYCHOLOGY

General 0621
Behavioral 0384
Clinical 0622
Developmental 0620
Experimental 0623
Industrial 0624
Personality 0625
Physiological 0989
Psychobiology 0349
Psychometrics 0632
Social 0451

THE UNIVERSITY OF MANITOBA

FACULTY OF GRADUATE STUDIES

COPYRIGHT PERMISSION

INTERACTIONS OF B16F1 MURINE MELANOMA CELLS WITH THE HEPATIC MICROVASCULATURE OF C56BL/6 MICE IN LIVER METASTASIS

BY

SANDRA E. SCHERBARTH

A Thesis/Practicum submitted to the Faculty of Graduate Studies of the University of Manitoba in partial fulfillment of the requirements for the degree of

MASTER OF SCIENCE

MASTER OF SCIENCE (1996) University of Manitoba

Winnipeg Manitoba

TITLE: Interactions of B16F1 murine melanoma cells with the hepatic microvasculature of C57bl/6 mice in liver metastasis

AUTHOR: Sandra Scherbarth B.Sc. (University of Western Ontario)

SUPERVISOR: F.W. Orr M.D.

NUMBER OF PAGES: x, 126

Softly, slowly, moving as if in a dream state
He pulsed quietly along the winding trail,
Slipping randomly from the large highways, through a tiny gate
To the journey's end - over and over without fail.

Suddenly, the pace quickens and he is forced to flee.
Large orbs of light invade, buffeting the protective wall.
Some stopping, standing, basking in their own glow for all to see.
Others slinking away, ashamed to watch the temple fall.

The seeds of light fade, but in the darkness, the orbs begin to grow,
Pushing their black fingers into the necks of their hosts
Who continue to struggle against strangulation, but know
That in the end all that will be left are ghosts.

Thus, blackness grows from the glorious shrine of old
And what was once peaceful and warm is now cold.

ABSTRACT

To seek a role for inducible vascular adhesion molecules in liver metastasis, $3x10^5$ B16F1 cells were injected into a mesenteric vein of C57bl/6 mice. Animals given 1.5 μg interleukin-1α intraperitoneally four hours before injections had an 11-22 fold increase in tumour burden after 7 days compared to control. Retention of [^{125}I]UdR-labelled B16F1 cells in livers of interleukin-1 treated animals was twice that of controls immediately after injection and seven fold that of controls after 24 hours. Intravital microscopy showed differences in the patterns and anatomical sites of arrest of calcein AM-labelled B16F1 cells. In interleukin-1 pre-treated mice, arrest occurred in larger vessels [median diameter 34 μm (27-31 μm) versus 16 μm (9-23 μm) in control animals] and cells travelled less far into sinusoids [0 μm (0-18 μm) versus 41 μm (0-74 μm)]. Entry velocities of cells in interleukin-1 pre-treated mice were slower [387 μm/s $\pm$ 27] versus 571 μm/s $\pm$ 69] and the maximum observed velocities were less [455 μm/s $\pm$ 27 versus 1470 μm/s $\pm$ 179]. Analysis of the flow of red blood cells in control and interleukin-1 pre-treated mice showed a non-significant decrease in hepatic venous flow rates of animals pre-treated with IL-1. Analysis of the velocities of 6 μm fluorescently labelled microspheres showed significantly slower velocities of the spheres in interleukin-1 treated animals. To look for effects of interleukin-1 on the adhesive properties of the liver microvasculature, $5x10^4$ B16F1 cells were incubated for 15 min on 5 μm frozen sections of liver. In livers from mice pre-treated with interleukin-1 there

was a significant increase in the total number of cancer cells adhered to the sections and an increase in the number of cancer cells adhered to sinusoids, hepatocytes and the wall of large vessels compared to control liver sections from mice pre-treated with saline. This interleukin-1 induced increase was completely blocked in the presence of 50 μM GRGDS peptide *in vitro*, but no inhibition of liver metastasis was observed *in vivo*. I postulate that pre-treatment of mice with interleukin-1α alters the interactions between cancer cells and the hepatic microvasculature resulting in an environment conducive to an increase in formation of tumour.

Acknowledgments

I would like to thank the many people who have supported and helped me during the course of this thesis. I would especially like to extend my appreciation to Rob Lafrenie for acting as a proof reader for this thesis but more importantly for his invaluable input on the contents of this document over the past three years. I would also like to thank Margaret McKay, Joanne Lee, Kate Hole and Tammy Hiller for their constant support and input. The support of my parents has also been a source of continued motivation and strength, even from a distance. I would like to thank them for demonstrating, on a daily basis, the value of conscience and a strong work ethic. I would also like to take this opportunity to thank the examination committee, Dr. M. Del Bigio and Dr. G. Minuk for taking the time to review this thesis and taking part in the examination. Lastly, I would like to thank my supervisor Dr. F.W. Orr who has taught me, by example, many things not only about science but about life.

TABLE OF CONTENTS

1.0 BACKGROUND

1.1 Clinical Aspects of Hepatic Metastasis

Liver metastases are more common than primary liver cancer and their incidence is exceeded only by lymph node metastases. Thirty to 50% of patients dying of malignancies present with liver metastases. This condition causes significant morbidity and results in a poor prognosis (Zavadsky and Lee, 1994). The primary tumour sites which most commonly result in liver metastases are the eye (McCartney, 1995), breast (Weiss, 1992), and gastrointestinal tract (gallbladder, extrahepatic bile ducts, colon, rectum, and stomach) (Meijer *et al.*, 1990). The mechanisms responsible for liver metastasis are poorly understood and despite advances in more non-invasive therapies, surgical resection remains the only treatment which gives a reasonable chance of long term survival (Zavadsky and Lee, 1994).

1.2 Tumour Cell/Endothelial Cell Interactions

1.2.1 Metastatic Cascade

The process of the spread of cancer from a primary tumour to a secondary site is a complex one, typically involving the growth and invasion of primary tumours into the lymphatics or blood vessels. It appears that the haematogenous spread of cancer is the more important route. Steps in the metastatic cascade include: 1) the release of cancer cells from the primary tumour, 2) the invasion of these cells through the vessels and into the circulation, 3) the spread of the cells through either the lymphatics or

circulatory system, 4) the arrest of cells at a secondary site and 5) the extravasation, growth and proliferation of the cells at the secondary site. (Fidler, 1991) Most of the cells that enter this process are killed and do not survive to form metastatic colonies.

1.2.2 Arrest of Tumour Cells in the Vasculature

1.2.2a Mechanical Arrest

The bloodstream is the most important anatomical pathway for the dissemination of cancer cells (Weiss, 1992). Interaction of intravascular tumour cells with the endothelium, or cancer cell arrest, appears to be a requisite for metastasis (Crissman *et al.*, 1985; Crissman *et al.*, 1988). Cancer cell arrest has been attributed to mechanical trapping of cells in the microvasculature. That is, cancer cells could be trapped by size restrictions in the first microvascular bed they encounter. Therefore, it has been postulated that blood flow to the specific organ is the major factor influencing the rate of metastasis in that organ. Recent evidence to support the theory of cancer cell arrest by mechanical trapping is provided using intravital microscopy of both murine liver and rat cremaster muscle (Morris *et al.*, 1993).

1.2.2b Adhesion Molecules in Arrest

Adhesive interactions between surface adhesion molecules on cancer cells and endothelial cells are also implicated in the arrest process. (Table 1) Constitutively expressed endothelial adhesion molecules may cause adhesion of cancer cells to the endothelium of specific organs to which these cells

preferentially metastasize *in vivo*. Auerbach *et al.* (1987) demonstrated that tumour cells will adhere preferentially to specific capillary endothelium derived from different organs *in vitro*. The novel adhesion molecule, Lu-ECAM-1, found exclusively on lung endothelium, was shown to mediate the adhesion of B16F10 murine melanoma cells *in vitro* and *in vivo* (Zhu *et al.*, 1991). More recently it has been found that endothelial CD44H mediates the adhesion of a human melanoma cell line to quiescent endothelium (Price *et al.*, 1996). In contrast, inducible endothelial adhesion molecules are postulated to regulate metastasis in the same way as they regulate leukocyte adhesion and migration during inflammation. In inflammation, leukocytes marginate once they come in contact with the activated endothelium. They initially make transient contacts with selectin molecules on the surface of the endothelium. This results in rolling of the leukocytes over the endothelium and has been demonstrated *in vitro* using a flow chamber (Abbassi *et al.*, 1993; Lawrence and Springer, 1991) and *in vivo* as observed by intravital microscopy of mesenteric venules (Dore *et al.*, 1993; Arndt *et al.*, 1995). Rolling is blocked *in vivo* using selectin deficient mice (Mayadas *et al.*, 1993; Ley *et al.*, 1995) or the addition of polysaccharide fucoidin (Granert *et al.*, 1994; Ley *et al.*, 1993). Firm adhesion of the leukocytes to the endothelial surface appears to be the result of integrin/receptor interactions (Lawrence and Springer, 1991; Elices *et al.*, 1990). A new sialoglycoprotein, VAP-1, also appears to be involved in lymphocyte adhesion to endothelial cells (Salmi and Jalkanen, 1996). Recent

studies have simulated the shear stress present in the vessels of various sizes through the use of flow chambers. By flowing cancer cells over endothelial monolayers it has been shown that E-selectin (Tozeren *et al.*, 1995; Giavazzi *et al.*, 1993), VCAM-1 (Giavazzi *et al.*, 1993) and Lu-ECAM-1 (Goetz *et al.*, 1996) can mediate cancer cell attachment to endothelium under conditions of shear. This suggests that these molecules may have the ability to cause arrest of cancer cells *in vivo.*

1.3 Adhesion Molecules on Cancer Cells

On cancer cells there appears to be an ordered change of expression of adhesion molecules during tumour progression. For example, the increased expression of MUC 18 (Sers *et al.*, 1994) or α4 integrin subunit (Schadendorf *et al.*, 1995) in melanoma, or α6 integrin in breast cancer (Friedrichs *et al.*, 1995) correlates with a poor clinical prognosis. Binding of colon cancer cells to E-selectin on activated endothelium correlates with malignancy of the cells, activation status of the endothelium, and expression of SLE(a) or SLE(x) (Iwai *et al.*, 1993). The invasive behaviours of some tumours may also correlate with the expression of these adhesion molecules or their receptors.

1.4 Adhesion Molecules Involved in Attachment of Cancer Cells to Endothelium

Early data on cancer cell adhesion systems were obtained using static assays (Rice and Bevilacqua, 1989; Kawaguchi *et al.*, 1992; Rice *et al.*, 1991). These assays also served to illustrate that the adhesive interactions between

cancer cells and endothelial cells could be up-regulated by using various agents to perturb the endothelium. The effects of interleukin-1 (Rice *et al.*, 1988; Lafrenie *et al.*, 1992a; Bereta *et al.*, 1991; Dejana *et al.*, 1988; Lafrenie *et al.*, 1994), thrombin (Neirodzik *et al.*, 1992; Wojtukiewicz *et al.*, 1992), tumour necrosis factor (Okahara *et al.*, 1994) and 12(S)-HETE (Tang *et al.*, 1994) have all been examined and pre-treatment of endothelial monolayers with these agents results in an increase in various adhesion molecules. *In vivo* pre-treatment of animals with interleukin-1, thrombin or tumour necrosis factor before the intravenous injection of cancer cells results in an increase in the number of metastases in the target organs (Okahara *et al.*, 1994; Neirodzik *et al.*, 1992; Lauri *et al.*, 1990; Bertomeu *et al.*, 1993). These observed increases in metastasis can be blocked by the use of synthetic peptides that mimic or interact with adhesive sites on the endothelium (Humphries *et al.*, 1988; Hardan *et al.*, 1993; Humphries *et al.*, 1986), and by interleukin-1 receptor antagonist (Vidal-Vanaclocha *et al.*, 1994; Chirivi *et al.*, 1993). These mediators of endothelial cell perturbation can also elicit a variety of endothelial cell responses, apart from the induction of adhesion molecules, which are potentially relevant to metastasis, including retraction of endothelial cells (Lafrenie *et al.*, 1992b; Honn *et al.*, 1994a; Honn *et al.*, 1994b) or production of soluble factors. These soluble factors include, interleukin-1 which can act as a tumour cell chemoattractant (Orr, 1994), and interleukin-6. Activation of tyrosine kinases which have been postulated to promote the growth of

malignant tumour clones (Rak *et al.*, 1995). The endothelium also produces factors that are detrimental to the growth of tumour cells such as nitric oxide, which is toxic to some tumour cells (Denhardt and Chambers, 1994). Cancer cells can also express cytokines (Mattei *et al.*, 1994; Takeda *et al.*, 1991) that could be involved in the perturbation of the endothelium.

1.5 Mechanisms of Hepatic Metastasis

1.5.1 Liver Anatomy

The liver possesses a dual blood supply: the hepatic artery and the portal vein. The main role of the hepatic artery is to carry an adequate supply of oxygenated blood to the liver. The portal vein carries nutrient-rich venous blood from the capillary system of the digestive tract, spleen, pancreas and gallbladder (Rappaport and Wanless, 1993; Warren, 1982). The vessels enter the liver at the porta hepatis, divide into interlobar branches and these break into interlobular branches (Figure 1). This segmentation is continued at a microscopic level in the liver acinus where short branches from the interlobular veins break up into hepatic sinsuoids which flow on either side of the hepatocytes. The liver acinus is considered to be the basic unit of the liver with the final division of the hepatic artery at its core. The acinus is a hexagonal mass of parenchymal tissue that is divided into three zones differentiated by their distance from the terminal portal vein. The blood enters the sinusoids at zone 1 and exits via the central vein at zone 3 (Figure 2). The lining of the sinusoids differ from that of the larger vessels in that the sinusoids are

FIGURE 1. Hepatic blood circulation. Adapted from (Rappaport and Wanless, 1993).

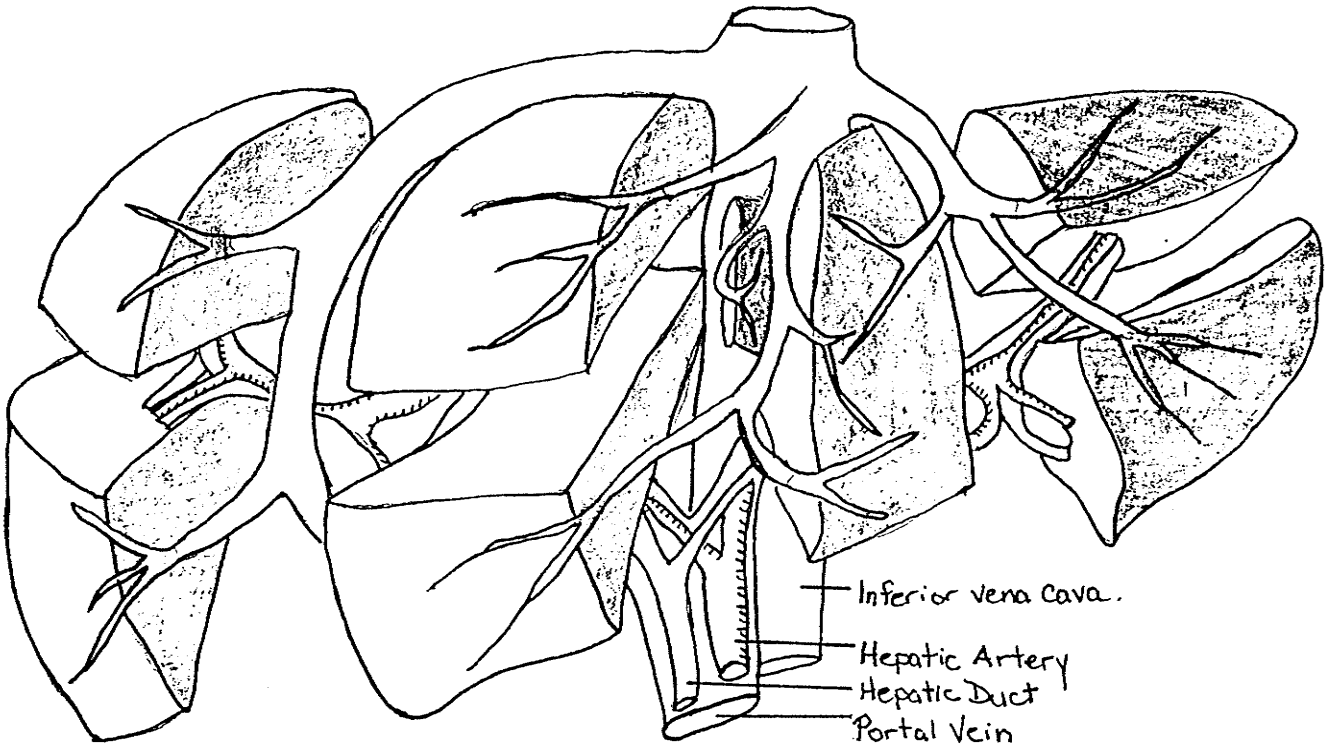
Inferior vena cava.
Hepatic Artery
Hepatic Duct
Portal Vein

fenestrated, have no basement membrane and are of two distinct cell types, endothelial cells and macrophages (Kupffer cells).

1.5.2 Endothelial cells

Liver sinusoidal endothelial cells form a discontinuous, fenestrated lining of the hepatic sinusoids (Smedsrod *et al.*, 1994) and are separated from hepatocytes by the space of Disse. The primary function for the fenestrated endothelium is believed to be as a selective barrier between blood and liver parenchyma (Brouwer *et al.*, 1988). Sinusoidal endothelial cells are able to endocytose an array of substances, mainly through receptor-mediated endocytosis (Smedsrod *et al.*, 1994). It is now known that this reflects an important role for these cells as a part of the scavenger system that clears waste products originating in different tissues and which are brought to the liver via the blood stream. Hyaluronan (Smedsrod *et al.*, 1984) and chondriotin sulphate (Smedsrod *et al.*, 1985) are almost exclusively cleared by the sinusoidal endothelial cells. The sinusoidal endothelial cells are also known to produce and secrete effector molecules such as prostaglandins (Smedsrod *et al.*, 1994),interleukin-1 (Feder *et al.*, 1993) and interleukin-6 (Feder *et al.*, 1993; Luster *et al.*, 1994) along with C3b, which has been identified as a paracrine migration stimulating factor for tumour cells (Hamada *et al.*, 1993). Blocking the interleukin-1 receptor *in vivo* results in the reduction of hepatic metastasis and the reduction in melanoma cell adhesion to cultured hepatic sinusoidal endothelial cells (Vidal-Vanaclocha *et al.*, 1994). Recently, liver

FIGURE 2. Schematic illustration of hepatic acinus showing positions of zones. C = central vein, V = portal vein, A = hepatic artery, D = hepatic duct.

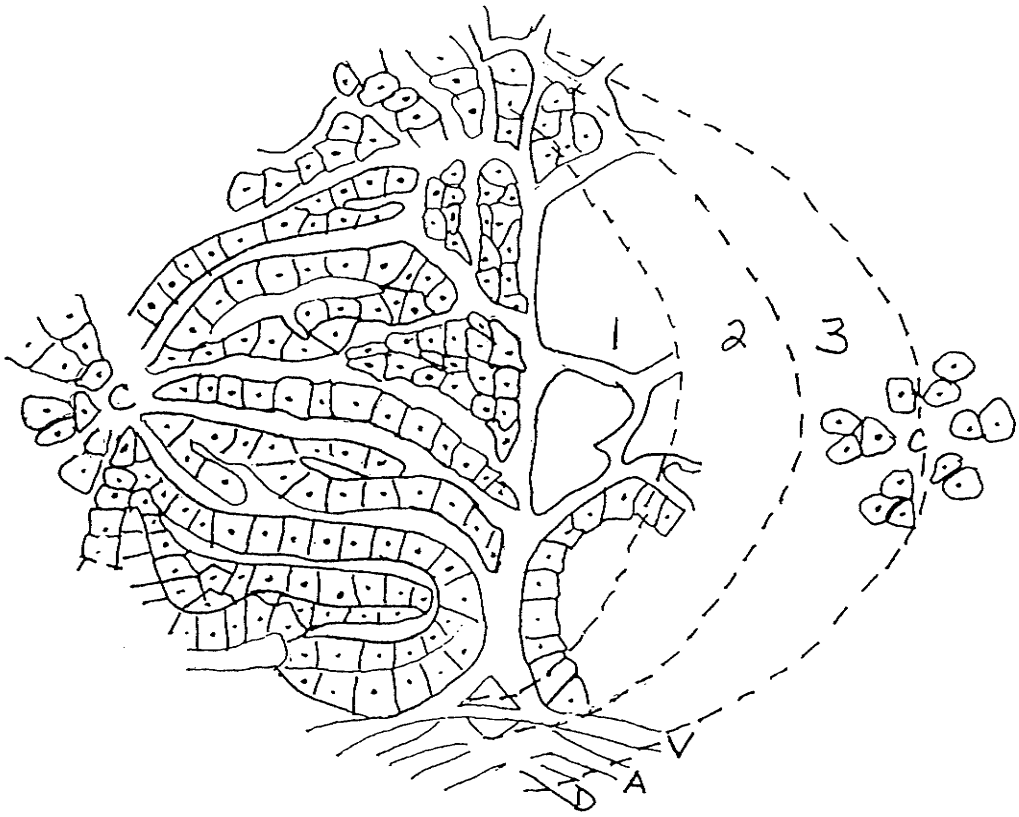
1
2
3
C
C
V
A
D

endothelial cells have been found to also produce nitric oxide. This production has been linked to the T cell- dependent host resistance to lymphoma cells and to the decrease in metastasis of these cells *in vivo* (Rocha *et al.*, 1995).

1.5.3 Kupffer Cells

Kupffer cells are a form of macrophage specific to the liver. They are recruited from the bone marrow but also have the ability to propagate in the liver (Heuff *et al.*, 1993; Decker, 1990). Kupffer cells reside in the sinusoids of the liver in close contact with the sinusoidal endothelium (Figure 3). They are usually observed in higher numbers in the periportal region than in the central vein region and therefore present the first line of defense against viruses, bacteria, and other noxious agents that enter the liver from the gut by way of the portal vein. This defense is their main function and they accomplish it by receptor mediated phagocytosis and cytotoxicity. Kupffer cells also possess the ability to secrete peptide mediators, the best characterized of these are interleukins 1 and 6 (Feder *et al.*, 1993; Luster *et al.*, 1994), tumour necrosis factor (TNF) (Luster *et al.*, 1994) and interferon-α/β (Werner Wasik *et al.*, 1989). Functional differences between the ability of normal and activated rat Kupffer cells to secrete tumour necrosis factor α have been found. Macrophages that had been primed and then activated with lipopolysaccharide did not differ in their capacity to take up lipopolysaccharide when compared to controls but stimulated macrophages released significantly more tumour necrosis factor α (Kayano *et al.*, 1995). Kupffer cells also secrete prostanoids

and oxygen species (Smedsrod *et al.*, 1994). These substances appear to modulate hepatic sinusoidal endothelial cell functions such as endocytosis (Deaciuc *et al.*, 1994). Kupffer cell secretions (proteases, tumour necrosis factor, prostaglandins and oxygen radicals) have been implicated in the damage that occurs during liver reprofusion injury. The *in vitro* demonstration of a rapid increase in the amount of xanthine oxidase present in Kupffer cells (Wiezorek *et al.*, 1994) and the evidence of improvements in prognosis of liver grafts after the removal of Kupffer cells (Bremer *et al.*, 1994) seem to support this theory. But other investigators have found that Kupffer cells do not modify the effects of 24 hour cold ischemia reprofusion in rat livers (Imamura *et al.*, 1995). Many of the Kupffer cell secretions have also been implicated in tumouricidal activities. Kupffer cells have been observed interacting with both colorectal cancer cells (Meterissian *et al.*, 1994) and Friend erythroleukemia cells (McCuskey *et al.*, 1994). Barbera-Guillem *et al.* (1993) have shown that 90% of the cells introduced into the liver by intrasplenic injection are dead in zone 1, the periportal region of the acinar structure, 1 hour after injection of the cells.

1.6 Arrest of Cancer Cells

There are parallels between the vascular phase of metastasis described in section 1.2.1 and events which occur in liver metastasis. Most cancer cells seed the liver in the portal venous or hepatic arterial blood. This is likely to occur early in the clinical course of the disease since cancer cells have been

FIGURE 3. Schematic representation of the liver sinusoid.

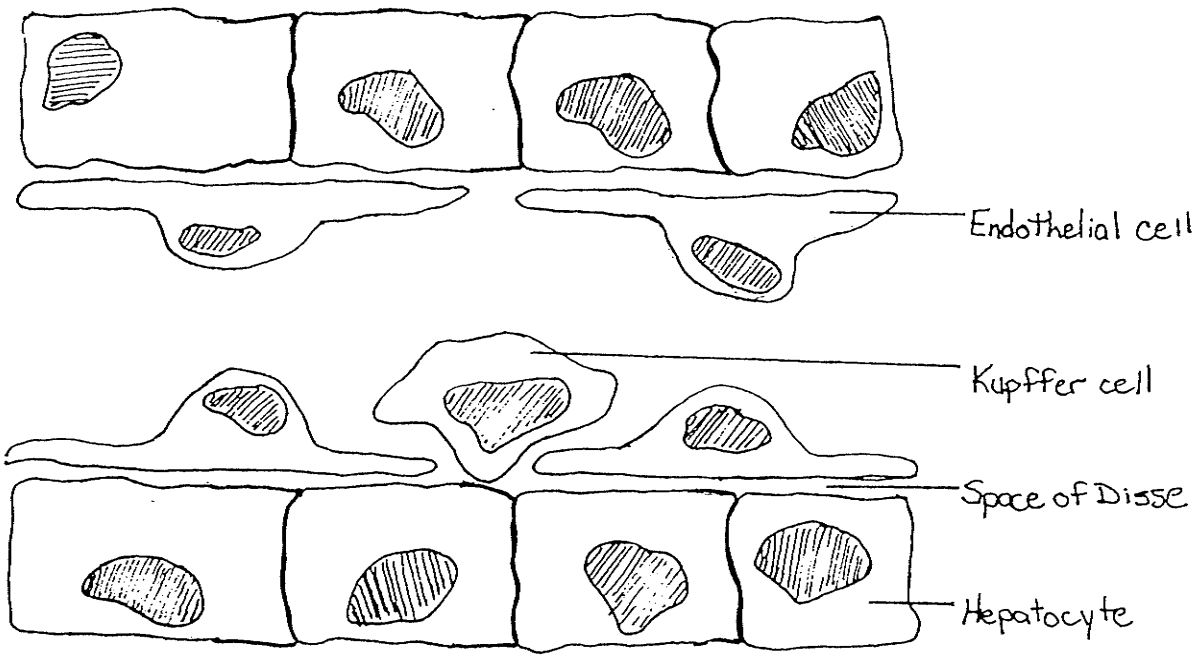
Endothelial cell
Kupffer cell
Space of Disse
Hepatocyte

detected in the blood (Burchill *et al.*, 1995; Tobal *et al.*, 1993), marrow (Gerhard *et al.*, 1994) and liver (Inoue *et al.*, 1995) at the time of surgery for primary tumours which typically form liver metastasis. There is evidence that both mechanical trapping (Barbera-Guillem *et al.*, 1993; Morris *et al.*, 1993) and vascular adhesion molecules can mediate tumour arrest. For example Tressler *et al.* (1993, 1994) have identified two molecules on RAW117 lymphoma cells, annexin II and annexin VI, that mediate the adhesion of these cancer cells to liver microvascular endothelial cells in a calcium-dependent manner. Some adhesive events appear to be susceptible to modulation. The laminin α1 chain, in peptide form, has been implicated in up-regulating the liver colonizing ability of human colon cancer cells (Bresalier *et al.*, 1995). Also, spontaneous metastasis as well as experimental liver metastases of a highly metastatic lymphoma cell line was increased by treatment of animals with tumour necrosis factor (Orosz *et al.*, 1995). *In vitro*, the adhesion of these cells to mouse endothelioma cells was inhibited by antibodies which block VCAM-1/$\alpha_4\beta^1$ interactions. Similarly, hepatic sinusoidal cells have been reported to express E-selectin after exposure to tumour necrosis factor α. An anti-E-selectin antibody blocked H59 cell adhesion to these cells and also blocked metastasis (Brodt *et al.*, 1994). Transgenic mice expressing E-selectin in all tissues which were injected with B16F10 cells transfected to express E-selectin showed massive infiltrating liver tumours. Normal mice injected with transfected B16F10 cells formed lung tumours exclusively. This would suggest that E-

selectin can redirect metastasis of tumour cells expressing appropriate ligands *in vivo* (Biancone *et al.*, 1996).

1.7 Distribution of Endothelial Adhesion Molecules

As discussed above, the hepatic circulation is divided into distinct subunits. It appears that each of these subunits express a unique family of vascular adhesion molecules (Table 2). Specifically, VCAM-1 is expressed on sinusoidal cells but not on portal capillary endothelium and is known to interact with $\alpha 4$ integrins to bind tumour cells of varying histogenesis to endothelial cells (Lafrenie *et al.*, 1994). The mRNA expression of ICAM-1 has been shown to increase in the livers of mice after treatment with tumour necrosis factor α but has not been related to the zonal anatomy of the liver (Essani *et al.*, 1995). ICAM-1 had also been implicated in the binding of glioma cells to endothelial cells *in vitro* (Tamaki *et al.*, 1995). E-selectin is reported to be absent from the portal capillary and sinusoidal endothelium, but Brodt *et al.* (1994) has recently reported that this molecule is expressed by tumour necrosis factor α-stimulated hepatic sinusoidal cells *in vitro*. In man, normal liver shows intra-acinar variation in structural and functional markers for sinusoidal endothelial cells (Scoazec *et al.*, 1994; Scoazec and Feldmann, 1991). Sinusoidal endothelial cells also show a limited array of the $\beta 1$ family of integrins in comparison to other tissues of the liver (Volpes *et al.*, 1991). The repertoire of expression of these adhesion molecules changes during the development of hepatitis (Volpes *et al.*, 1992), cirrhosis (Couvelard *et al.*, 1993) and transplant rejection

(Steinhoff *et al.*, 1993). In the mouse, differences in the expression of wheat germ agglutinin-binding sites between the periportal and perivenous regions have allowed the isolation of two sinusoidal endothelial cell subpopulations from sublobular liver compartments (Vidal-Vanaclocha *et al.*, 1993). These differences in sinusoidal cell populations might contribute to the definition of distinct microenvironments within the human liver. Heparin sulfate proteoglycans have recently been found to be expressed in normal human liver. It is postulated, due to the differential expression of these molecules in different compartments of the liver, that each one has a specific function in the interplay of cells, matrix molecules, growth factors and proteinases (Roskams *et al.*, 1995). Other groups have identified what they believe to be specific adhesion systems on lymphoma cells and carcinoma cells that allow them to interact specifically with the liver microenvironment and form metastasis (Kemperman *et al.*, 1995; Kemperman *et al.*, 1994). Recently, the presence of LFA-3 on gastric carcinomas has been correlated to giving these cells a selective advantage in establishing distant metastases in the liver and peritoneum (Mayer *et al.*, 1995). These systems are in the process of being further defined and an accurate portrait of the specific and relevant hepatic endothelial adhesion molecule/tumour cell interactions are being developed both *in vivo* and *in vitro*.

1.8 Intravital Microscopy

The technique of intravital microscopy (IVM) uses a video camera attached to a light microscope to visualize, record, and analyze the movement of blood through microcirculatory pathways of intact organs and tissues in living animals (Chambers *et al.*, 1995). It has been used with great success to elucidate the interactions between leukocytes and the vascular endothelium in inflammation. The phenomenon of leukocyte rolling in mesenteric venules has been extensively investigated through the used of IVM. It has been found that rolling of leukocytes in inflammation does not occur in mice deficient in P-selectin (Mayadas *et al.*, 1993; Dore *et al.*, 1993) or L-selectin (Ley *et al.*, 1995). Recently, it has been discovered that P-selectin is not only involved in the early events of inflammation but is additionally responsible for leukocyte rolling and macrophage recruitment in more prolonged tissue injury (Johnson *et al.*, 1995). More specifically, P-selectin and E-selectin have been implicated in contributing to the adhesion of leukocytes to the intestinal wall resulting in granulocyte accumulation in chronic intestinal inflammation (Arndt *et al.*, 1995). The transmigration of leukocytes has also been examined through the use of IVM and the mediators of this process are being examined through the effects of endogenous inflammatory products (Nourshargh *et al.*, 1995) as well as specific anti-inflammatory drugs (Mancuso *et al.*, 1995). In fact, this technique of leukocyte watching is now being used in the study of many specific disease processes such as ischemia/reperfusion injury (Kubes *et al.*, 1995), cholestatis

(Swain *et al.*, 1995), atherosclerosis (Lehr *et al.*, 1994; Lehr *et al.*, 1995; Gauthier *et al.*, 1995) and haemorrhagic shock (Bauer *et al.*, 1995; Marzi *et al.*, 1995) as well as to examine the effects of specific mediators such as nitric oxide (Gauthier *et al.*, 1995; Minnicozzi *et al.*, 1995) and endothelin-1 (Zhang *et al.*, 1995).

Most experimentation with IVM involve studying endogenous systems, but the injection of cancer cells into the circulation of animals has also been employed to investigate the process of metastasis. Wood, (1958) was one of the first to investigate the process of metastasis using intravital microscopy of the V2 squamous-cell carcinoma in the rabbit ear. This model allowed the observation of the process of metastasis from the initial lodging of the cancer cells in the vasculature, through growth and angiogenesis of the forming tumour. In his paper, Wood outlined suggestions for many of the techniques now employed in this study and one of the first accounts of the interactions between the endothelium and cancer cells. More recent studies have expanded on Wood's initial observations and have provided novel information on the vascular phases of metastasis. Chambers' *et al.* (1992) began studies of haematogenous metastasis using the model of the chorioallontoic membrane of chick embryos. Initial data showed that eight hours after injection of cancer cells, 83% of the cells had extravasated and the rest were in the process of extravasation. Cancer cell division was seen only after extravasation (Chambers *et al.*, 1992). These results were extended to a murine model

where it was reported that even though cells went through extensive deformation in the process of mechanical trapping in the vasculature of the muscle and liver, over 97% of cells maintained membrane integrity (Morris *et al.*, 1993). This challenges the existing dogma of metastatic inefficiency by haemostatic destruction, which suggests that the majority of cancer cells are killed quickly by the stress of the circulation (Weiss, 1990). Further experimentation using high and low metastatic cell lines and a cell line over-expressing metalloproteinase inhibitors showed no differences in the extravasation potential of these cells. In both situations Chambers *et al.* report no differences in the extravasation ability of these cells compared to control cells, with more than 95% of the observed cells extravasating, but report differences in the cells' abilities to migrate and subsequently grow (Morris *et al.*, 1994; Koop *et al.*, 1994). Recent data by Chambers *et al.* have shown that normal murine fibroblasts extravasate with the same ability as the cancer cell lines examined (personal communication). Contrary to this, experimentation with colorectal carcinoma cells of high and low metastatic potential have shown a difference in the retention of cells in the liver (Ishii *et al.*, 1996). The highly metastatic cell line showed more cells in the liver and cells present in aggregates of 8-12 cells whereas the less metastatic line showed only a few single cells 72 hours after injection.

Based on extensive experience with the technique of intravital microscopy, Chambers *et* alhave made several conclusions about hepatic

metastasis: a) Initial arrest occurs by size restriction; b) Cells extravasate through sinusoids; c) The vast majority of cells arrested in the microcirculation successfully extravasate; d) extravasation involves adhesion to the sinusoidal wall and active migration (Chambers *et al.*, 1995).

Table 1. Endothelial surface adhesion molecules involved in interactions with cancer cells

Endothelial Cell Surface Molecule	Tumour Cell Counter-Receptor	Known Cell Types	References
Selectin Family of Adhesion Molecules			
E-selectin[1]	SLE(a) SLE(x)	Colon Carcinoma	(Ye *et al.*, 1995; Tozeren *et al.*, 1995)
Immunoglobulin Super Family			
CEA	CEA	Breast Cancer Colon Cancer	(Majuri *et al.*, 1994)
ICAM-1	β_2	C6 Glioma	(Tamaki *et al.*, 1995)
VCAM-1 [2]	α_4 integrins	Renal Carcinomas	(Tomita *et al.*, 1995)
	$\alpha_4\beta_1$	Melanomas	(Garofalo *et al.*, 1995)
		Sarcomas	(Wojtukiewicz *et al.*,1993; Paavonen*et al.*, 1994)
MUC18 [3]	MUC18	Melanomas	(Shih *et al.*, 1994)

[1]Seen on intratumour vessels where its expression correlates inversely with the distance from the tumour. *In vitro*, inducible by cytokine stimulation where expression is associated with attachment of cancer cells to endothelium in static assays or under flow and with an invasion of endothelial monolayers.

[2]Increased expression seen *in vivo* after injection of interleukin-1.

[3]Constitutive expression on some endothelial cells.

Table 1. Endothelial surface adhesion molecules involved in interactions with cancer cells (continued).

Endothelial Cell Surface Molecule	Tumour Cell Counter-Receptor	Known Cell Types	References
Immunoglobulin Super Family (con't)			
MADCAM-1	α_4 integrins	Postulated[4]	(Piali *et al.*, 1995)
Integrin Adhesion Molecules			
α_6 integrins $\alpha_6\beta_1$ $\alpha_6\beta_4$	$\alpha_6\beta_1$	B16/129 Melanomas	(Ruiz *et al.*, 1993)
$\alpha_v\beta_3$[5]	Unknown[6]	Multiple tumour types	(Lafrenie *et al.*, 1994)
Other Adhesion Molecules			
Thrombospondin(Tsn)	Tsn and Tsn Receptors	MCF7 Breast Cancer	(Incardona *et al.*, 1995)
Heparin Sulphate	NCAM		(Zocchi *et al.*, 1993)

[4]Known to interact with α_4 integrins on leukocytes. Could theoretically interact with cancer cells carrying this same adhesion molecule.

[5]Synthesis increased after interleukin-1 treatment. Increased expression may also relate to translocation from the cytoplasm to cell membrane.

[6]In leukocytes, can interact with CD31/PECAM.

Table 2. Adhesion molecules in the human hepatic microvasculature.

	PORTAL TRACT		SINUSOIDS		
	PV	PCE	SE	K	SLE
Selectin Family					
E-selectin	+/-[a]	-	-	-[b]	
P-selectin	+/-[a]	-	-	-	
Immunoglobulin Superfamily					
ICAM-1	-[c]	-	+	+	+[a]
ICAM-2	-[c]	+	+	+	+
ICAM-3	-		-	+	
VCAM-1	-[b]	-	-[b]	+	-[a]
LFA-3	-[c]		+	+	+/-[c]
Integrin Family					
β_1	+	+	+		+
β_2		+		+	
β_3		+[e]	+		
β_4		+	-		
α_1	+	+	+		+
α_2	+	+	-		+/-
α_3	+	+	-		-
α_4	-	+	-	+[d]	-[e]
α_5	+	+	+		+[e]
α_6	+	+	-[d]		-
α_{IIb}		+	+/-		
α_v		+	+[d]		

Data obtained from (Volpes *et al.*, 1992; Scoazec and Feldmann, 1994; Volpes *et al.*, 1991; Scoazec and Feldmann, 1991; Couvelard *et al.*, 1993; Scoazec *et al.*, 1994; Steinhoff *et al.*, 1993)

[a] Upregulated in acute and chronic non-reversible rejection and in cholangitis, sepsis and viral infection (Steinhoff *et al.*, 1993)

[b] Upregulated in acute and chronic hepatitis and in chronic active hepatitis (Volpes *et al.*, 1992)

[c] Upregulated in chronic irreversible rejection (Steinhoff *et al.*, 1993)

[d] Upregulated in cirrhosis (Couvelard *et al.*, 1993)

[e] Upregulated in inflammation and cholestasis (Volpes *et al.*, 1991)

Abbreviations PV = portal vein, PCE = portal capillary endothelium, SE = sinusoidal endothelium, K = Kupffer cells, SLE = sinusoidal lining cells (unspecified).

2.0 HYPOTHESIS AND APPROACH:

The major hypothesis of this work is that cancer cells become arrested in the liver microvasculature by non-mechanical, regulatable means and that this arrest leads to the formation of liver metastasis.

There are two main theories on how cancer cells become arrested in the vasculature. First, is the theory of mechanical trapping. This theory is supported by autopsy data that shows that in a large number of patients with metastasis, the secondary tumour is found in the first microvascular bed that is encountered after entering the circulation (Weiss and Ward, 1982; Weiss, 1992). The cells are trapped, extravasate and form metastases. Recent data also support this hypothesis Morris *et al.* (1993) show by intravital microscopy that B16 melanoma cells become mechanically trapped in the muscle and liver vasculatures. The second theory is that adhesive interactions between endothelial cells and cancer cells result in the arrest of cancer cells in the vasculature and lead to their subsequent extravasation and growth. The organ specificity of some cancer cells supports a special adhesive interaction between these cells and specific endothelial cells (Rusciano and Burger, 1992; Zetter, 1990; Nicolson, 1988; Verschraegen *et al.*, 1991; Weiss *et al.*, 1984; Pauli *et al.*, 1990; McCarthy *et al.*, 1991). *In vitro* data show that cancer cells can interact with endothelial cells through a variety of adhesion molecules and that these interactions can be regulated (Lafrenie *et al.*, 1994; Lafrenie *et al.*, 1992a; Rice *et al.*, 1988; Vidal *et al.*, 1992; Bereta *et al.*, 1991; Martin-Padura

et al., 1991; Dejana *et al.*, 1988). Also, *in vivo* experimentation has shown that an up-regulation in tumour burden due to IL-1 can be blocked using inhibitory peptides (Bertomeu *et al.*, 1993; Lauri *et al.*, 1990) and IL-1 receptor antagonists (Chirivi *et al.*, 1993; Vidal-Vanaclocha *et al.*, 1994).

The experiments in this thesis were designed to investigate a role for non-mechanical arrest of cancer cells in the liver microvasculature, with particular emphasis on manipulation of the arrest with recombinant interleukin-1 α. Therefore, to assess if pre-treatment of C57bl/6 mice with recombinant interleukin-1 α resulted in increased experimental liver metastasis of B16F1 murine melanoma cells, analogous to the increase in adhesion seen *in vitro* and in the lung, a model of liver metastasis was developed. B16F1 cells were injected via a mesenteric vein, allowing direct seeding of the liver. This technique was used to explore the up-regulation of tumour burden with recombinant interleukin-1 α pre-treatment, the retention of cancer cells in the liver at early time points, the effect of GRGDS and GRGES peptides on metastasis and the arrest patterns of the cancer cells as visualized by intravital microscopy. A modified Stamper-Woodruff assay was developed to attempt identification of a specific adhesion molecules which might be responsible for the results obtained *in vivo*.

3.0 MATERIALS AND METHODS

3.1 MATERIALS

Cell culture media and Thermanox discs™ were obtained from GIBCO, Edmonton, Alberta. Plasticware for tissue culture was supplied by Fisher Scientific, Winnipeg, Manitoba. B16F1 murine melanoma cells were purchased from the American Type Culture Collection (Rockville Maryland). Female C57bl/6 mice were obtained from Charles River, Montreal, Que. The recombinant human interleukin-1α (rIL-1α) was a gift from Richard Chizzonite of Hoffman-LaRoche, Nutely, New Jersey. The [^{125}I]-iododeoxyuridine (2000 Ci/mmol) was obtained from Flow/ICN Biomedicals Inc., Mississauga, Ontario. Glycyl-arginyl-glycyl-aspartyl-serine (GRGDS) and glycyl-arginyl-glycyl-glutamyl-serine (GRGES) peptides were purchased from Novabiochem, La Jolla California. Calcein AM was obtained from Molecular Probes, Eugene Oregon, and the 0.05 and 6μm fluorescent latex microbeads were obtained from Polysciences, Warrington Pennsylvania. The Leitz DMIL microscope and the Volpi Intralux 5000-1 fiberoptic light source were obtained through Leica, Toronto, Ontario. The VE-1000 system control board and the Dage Video monitor were obtained from Dage MTI Inc., Michigan City, IN. The time/date generator and the Panasonic super VHS VCR were bought from Hill's Bros. Ltd. in Hamilton Ontario.

3.2 CELL CULTURE

3.2.1 Cancer Cell Maintenance

B16F1 murine melanoma cells were cultured in T75 flasks in αMEM supplemented with 10% fetal bovine serum and 100U/ml penicillin and 100μg/ml streptomycin at 37°C, 5% CO_2 and 100% humidity. Confluent monolayers were harvested by incubating with either 1% Trypsin/ethylenediaminetetraacetic acid (EDTA) or 5 mM ethyleneglycotetraacetic acid (EGTA) in phosphate buffered saline at Ph 7.4, collected by centrifugation at 1000 rpm for 5 min and replated at dilutions of 1:4 to 1:10.

3.2.2 B16F1 Cultures from Passaged Tumours

Passaged B16F1 cells, obtained from ATCC were expanded as described, and $3x10^5$ cells in 0.1 ml were injected subcutaneously into the left shoulder of C57bl/6 mice. The cells were harvested when a tumour of 5-10 mm was observed. The tumour was harvested under sterile technique, washed in supplemented αMEM, minced and dispersed into a single cell suspension by treatment with 0.5% Trypsin/EDTA in calcium-magnesium free phosphate buffered saline. The cell suspension was plated onto T75 flasks and allowed to grow to confluent monolayers. The cells were then harvested, suspended in media containing 30% FBS and 10% DMSO, quick-frozen and stored in liquid nitrogen.

3.2.3 Harvesting for Experimentation

Cells to be used in adhesion assays or for animal experiments were harvested by incubation with 5 Mm EGTA in phosphate buffered saline washed once with supplemented media and twice with unsupplemented media. The cells were passaged through a 20 gauge needle to obtain a single cell suspension and resuspended at appropriate concentrations. Cell viability was assessed using the trypan blue exclusion method.

3.3 CELL LABELLING

3.3.1 Fluorescent Microbeads

Monolayers were grown to 75% confluence, washed 3 times with unsupplemented Opti-MEM™ medium and 7.5 ml of Opti-MEM™ was added to each monolayer. The cells were fluorescently labelled by incubation with 75μl of 0.05μm latex beads at 37°C, 50% CO_2 and 100% humidity for 60 minutes with periodic rocking (Morris *et al.*, 1994). The media and remaining beads were aspirated, the monolayer washed three times with Opti-MEM™ to remove excess beads and incubated for 4 hours with αMEM supplemented with 10% fetal bovine serum or overnight with αMEM media supplemented with 1% FBS. The monolayer was detached by incubation with 5 Mm EGTA and harvested as described in section 3.2.3.

3.3.2 Calcein AM

Confluent monolayers were washed twice with phosphate buffered saline and 4 μl of calcein stock (5 mg/ml in DMSO) was added to 10 mls of PBS

and incubated with the monolayer at 37°C for 45 minutes (Morris *et al.*, 1993). The cells were then harvested by incubation with 5 Mm EGTA as described.

3.3.3 Fluorescein Isothiocyanate (FITC)

A fluorescein isothiocyanate (FITC) solution was prepared by adding 0.03 g of FITC (isomer 1) to 50 ml PBS and shaking the mixture in a water bath at room temperature for 2 hours. The mixture was centrifuged for 15 minutes at 3000 rpm to remove undissolved FITC. The solution was filtered through a 2μm filter and the O.D. measured at 495 nm to determine the concentration in μg/ml using the formula:

$$\text{concentration} = \frac{Abs_{495} \times MW_{FITC} \times \text{dilution factor}}{E \times C}$$

where $E = 6.8 \times 10^4$, $C = 1.0$ cm and $MW_{FITC} = 389.4$ g/mol.

Monolayers were labelled by incubation in 5 ml supplemented αMEM and 5 ml PBS. The desired concentration of FITC was added and allowed to incubate for 20 min at 37°C (Butcher *et al.*, 1980; Butcher and Weissman, 1980). The monolayers were washed with αMEM, detached and harvested as described.

3.3.4 [^{125}I]-iododeoxyurine labelling

Cells were subcultured at a ratio of 1:4-1:6 the day before labelling. The subconfluent cancer cells were incubated with 2μCi/ml of [^{125}I]-iododeoxyuridine [^{125}I]-UdR for 48 hours at 37°C (Fidler, 1970). Cells were harvested as described above. (section 3.2.3)

3.4 IN VIVO STUDIES

3.4.1 Metastasis Assay

Eighteen to twenty-two gram, female, C57bl/6 mice were injected intraperitoneally with either 1.5 μg of recombinant interleukin-1α or with an equal volume of saline at half hour intervals, alternating treated and untreated animals. Four hours after injection the animals were anaesthetized with Avertin, (1 g of tribromomethyl alcohol in 1 ml 2-methyl-2- butanol) at a dose of 0.02 ml/gm of mouse, and prepared for surgery. A mid-line incision was made over the lower abdomen of the mouse and an appropriate mesenteric vein exposed and cannulated. $3x10^5$ B16F1 melanoma cells in 0.1 ml were injected over a period of 30 seconds. The incision was closed and the mouse allowed to recover under an external heat source to maintain body temperature. The animals were returned to the housing facility until the endpoint of the experiment when they were euthanized using CO_2 and autopsies carried out. An incision was made from beneath the chin to the external genitalia and the chest cavity exposed by removing the rib cage. The trachea was cannulated and the lungs filled with neutral buffered formalin. The organs were removed in mass and fixed in 10% neutral buffered formalin. Twenty-four to 48 hours later the organs were dissected and examined for overt tumour burden. Liver tumour burden was quantified macroscopically by counting the visible nodules on the liver surface and microscopically by examining 3 sections from each liver in both experimental groups. The lobes of the liver were dissected and the two

largest lobes and one smaller lobe was used. The 1-2 mm thick sections were cut horizontally through the widest part of the liver lobe and placed in histological cassettes for further processing. Each experiment employed the same choice of liver lobes, cut in the same manner. The sections were embedded in paraffin, stained using haematoxylin and eosin (H&E) and the percent area of normal liver, tumour and necrotic tissue was determined for each section by microscopy using a Mertz graticule. The intersection of the tissue types with points on the Mertz graticule was observed microscopically at 10x's magnification. The percent area occupied by each of tumour tissue, normal liver tissue, or necrotic tissue was calculated for each field observed over the section of the liver. All three sections of liver from each animal were scanned in a systematic fashion to ensure accurate quantification. The mean value for the percent area of each tissue type was determined for each animal and the median of these values represented the total percent occupied by each tissue type.

The effect of GRGDS and GRGES peptides on metastasis in both control and interleukin-1 treated animals was assessed. 3 mg of peptide/mouse (Humphries *et al.*, 1988; Humphries *et al.*, 1986) were added to the cell suspension immediately before they were injected into the mesenteric vein as described above.

3.4.2 Radioactivity Study

B16F1 cells were radio-labelled with [^{125}I]-UdR and then injected into the

mesenteric vein as described. The animals were euthanized at time points ranging from 0-24 hours and the animals autopsied immediately. The organs were dissected and fixed in 10% neutral buffered formalin for 48 hours and the liver, spleen, kidney, intestines and lungs put into scintillation vials and counted in a gamma counter. Background radioactivity was determined by counting empty scintillation vials. The number of cells in each organ was determined by subtracting the background counts and dividing by the counts found in the total number of cells injected. The control cells were introduced directly into a scintillation vial via a canula at the time of harvest.

3.5 INTRAVITAL MICROSCOPY

3.5.1 Construction of the Intravital Microscope

The technique of intravital microscopy requires the use of an inverted microscope with a ultraviolet light source, connected to a video camera, and a super VHS VCR. Oblique or trans-illumination of the tissue was provided by a fibre optic light source. Transillumination of the tissue resulted in a shadowing effect that increased the contrast and imparted a 3-dimensional quality to the image. The stage of the inverted microscope was modified to accommodate the animal and the insertion of a 6.5 cm x 4.5 cm glass coverslip. The liver of the mouse rested on the glass coverslip window above the objective lens (16-100x) and was completely stabilized with a minimal amount of external pressure (Chambers *et al.*, 1995) (Figure 4). This resulted in the tissue of interest remaining relatively stationary, flat, in the plane of focus and gave a

FIGURE 4. Schematic illustration of an intravital microscope.

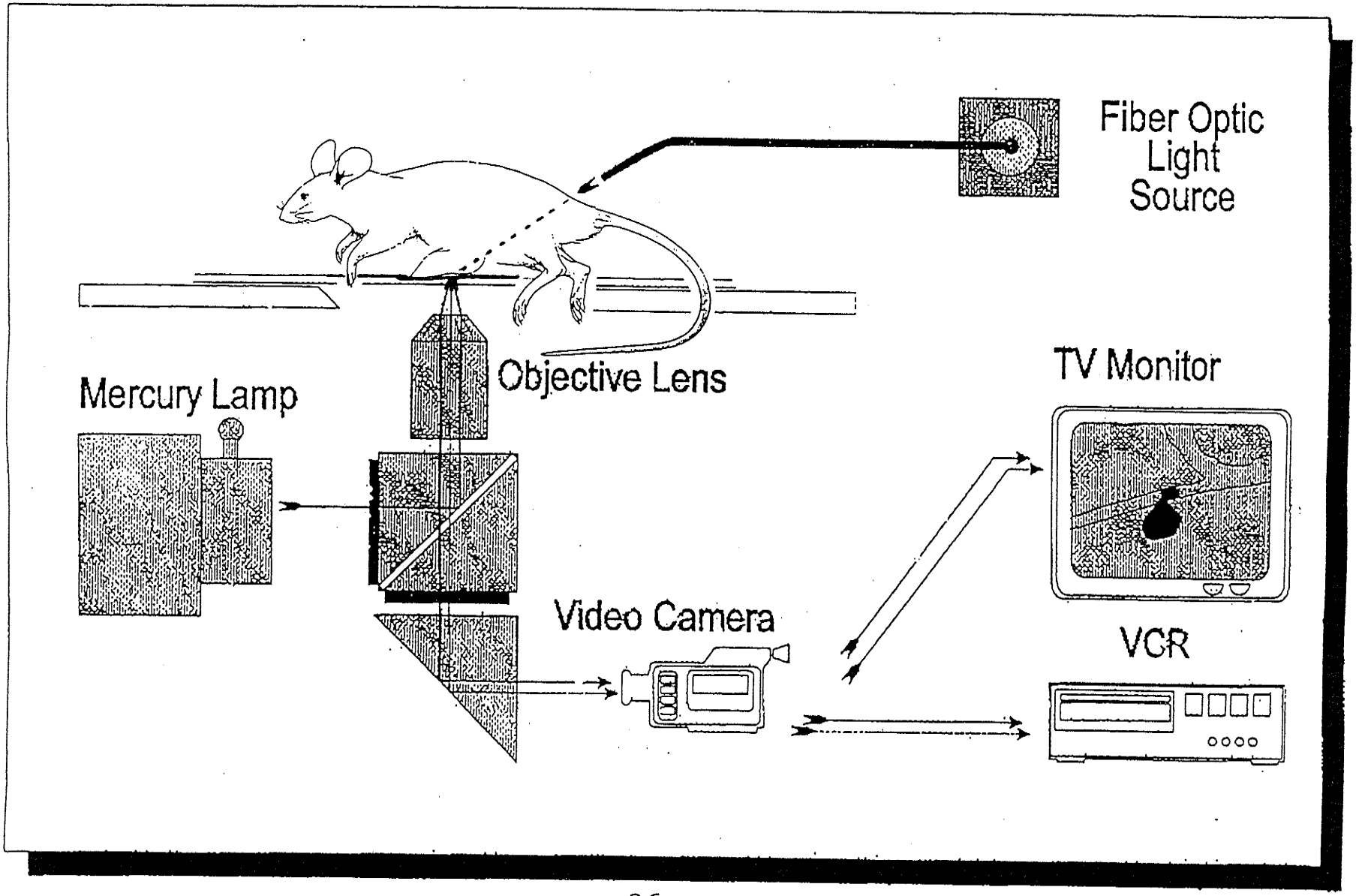
Fiber Optic
Light
Source
Objective Lens
TV Monitor
Mercury Lamp
Video Camera
VCR

large working area over which observations were made. The features of this system yielded images of high resolution which could be quantified as described.

3.5.2 Experimentation using Intravital Microscopy

Cells were fluorescently labelled, as previously described, with either latex microbeads (section 3.3.1) or Calcein-AM (section 3.3.2). Animals were injected intraperitoneally with either 1.5 μg interleukin-1 α or an equal volume of saline. Four hours later the animals were anaesthetized using Avertin. A canula was introduced intraperitoneally to administer anaesthetic as needed. The mouse was prepared for surgery and a midline incision made from the sternum to the external genitalia exposing both the liver and the intestinal area. An appropriate mesenteric vein was found, cannulated and the canula was splinted into place. The liver was exposed and one lobe was placed onto the modified stage of the microscope. A 40x's field was found that showed a incoming portal vessel, with good blood flow, in the plane of view. Fluorescently-labelled B16F1 cells ($1x10^6$ per 0.1ml) were injected into the cannulated mesenteric vein until the cells could be observed in the portal tract capillary projected onto a video monitor. The rate of appearance of cells could be controlled by the speed of injection. The sequence of events was recorded so that later analysis and quantification of tumour cell/endothelial cell interactions could be carried out. The outlines of the vessel system were traced from the monitor and the anatomical arrest points of the fluorescent cells were

marked. From these drawings, the distance cells travelled into the sinusoids and the calibre of the vessel in which cells arrested was determined manually. The velocity of the cells was determined by tracing the movement of the cancer cells on the video record frame by frame onto the outline of the vessel system. The distance that the cell moved from frame to frame was measured and the time between frames was recorded. From this information a velocity profile was established for each cell. The data for each cell were pooled to obtain overall velocity versus time and velocity versus distance profiles in which the movements of cells in control and in interleukin-1 treated animals were compared. To observe the effects of GRGDS and GRGES peptides on cell movement, in some experiments 3 mg of the peptides were added to the cell suspension immediately before they were injected (Humphries *et al.*, 1988; Humphries *et al.*, 1986). The remainder of the protocol was as described above.

3.6 *IN VITRO* STUDIES

3.6.1 Frozen Section Assay

Mice were treated intraperitoneally with 1, 1.5 or 2 μg of interleukin-1α or an equal volume of suspending vehicle at half hour intervals. Four hours later, the animals were euthanized using CO_2 and their livers excised, divided into lobes and sub-lobes, mounted onto cork with OCT™ compound, and snap frozen in methyl-butane cooled in liquid nitrogen. The tissue was stored at -80°C until sections were to be taken. The necessary blocks were warmed to -

30°C in a cryostat, 5 μm sections were cut, mounted onto Thermanox™ discs and placed in 24 well plates. B16F1 cells were harvested as described in section 3.2.3 and resuspended to a concentration of $5x10^4$ cells/ml in Hanks' Balanced Salt Solution (HBSS). One ml of the cell suspension was placed over each frozen section and allowed to incubate for 15 minutes at room temperature. The medium containing non-adherent cells was aspirated and the sections washed 3 times in HBSS to remove any non-adherent cells. The sections were then fixed by incubation in 70% ethanol for at least 1 hour. To examine the effect of GRGDS and GRGES peptides on the adhesion of cancer cells to the liver sections, 500 μl of solution containing either 50 or 100 μM of the peptide in HBSS was placed onto the frozen section 30 seconds before the cells were added. In this case, the cells were resuspended at a concentration of $1x10^5$ cells/ml and 500 μl of the suspension added to the sections. The sections were stained with Haematoxylin and Eosin, mounted on glass slides, and examined microscopically. The total number of adherent cancer cells and the proportion of cells adherent to hepatocytes, sinusoids, and the wall of large vessels was determined. All experiments included 25 random fields per slide and were done in replicates of 6 slides per condition with each experiment being performed at least 3 times.

3.7 STATISTICS

For all animal work, median values and ranges were used and statistics were done using the Mann-Whitney U-test. In the *in vitro* adhesion assays mean ± standard deviation or standard error of the mean was used and statistics calculated using the Student's t-test or Anova.

4.0 RESULTS

4.1 METASTASIS ASSAY

4.1.1 Rationale

To investigate a role for non-mechanical arrest during the process of metastasis an animal model system had to be developed. An appropriate cell line, mouse strain, target organ and injection route had to be determined. This system had to give consistent reproducible results, be amenable to modulation and be adaptable to experimentation on the intravital microscope.

4.1.2 Characterization of Parameters for Metastasis Assay

B16F1 melanoma cells were injected, via a mesentery vein, directly into the liver at varying concentrations and allowed to grow for different time periods ranging from 7-21 days. Upon autopsy it was determined that the B16F1 cells formed colonies in the livers of C57bl/6 mice, were also present in the mesentery and to a lesser extent in the lung. The tumour burden was quantitated by counting nodules on the liver surface and by determining changes in weight of individual organs (Table 3). The organ weights showed an increase in the mass of the spleen and intestine in all groups, an increase in the mass of adrenal glands 21 days after injecting $2x10^4$ cells and in the liver mass 14 days after injecting $5x10^5$ cells when compared to non-treated controls. Quantisation of discrete nodules in the organs was only possible for animals euthanized 14 days after the injection of $3x10^5$ B16F1 cells. Time course experiments demonstrated that euthanizing animals 21 days after the

injection of $3x10^5$ cells resulted in high numbers of nodules in both the liver and in the mesentery with a number of metastasis in the lung. Animals euthanized 14 days after had quantitatable tumour growth in the liver and in the mesentery but did not have lung metastasis. Mice euthanized 7 days after injection had quantitatable tumour growth in the liver with little or no detectable growth in mesentery or lung. The weights of organs were significantly increased for the intestine and liver only in animals 21 days after injection, for the kidney 14 days after injection and for the brain at 7 and 14 days after injection (Table 4).

4.1.3 Effect of Interleukin-1 Pre-treatment on Tumour Burden

Mice pre-treated with 1.5 μg interleukin-1α, injected with $3x10^5$ B16F1 cells and euthanized after 7 days, showed a 7 fold increase in the number of liver tumour nodules compared to animals pre-treated with saline only. No tumour was detectable in the mesentery or lung in either group (Table 5a). Organ weights showed significant increases in the liver, intestine, kidney and spleen of both saline treated and interleukin-1 treated animals compared to a group of non-treated control animals (Table 5b). Histomorphometric analysis showed a 28 fold increase in liver tumour burden and a significant increase in the amount of necrotic tissue present in animals pre-treated with interleukin-1 (Table 6). Weights were shown to be an imprecise method of quantisation in this experiment and this approach was discontinued. A second, identical experiment showed a 3.7 fold increase in the number of liver nodules present in mice pre-treated with interleukin-1 and a 15 fold increase in the percent area

occupied by tumour. A third repetition of the experiment, to ensure reproducibility, showed an increase of 2.5 fold in the number of liver tumour nodules and a 17.5 fold increase in the percent area occupied by tumour in animals pre-treated with interleukin-1 (Table 6). The cells for this experiment had been fluorescently labelled with 0.05 μm latex microbeads. No differences were apparent when compared to the previous experiments.

The growth of early metastasis was noted predominantly in the area of the portal triads with little growth seen in the mid-zonal or central vein region in either control animals or animals pre-treated with interleukin-1 (Figure 5). Thus, early tumours grew predominantly in a specific portion of the liver.

Table 3. Quantitation of tumour burden in C57bl/6 mice injected via a mesenteric vein with B16F1 melanoma cells.*

Number of Nodules

Organ	Control	$2x10^4$ cells	$3x10^5$ cells	$5x10^5$ cells
		21 days	14 days	14 days
	n=8	n=2	n=7	n=3
Liver	0	Confluent	37(2-66)	17-Confluent
Intestine	0	Confluent	6(1-38)	69-Confluent
Lung	0	84(0-168)	0	4(0-4)

Weight(grams)

Organ	Control	$2x10^4$ cells	$3x10^5$ cells	$5x10^5$ cells
		21 days	14 days	14 days
	n=8	n=2	n=7	n=3
Brain	0.42(.37-.47)	0.53 (n=1)	0.49(.39-.52)	0.42(.37-.51)
Spleen	0.07(.06-.11)	0.16(.13-.18)$^+$	0.10(.1-.12)$^+$	0.13(.12-.15)$^+$
Adrenals	0.005(.004-.01)	0.04(.01-.08)$^+$	0.01(.004-.02)$^+$	0.01(.004-.007)
Kidney	0.14(.12-.24)	0.14(.14-.18)	0.20(.17-.23)	0.17(.13-.21)
Intestine	2.6(2.2-5.3)	8.5(6-11)$^+$	3.8(3.6-4.5)$^+$	4.5(4.5-9.5)$^+$
Liver	1.2(1.1-2.2)	1.9(1.7-2.1)	2.2(2.0-3.2)	2.4(1.2-4.5)$^+$

A serum free cell suspension of B16F1 murine melanoma cells was injected into a mesenteric vein of female C57bl/6 mice at the indicated concentration and the animals euthanized at the indicated time points. Discrete tumour nodules were counted by visual inspection excluding areas of confluence. Control animals were not injected with cancer cells and represent standard weights of organs.

* values presented are median and (range)

$^+$ values are statistically significant ($p<.05$)

Table 4. Quantitation of tumour burden in C57bl/6 mice injected via a mesenteric vein with $3x10^5$ B16F1 melanoma cells.* - Effect of time after injection on numbers of metastases.

Number of Nodules

Organ	7 days n=8	14 days n=8	21 days n=7
Liver	21 (0-200)	81 (25-200)	>200 (24-200)
Intestine	0 (0-3)	21 (0-75)	>200 (70-200)
Lung	0	0	4 (0-53)

Weight

Organ	Control n=6	7 days n=8	14 days n=8	21 days n=7
Brain	0.41(.37-.50)	0.51+(.45-.55)	0.47(.42-.50)+	0.46(.39-.50)
Spleen	0.07(.06-.09)	0.08(.06-.11)	0.08(.06-.12)	0.09(.05-.14)
Adrenals	0.005(.004-.008)	0.005(.004-.01)	0.005(.003-.007)	0.005(.003-.006)
Kidney	0.13(.12-.15)	0.14(.11-.17)	0.16(.13-.18)+	0.15(.09-.19)
Intestine	2.5(2.2-2.7)	2.5(2.1-2.6)	2.6(2.3-3.1)	3.8(2.0-5.0)+
Liver	1.2(1.1-1.5)	1.3(1.1-1.6)	1.9(1.6-3.6)	3.4(1.9-5.5)+

A serum free cell suspension of $3x10^5$ B16F1 murine melanoma cells was injected into a mesenteric vein of female C57bl/6 mice with the animals being euthanized at the indicated time points Discrete tumour nodules were counted by visual inspection excluding areas of confluence. Control animals were not injected with cancer cells and represent standard weights of organs.

* values presented are median and (range)

+ values are statistically significant ($p<.05$)

Table 5a. Effect of interleukin-1 pre-treatment of the number of metastatic nodules in organs after mesenteric vein injection of $3x10^5$ B16F1 melanoma cells*.

	TREATMENT GROUPS	
	Control	Interleukin-1
Experiment 1 (n=12)		
Liver	19 (0-300)	129+ (22-300)
Intestine	0	0
Lung	0	0
Experiment 2 (n=14)		
Liver	43 (0-135)	159+ (68-292)
Intestine	0	0 (0-10)
Lung	0	0
Experiment 3 (n=13)‡		
Liver	48 (24-300)	122+ (68-292)
Intestine	0	0
Lungs	0	0

Female C57bl/6 mice were pre-treated for 4 hours prior to surgery with an intraperitoneal injection of 1.5 μg interleukin-1 α or an equal volume of saline. A serum free cell suspension of $3x10^5$ B16F1 murine melanoma cells in .1 ml was injected into a mesentery vein. Seven days later the animals were euthanized and the tumours quantitated by counting discrete nodules. The values presented do not include areas of confluence.

* values represent median(range)

+ values significantly different by Student's t-test ($p<.001$).

‡ B16F1 cells labelled with 0.05 μm latex beads.

Table 5b. Effect of interleukin-1 pre-treatment on organ weights after mesenteric vein injection of $3x10^5$ B16F1 melanoma cells.*

Organs	No Treatment n=9	Saline Treatment n=12	IL-1 Treated n=12
Brain	0.48 (.38-.52)	0.48 (.41-.51)	0.47 (.44-.50)
Spleen	0.07 (.06-.07)	0.09 (.07-.12)+	0.08 (.06-.10)+
Adrenals	0.005 (.004-.007)	0.005 (.003-.008)	0.005 (.003-.007)
Kidney	0.16 (.14-.19)	0.18 (.15-.21)+	0.18 (.15-.21)+
Liver	1.4 (1.2-1.7)	1.8 (1.3-1.9)+	1.8 (1.5-1.9)+
Intestines	2.8 (2.2-3.4)	3.7 (3.0-4.1)+	3.5 (2.9-4.5)+

Female C57bl/6 mice were pre-treated for 4 hours before surgery with an intraperitoneal injection of 1.5 μg interleukin-1 or an equal volume of saline. A serum free cell suspension of $3x10^5$ B16F1 cells in 0.1 ml was injected into a mesentery vein. The animals were euthanized 7 days later, the organs fixed in formalin, dissected apart and weighed. The "no treatment" animals were not injected and served to give standard weights of the various organs.

* values represent median (range)

+ values are statistically significant from no-treatment group ($p<.05$)

Table 6. Histomorphometric analysis of hepatic tumour burden in control and interleukin-1 treated mice.

	TREATMENT GROUPS	
	Control	Interleukin-1
Experiment 1 (n=12)		
% Normal	99.0 (82-100)	78.0 (60-92) +
% Tumour	0.8 (0-17)	21.0 (8-35) +
% Necrotic	0 (0-.02)	2.0 (.4-8) +
Experiment 2 (n=14)		
% Normal	100.0 (87-100)	93.0 (87-100) +
% Tumour	0.4 (0-12)	7.0 (0-13) +
% Necrotic	0 (0-.01)	0.1 (0-2) +
Experiment 3 (n=13)‡		
% Normal	99.0 (96-100)	88.0 (72-96) +
% Tumour	0.8 (0-4)	11.0 (4-25) +
% Necrotic	0 (0-.01)	2.0 (0-7) +

Female C57bl/6 mice were pre-treated four hours prior to surgery with an intraperitoneal injection of 1.5μg IL-1α or an equal volume of saline. A serum free cell suspension of $3x10^5$ B16F1 murine melanoma cells in 0.1 ml was injected into a mesentery vein. Seven days later the animals were euthanized and three sections of each liver were made, processed in paraffin, stained using haematoxylin and eosin and quantitated histomorphometrically using a Mertz graticule.

* values represent median(range)

+ values significantly different by Student's t-test ($p<.02$).

‡ B16F1 cells labelled with 0.05 μm latex microbeads.

Figure 5. The presence of tumour around the portal vein but not in central vein or mid zonal region. (magnification 400x)

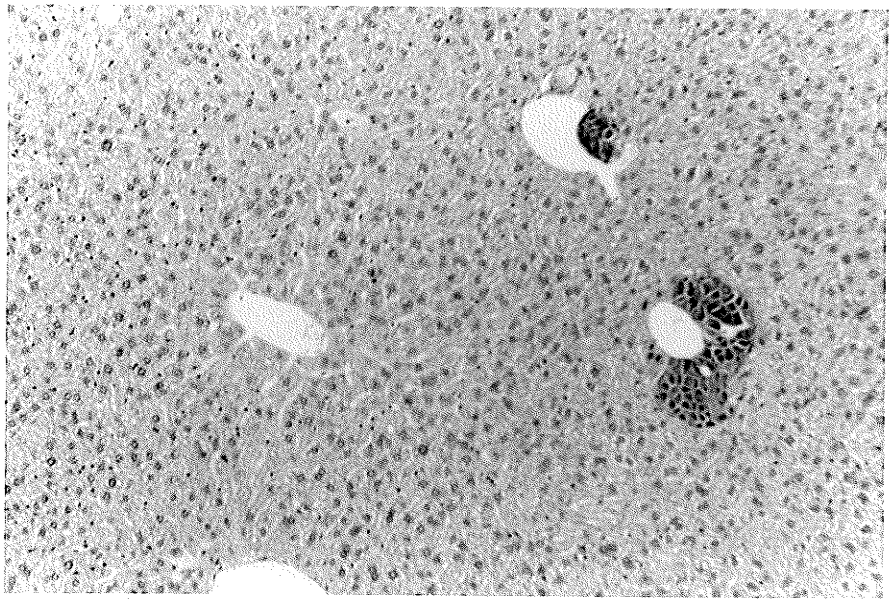

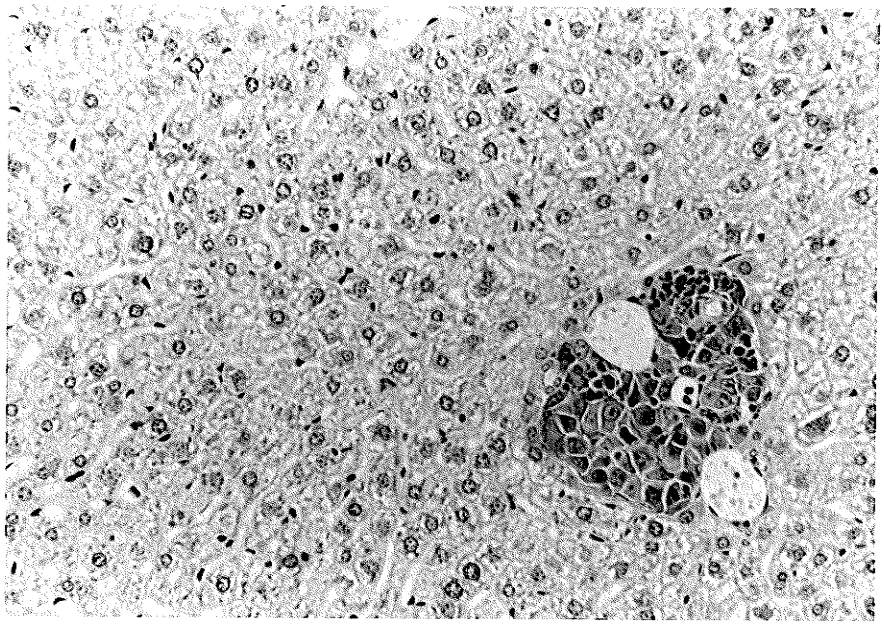

4.2 RADIOACTIVITY STUDY

4.2.1 Rationale

If the interleukin-1 dependent increase in metastasis observed in the experimental metastasis assay were due to changes in the adhesion molecules present on the hepatic endothelium, I predict that this might be reflected as a difference in the hepatic retention of radioactively labelled B16F1 cells at various times after their injection.

4.2.2 Retention of Radiolabelled B16F1 Cells in the Liver

To test if interleukin-1 treatment affected cell arrest a preliminary study determining the number of radio-labelled B16F1 cells retained in the livers of mice, after mesenteric vein injection, at various times was performed. This showed an approximate 2 fold increase in retention of radioactivity in animals pre-treated with interleukin-1 at 2 and 8 hours (Figure 6). There was no difference in the amount of radioactivity retained at 0 min or 24 h. The only organs showing appreciable levels of radioactivity were the liver and the intestines (Table 7). This data represents 4 animals per group and is not statistically significant at any point.

A second study was carried out using 10 animals per group and showed a more defined trend. There was a 2 fold increase in retention of radioactivity in the livers of interleukin-1 pre-treated animals killed immediately after injection. There was also an increase in the number of cells found in the lungs and kidneys of interleukin-1 treated animals at this time point. There was no

difference in the values at 2 h but at 8 h an 3 fold increase was observed and at 24 hours there a 7 fold increase of the number of cells retained in the livers of interleukin-1 pre-treated mice compared to controls. Figure 7 shows that both control and interleukin-1 pre-treated groups lost at least half of the cells originally observed at the 0 time point by 2 h. The control curve continued to decrease steadily until reaching approximately 1.5% of the original number of cells injected. The interleukin-1 curve appeared to stabilize, instead of decreasing steadily, and at 24 h 10% of the original number of injected cells remained in the livers. The number of cells associated with the other organs remained relatively constant throughout the 24 hour period with no notable differences between control and interleukin-1 except (Table 8).

FIGURE 6. Retention of [^{125}I]-UdR labelled B16F1 cells in the livers of mice pre-treated with 1.5 μg interleukin-1α (-○-) or saline (-●-) 4 h before mesenteric vein injection of $3x10^5$ cells. (n = 4) [Experiment 1]

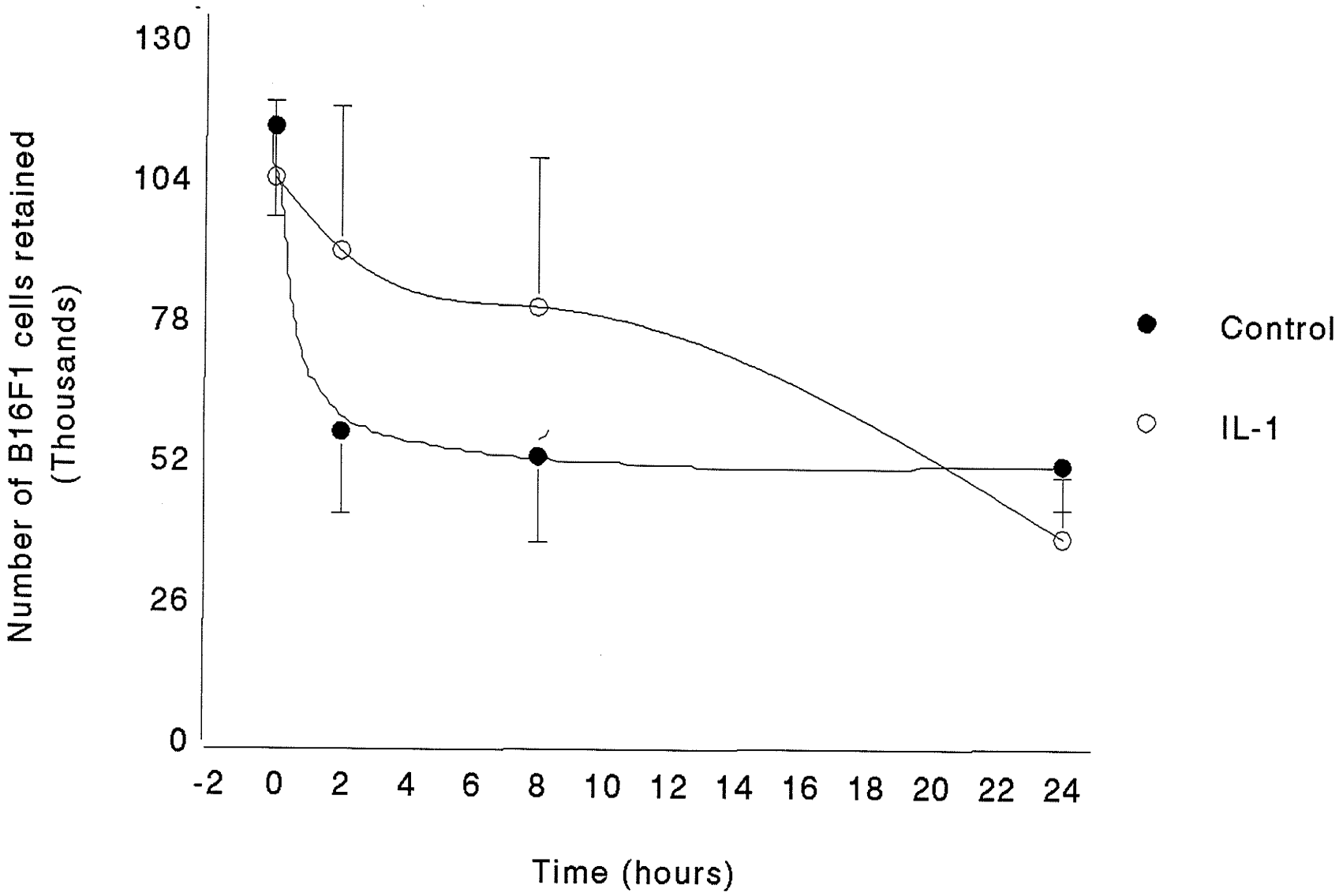
Number of B16F1 cells retained
(Thousands)
130
104
78
52
26
0
-2
0
2
4
6
8
10
12
14
16
18
20
22
24
Time (hours)
Control
IL-1

Table 7. Counts per minute associated with organs of C57bl/6 mice after mesenteric vein injection of $3x10^5$ B16F1 cells. * (Experiment 1)

		BRAIN	LUNGS	SPLEEN	KIDNEYS	ADRENALS	LIVER	INTESTINES	OVARY
T=0	C	16 (10-28)	64 (3-83)	14 (1-16)	12 (4-30)	6 (0 -16)	10370 (7102-15375)	339 (150-625)	30 (10-46)
	IL-1	23 (5-30)	45 (20-175)	11 (5-28)	19 (15-27)	10 (2-15)	9384 (7542 -9720)	126 (36-311)	30 (22-39)
T=2 hrs	C	11 (7-24)	12 (6-18)	17 (5-23)	18 (10-25)	10 (6-13)	4515 (2012-10096)	241 (225-678)	23 (5-65)
	IL-1	24 (8-24)	26 (9-46)	14 (0-18)	20 (7-27)	4 (0-12)	10052 (3106-15805)	218 (89-304)	24 (14-45)
T=8 hrs	C	8 (4-12)	12 (2-23)	9 (5-20)	10 (4-25)	7 (0-20)	2987 (975-8669)	156(50-399)	13 (10-28)
	IL-1	22 (5-26)	12 (5-18)	9 (1-11)	19 (14-32)	9 (3-18)	6508 (1171-13135)	367 (253-649)	18 (10-26)
T=24 hrs	C	8 (4-11)	23 (0-44)	13 (10-33)	22 (10-25)	6 (0-9)	3953 (3397-5961)	382 (162-1051)	16 (0-35)
	IL-1	10 (0-29)	11 (9-26)	7 (4-15)	11 (3-23)	4 (0-16)	2610 (680-5391)	376 (101-413)	10 (8-31)

$3x10^5$ [^{125}I]-UdR labelled B16F1 melanoma cells were injected into a mesenteric vein of C57bl/6 mice. The organs were harvested fixed in 10% neutral buffered formalin and the counts per minute for each organ determined using a gamma counter.

* Values represent median (range)

No values are statistically significant by Mann Whitney U-test.

FIGURE 7. Retention of [^{125}I]-UdR labelled B16F1 cells in the livers of mice pre-treated with 1.5 μg interleukin-1α (-○-) or saline (-●-) 4 h before mesenteric vein injection of $3x10^5$ cells. (n = 10) [Experiment 2]

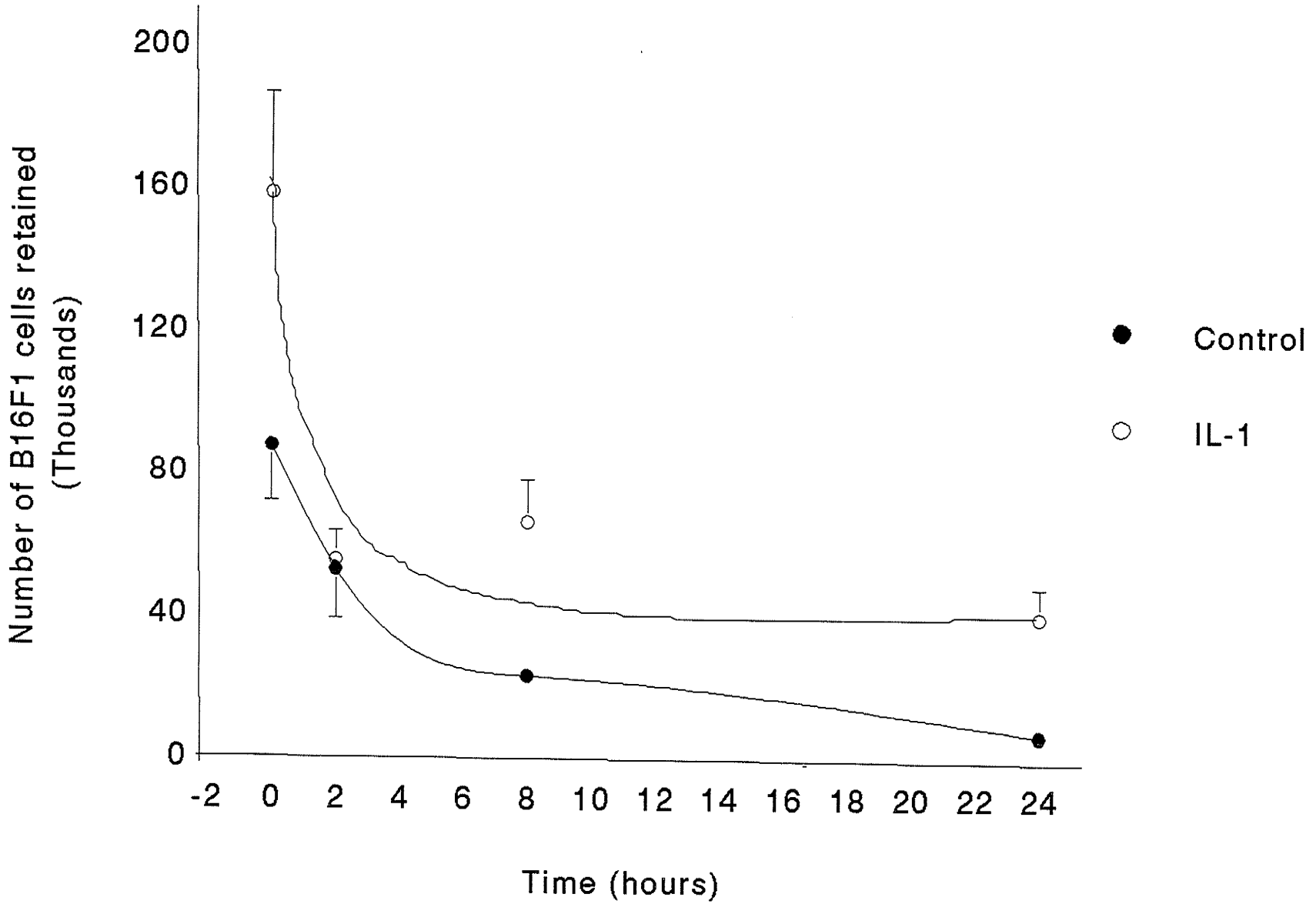
Number of B16F1 cells retained
(Thousands)
200
160
120
80
40
0
-2
0
2
4
6
8
10
12
14
16
18
20
22
24
Time (hours)
Control
IL-1

Table 8. Number of [^{125}I]-UdR labelled cells associated with organs of C57bl/6 mice after injection of $3x10^5$ cells via a mesenteric vein. * (Experiment 2)

		LUNGS	SPLEEN	KIDNEY	MESENTERY	LIVER
T=0h	C	323 (0-1032)	87 (0-440)	118 (0-548)	840 (300-2512)	75656 (33623-146333)
	IL-1	1032 (210-1668) +	192 (0-491)	327 (131-671) +	1602 (284-4697)	149308 (49529-277944) +
T=2h	C	295 (67-816)	192 (87-397)	467 (114-856)	2801 (878-5747)	34471 (2278-145151)
	IL-1	408 (90-848)	192 (0-888)	312 (70-720)	1507 (744-3383)	39503 (21490-115679)
T=8h	C	189 (0-438)	131 (0-340)	212 (45-493)	1463 (1255-2718)	21611 (15207-28093)
	IL-1	203 (0-732)	90 (0-746)	376 (90-793)	2266 (1477-4240)	68083 (14904-107604) +
T=24h	C	236 (30-377)	150 (0-732)	113 (0-344)	1476 (712-3280)	4399 (960-9309)
	IL-1	186 (0-411)	177 (0-315)	216 (0-659)	1911 (961-3562)	28766 (9389-84721) +

$3x10^5$ [^{125}I]-UdR labelled B16F1 melanoma cells were injected into a mesenteric vein of C57bl/6 mice. The organs were harvested fixed in 10% neutral buffered formalin, the counts per minute for each organ determined using a gamma counter and the number of cells calculated from the cpms divided by the total counts injected.

* Values represent median (range)

+ values are statistically significant by Mann Whitney U-test. ($p<0.05$)

4.3 INTRAVITAL MICROSCOPY

4.3.1 Rationale

The injection of radiolabelled cells demonstrated that twice as many cells were retained immediately after injection in the livers of animals pre-treated with interleukin-1. The technique of intravital microscopy would allow the observation of the cancer cell interactions with the hepatic microvasculature, in animals pre-treated with interleukin-1 and in controls, in real time. This would eliminate the "black box" effect of the metastasis assays and could allow us to better define the steps of cancer cell arrest and the immediate interactions between the cancer cells and the vasculature as the occur. Thus, intravital microscopy was used to elucidate the characteristics of the immediate differences in retention of cancer cells observed in the radioactivity study.

4.3.2 Cancer Cell Labelling

To provide an internal control the size distribution of B16F1 cells was determined (Figure 8). The median size of B16F1 cells, as measured using an ocular micrometer, proved to be 16 μm in diameter but the size ranged from 8-28 μm.

Before cancer cells could be injected, an appropriate fluorescent labelling technique providing high viability and a high specific fluorescent labelling was needed. Three fluorescent labels were examined, calcein AM (Morris *et al.*, 1993), fluorescently labelled latex microbeads (Morris *et al.*, 1994), and

fluorescein isothiocyanate (Butcher *et al.*, 1980; Butcher and Weissman, 1980). Two concentrations of microbeads and 2 labelling durations were used to assess appropriate labelling conditions. The viability of the labelled cells was assessed following three different treatments; after being resuspended using a pipette, after being passaged through a 20 gauge needle and after being passed through a 30 gauge canula. Table 9 shows that the only significant decrease in labelled cell viability compared to control was labelling with 75 μl of beads for 30 minutes. From this data 75 μl of beads incubated on the monolayer for 1 h was chosen as the optimal condition. It was found using these conditions that B16F1 cells would not detach from the flask after incubation with 5 mM EGTA for up to 1 hour. To explore ways to detach the cells without compromising their viability the labelled monolayers were incubated in media containing 10% fetal calf serum for 4 h or media containing 1% fetal calf serum overnight and detached as described in section 3.2.3. It was found that either treatment allowed the detachment of the cells without changing the viability of cells compared to control monolayers. To determine where the microbeads were localized in the cells, electron microscopy was done. Immediately after labelling the beads seemed to be within vacuoles present in the cytoplasm of the B16F1 cells (Figure 9). The protocol for calcein AM labelling was obtained from Dr. Alan Groom at the University of Western Ontario and carried out as stated in the methods. A panel of concentrations and time points was

investigated for labelling with fluorescein isothiocyanate. All labelling techniques were then compared in one experiment for the percent viability and the percent of viable fluorescently labelled cells (Table 10). From this data it was determined that calcein AM gave the highest viability and the best fluorescent labelling. This fluorescent label was subsequently used throughout the intravital microscope experiments.

4.3.3 Cancer Cell Interactions with the Microvasculature

By analyzing the anatomical sites of cancer cell arrest in both saline control animals and interleukin-1 pre-treated animals it was discovered that the cells injected into saline control animals arrested in vessels of a significantly smaller size than did the cells injected into interleukin-1 pre-treated animals. The median size of vessels in which cells injected into control animals arrested in was 16 μm (9-23 μm) compared to 34 μm (27-51 μm) in animals pre-treated with interleukin-1. An extension of this data showed that, in animals pre-treated with interleukin-1, cells do not enter the sinusoids 0 μm (0-18 μm) whereas cells injected into saline control animals travelled a median distance of 32 μm (0-74μm) into the sinusoids (Table 11 Figure 10 and 11). It was also observed that treatment with interleukin-1 decreased the entry velocities of the cells as well and a lower maximum velocity in comparison to saline treated control animals (Figure 12 and 13).

To assess the hepatic venous flow rates between saline treated and

interleukin-1 treated animals, the velocities of both red blood cells and injected 6 μm fluorescent latex microbeads were assessed. The velocities of red blood cells in saline treated control animals was 1.2 fold higher than the velocities seen in interleukin-1 treated animals. These results were not statistically significant. The velocity of latex microbeads in saline treated animals was 341 $\pm$ 13 μm/s compared to 214 $\pm$ 11 μm/s for IL-1 treated animals. This data showed a significant difference in the hepatic venous flow rate between interleukin-1 treated and control animals.

Figure 8. Size distribution of B16F1 cells measured using an ocular micrometer. (n = 300)

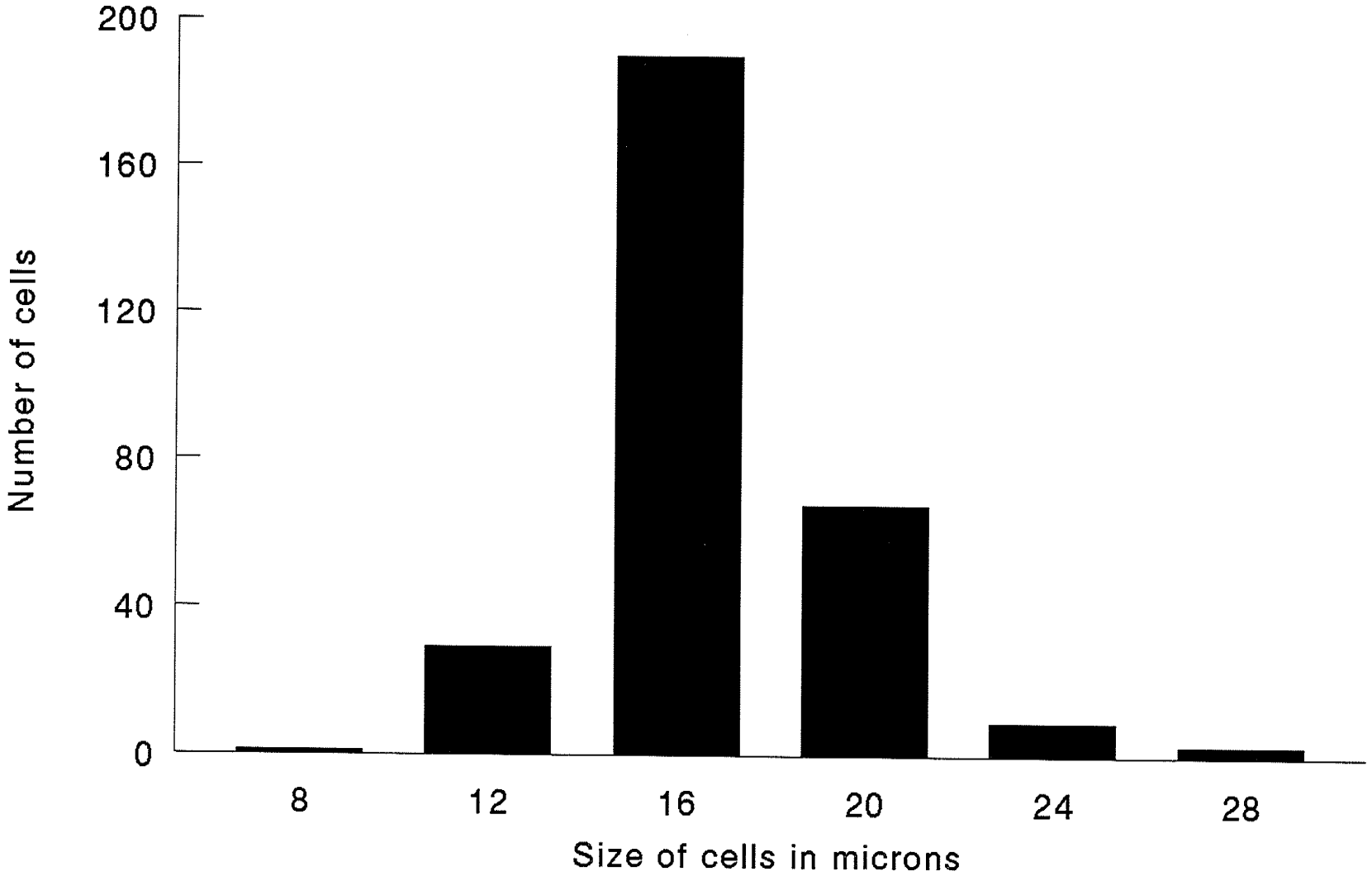
200
160
120
80
40
0
Number of cells
8
12
16
20
24
28
Size of cells in microns

Table 9. Comparison of the percent viability of B16F1 melanoma cells following different microbead labelling protocols.*

	Pipette	20 gauge needle	30 gauge canula
Control	96 ± 2.5	91 ± 4.8	96 ± 2.9
75μl:30min	82 ± 2.2[+]	85 ± 3.1	81 ± 14.6
150μl:30min	91 ± 5.3	85 ± 8.6	86 ± 5.1
75μl:60min	89 ± 9.1	85 ± 6.1	90 ± 3.6
150μl:60min	88 ± 9.1	89 ± 7.0	82 ± 10.7

The viability of B16F1 cells was determined by trypan blue exclusion after labelling with different concentrations of microbeads and treated as though they would be injected into animals. This would simulate the harvesting and resuspending protocol, the creation of a single cell suspension and the injection through the canula into the mouse.

[+] Values are significantly different from controls ($p < 0.05$)

* all values are mean ± S.D. and each condition was done in quadruplicate.

FIGURE 9. Electron micrograph showing location of fluorescent latex microbeads in B16F1 cells. (magnification 3000 x)

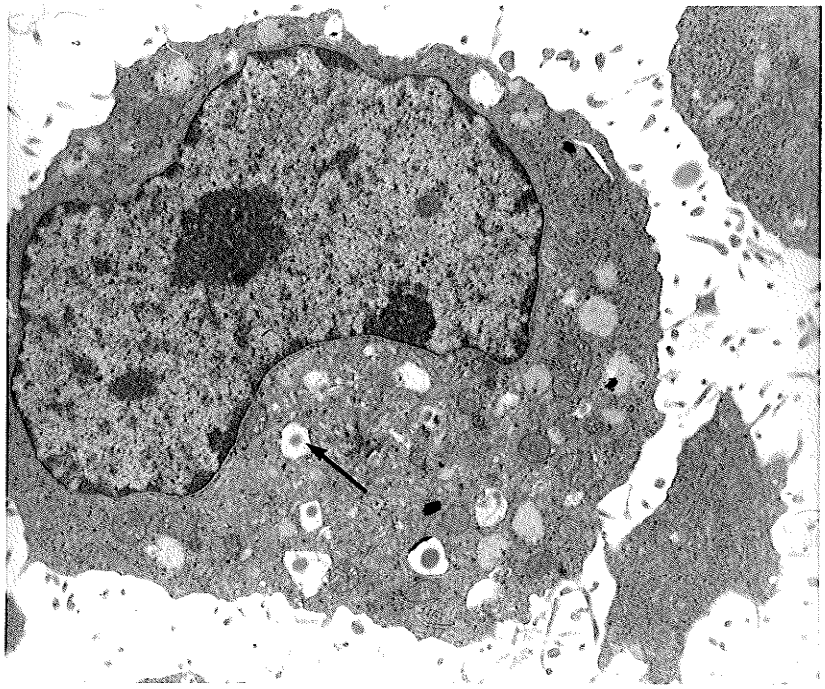

Table 10. Summary of % viability and % fluorescence of viable B16F1 cells using the labelling techniques of Calcein AM, latex microbeads and FITC.

LABELLING CONDITIONS	VIABILITY			% FLUORESCENCE		
	After harvesting	after 20 g needle	after 30g canula	after harvesting	after 20 g needle	after 30g canula
	Mean (S.D.)	Mean (S.D.)	Mean S.D.)	Mean (S.D.)	Mean (S.D.)	Mean (S.D.)
CALCEIN AM	94 (2.1)	92 (1.7)	93 (1.5)	98 (1.5)	99 (.96)	98 (1.2)
LATEX MICROBEADS	82 (.82)	77 (3.5)	79 (13.5)	60 (3.7)	57 (3.2)	57 (9.0)
FITC						
140mg/ml 20 min.	69 (6.0)	69 (5.6)	61 (3.6)	53 (5.3)	80 (11.0)	65 (8.1)
70mg/ml 20 min.	79 (4.9)	76 (2.5)	72 (2.1)	100 (0)	97 (2.1)	99 (0)
35 mg/ml 20 min.	80 (1.0)	77 (1.0)	81 (2.7)	98 (1.0)	98 (1.0)	98 (1.0)
70 mg/ml 15 min	84 (4.4)	87 (5.1)	84 (2.1)	99 (1.2)	97 (1.2)	99 (.6)
70 mg/ml 10min.	83 (2.1)	85 (2.7)	83 (3.0)	97 (2.1)	98 (.6)	97 (1.5)

B16F1 cells were fluorescently labelled and harvested according to the protocol in sections 3.2.3 and 3.3. The viability was assessed by trypan blue exclusion. Each number was obtained from three repeats of each condition. No values were significantly different by Student's t-test.

Table 11. Intravital microscopic evaluation of the arrest patterns of fluorescently labelled B16F1 cells in the hepatic microvasculature. *

	n	Size of Vessel	Distance into sinusoids
Control	10	16 (9-23)	32 (0-74)
Interleukin-1	9	34 (26 -51)$^{+}$	0 (0-18)$^{+}$

Female C57bl/6 mice were pre-treated 4 h before surgery with either 1.5μg IL-1 or saline intraperitoneally. The mice were prepared for microscopy and B16F1 cells ($1x10^6$ cells in 0.1ml) were injected until cells were viewed in the microvascular bed imaged on the monitor. The vasculature and arrested cells was traced from the image on the monitor. From these, the size of the vessels in which the cells arrested in and the distance they travelled into the sinusoids were determined.

n represents the number of animals

$^{+}$ values are statistically different from control by Mann-Whitney U-test ($p<.005$)

FIGURE 10. Digitized images of control hepatic microvasculature before and after injection of calcein AM labelled B16F1 cells via a mesenteric vein.

p.t.c = portal tract capillary

CONTROL

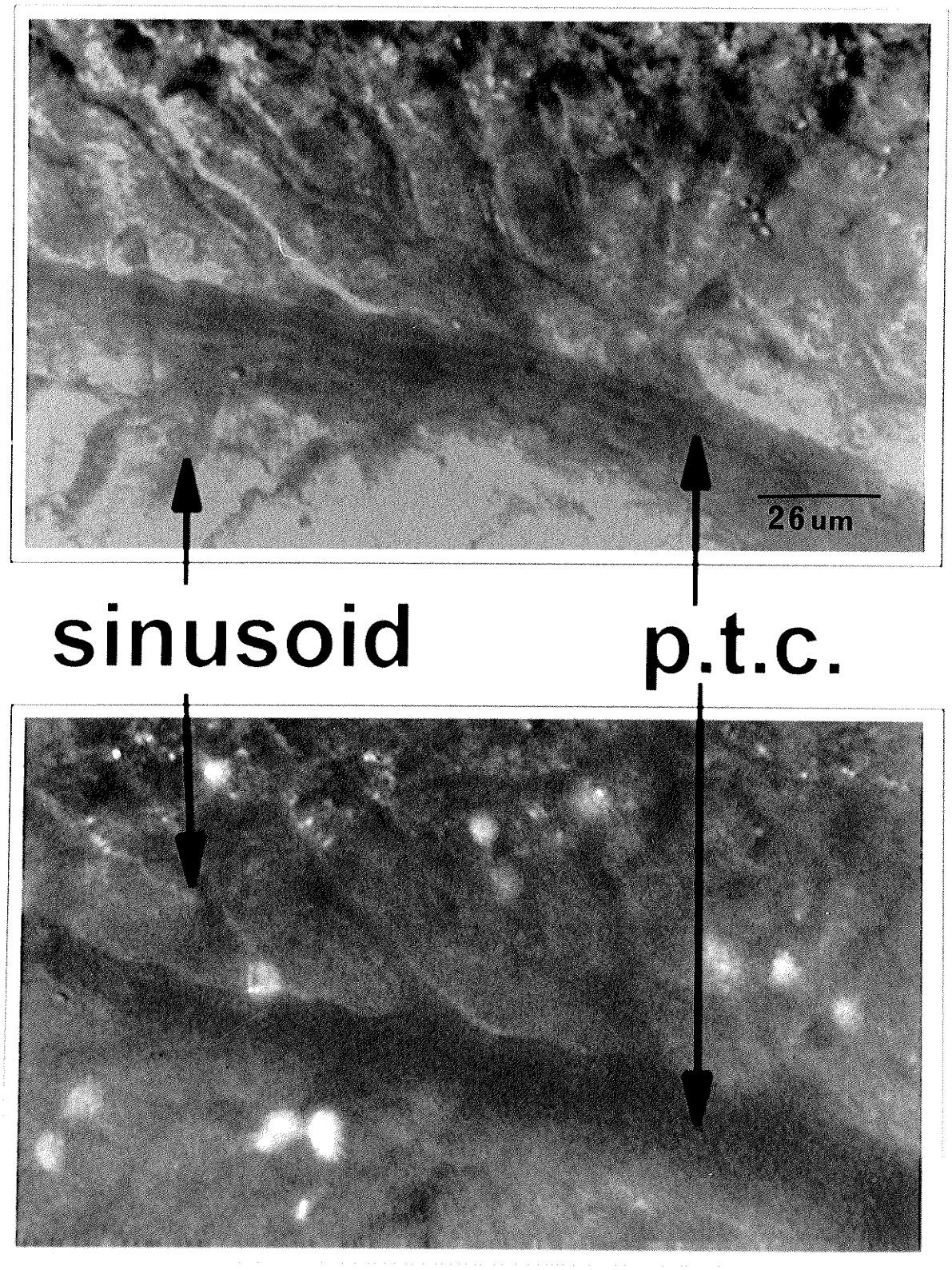

FIGURE 11. Digitized image of interleukin-1 pre-treated hepatic microvasculature before and after injection of calcein AM labelled B16F1 cells via a mesenteric vein.

p.t.c = portal tract capillary

INTERLEUKIN-1

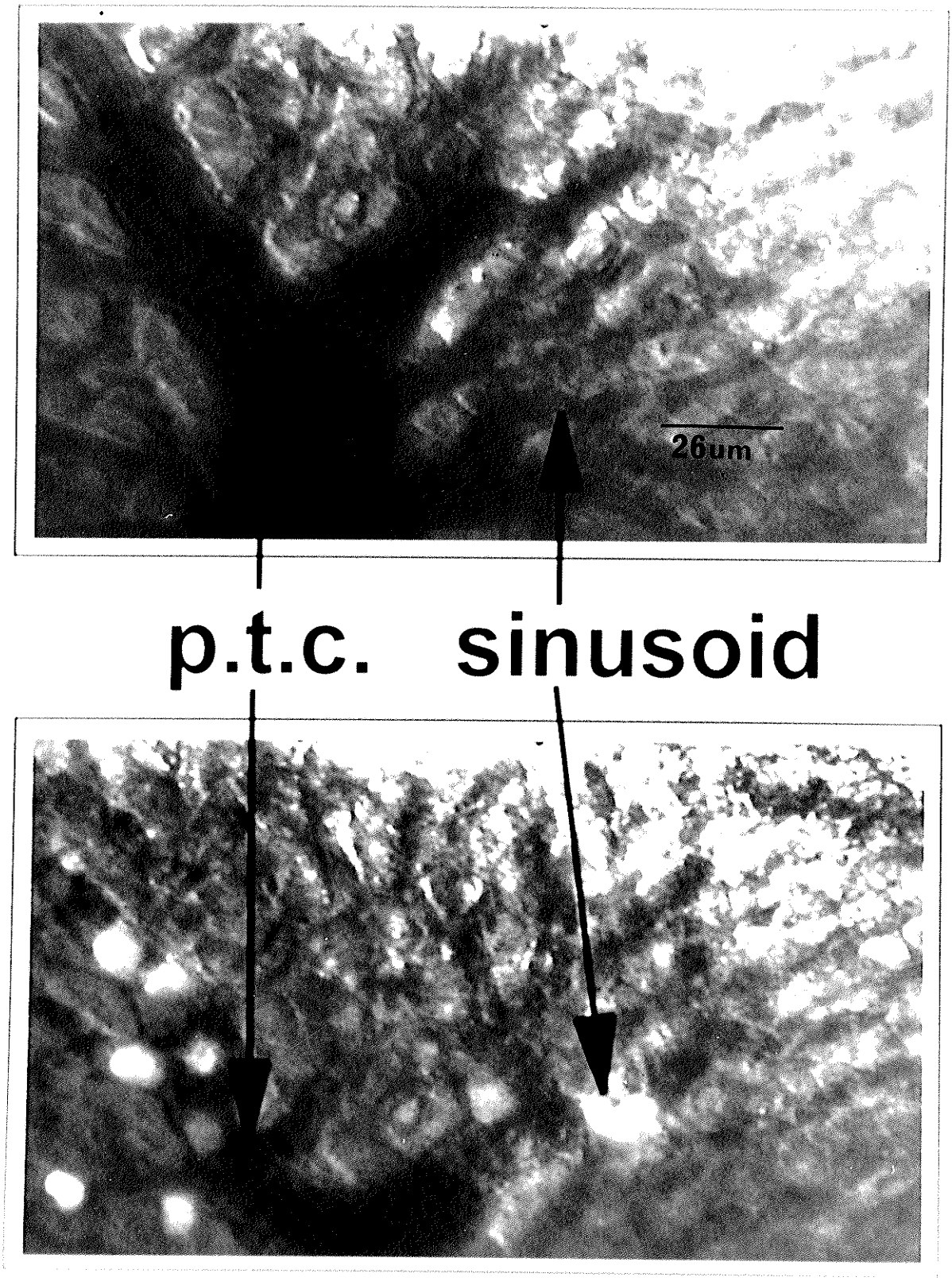

FIGURE 12. Quantisation of B16F1 cell interactions with the hepatic vasculature comparing velocity versus distance in control (-■-) and interleukin-1 pre-treated animals (-●-). Velocities were determined by frame by frame measurements of the distance cells travelled divided by the elapsed time. Distances were determined by making direct measurements from the image. (n/IL-1 group = 70 cells from 9 independent animals) (n/control group = 50 cells from 10 independent animals).

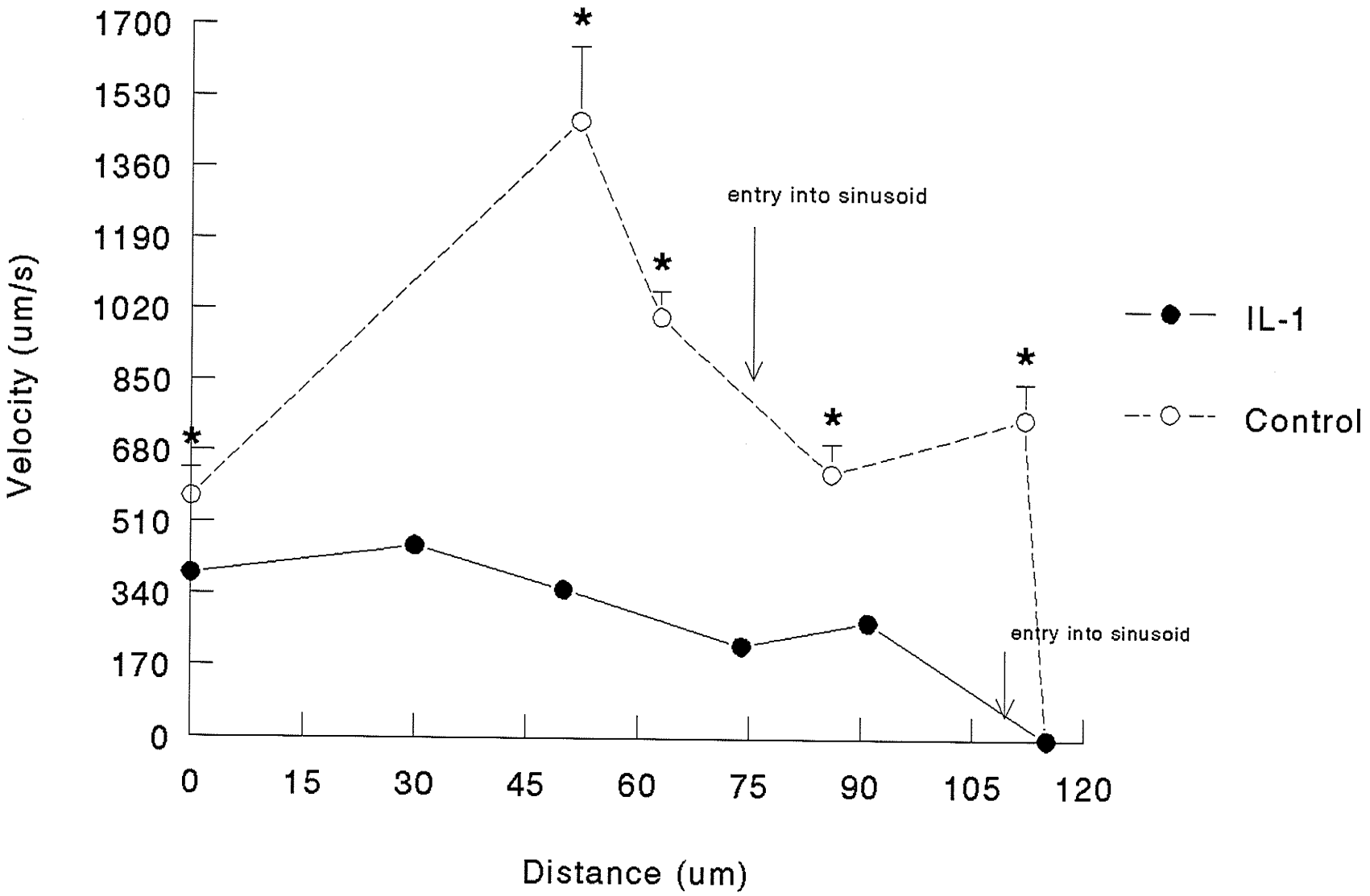
1700
1530
1360
1190
1020
850
680
510
340
170
0
Velocity (um/s)
0
15
30
45
60
75
90
105
120
Distance (um)
entry into sinusoid
entry into sinusoid
IL-1
Control
*
*
*
*
*

FIGURE 13. Quantisation of B16F1 cell interactions with the hepatic vasculature comparing velocity versus time in control (-■-) and interleukin-1 pre-treated animals (-●-). Velocities were determined by frame by frame measurements of distance cells travelled divided by the elapsed time. Distances were determined by making direct measurements from the image. (n/IL-1 group = 70 cells from 9 independent animals)

(n/control group = 50 cells from 10 independent animals)

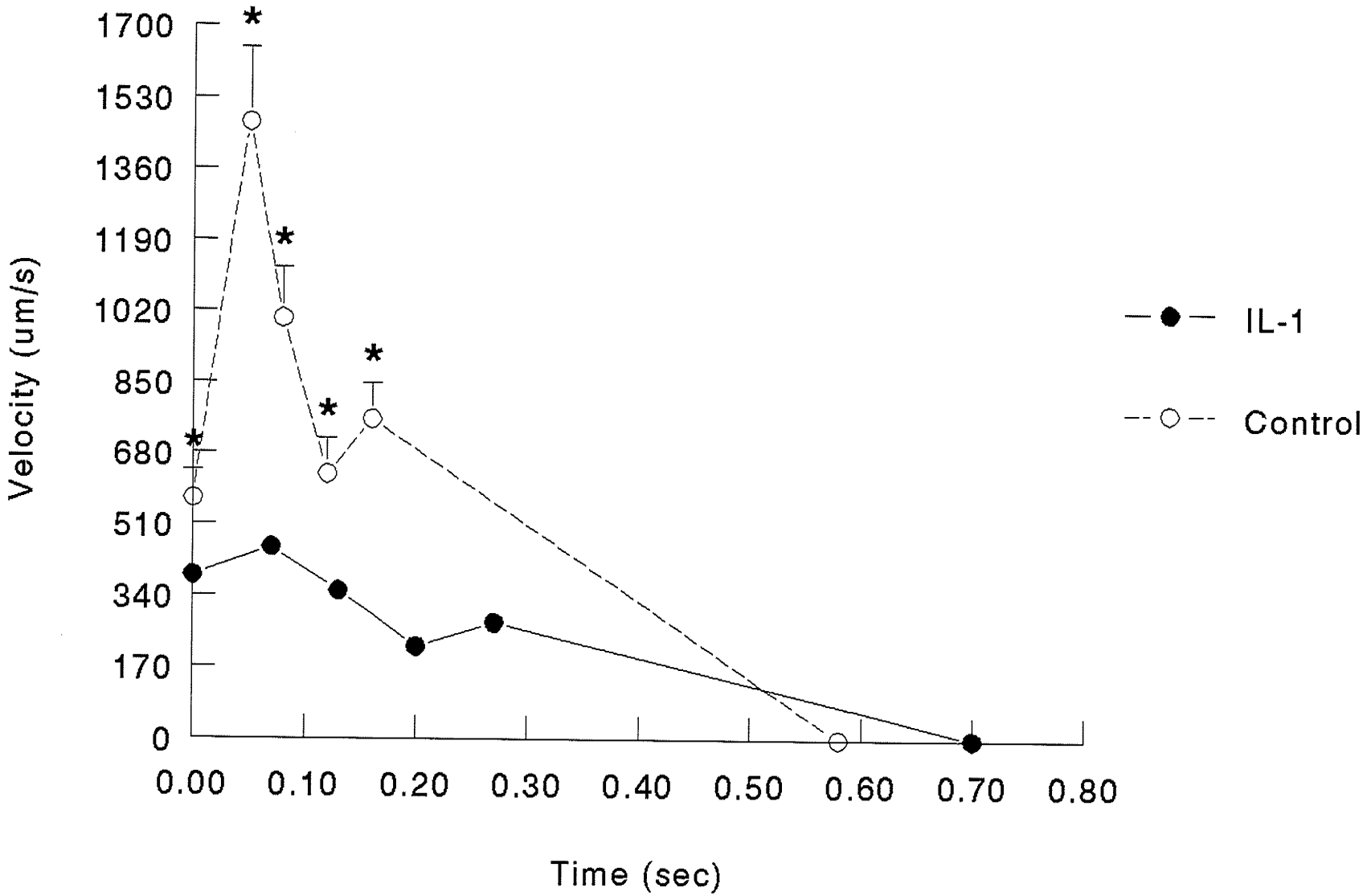
1700
1530
1360
1190
1020
850
680
510
340
170
0
Velocity (um/s)
0.00
0.10
0.20
0.30
0.40
0.50
0.60
0.70
0.80
Time (sec)
IL-1
Control

4.4 CANCER CELL ADHESION TO FROZEN LIVER SECTIONS

4.4.1 Rationale

The data presented thus far indicates, in an indirect fashion, a possible role for cancer cell adhesion in metastasis. To investigate this more directly an *in vitro* frozen section assay was developed. This system was modeled after the Stamper-Woodruff assay developed to investigate the role of adhesion molecules on high endothelial venules in relation of lymphocyte homing.

4.4.2 *In vitro* Cancer Cell/Liver Adhesion Model

The design of the frozen section adhesion assay was to mount 5 μm frozen sections of livers, from mice that had been pre-treated with either saline or interleukin-1 for 4 h, onto Thermanox™ discs which were placed into 24 well plates. B16F1 cells were added to the sections and incubated for a period of time to allow firm adhesion to occur. Then non-adherent cells were removed, the discs stained, the number of cells adhered to various anatomical locations on the liver assessed, by microscopic examination and trends compared.

To determine the appropriate number of cells to be added to the sections, a panel of cell numbers, ($2.5x10^4$, $5x10^4$, $1x10^5$ and $5x10^5$ cells) were added to untreated sections and allowed to incubate for 30 minutes (Figure 14). The goal was to have some cells adhered to control sections but not to non-specifically saturate the section to permit a postulated increase in specifically adherent cells to sections isolated from interleukin-1 pre-treated animals. From this experiment a dose of $5x10^4$ cells per section was chosen. This resulted in

a small number of adherent cells to each control section and accommodated a proposed increase in cancer cell adhesion that would be easily quantitatable.

To ensure that the chosen time point was long enough to allow firm adhesion to take place but not to long to saturate the section, permitting the proposed increase due to IL-1, a time course was done. The optimal time was determined by incubating $5x10^5$ cells per section for time periods of between 5 min to 2 h. The curve showed a large increase in the number of cells adhered to an unstimulated section between 15 and 30 min of incubation with the numbers reaching a plateau at 30 minutes. Therefore a 15 minute time point was chosen for experimentation (Figure 15).

4.4.3 Modulation of Adhesion Following Interleukin-1

To determine if there was an up-regulation of hepatic adhesion molecules following intraperitoneal pre-treatment of mice with interleukin-1 which mediated an increased adhesion of cancer cells to the liver, mice were treated by intraperitoneal injection with 1, 1.5, or 2 μg interleukin-1. Four hours later frozen sections of livers from these mice were cut and the adhesion assay, using B16F1 cells, carried out as previously described. The initial experiment showed a dose dependent increase in the total number of cells adhered per high power field on interleukin-1 treated sections. A dose of 1 μg interleukin-1 resulted in a 2.7 fold increase in the number of adhered cells, an increase of 3.7 fold was observed when the mice were pre-treated with 1.5 μg interleukin-1 but there was no increase in adhered cells over control when the mice were pre-

treated with 2 μg interleukin-1 (Table 12; expt 1). To assess the distribution of cancer cells on various areas of the section a classification scheme was designed to categorize the cells as adhered to hepatocytes, sinusoids, or to the walls of large vessels. When adherent cells were classified into these categories, the same trends were seen for adhesion to hepatocytes and to sinusoids as was seen for the total number of cells. Using this classification system, there was an increase in the number of cancer cells adhered to hepatocytes and to sinusoids in the 1 and 1.5 μg of interleukin-1 pre-treated animals and an increase in the number of cells adhered to large vessels in the 1.5 and 2 μg of interleukin-1 pre-treated animals (Table 12; expt 1) . A repeat of this experiment showed a significant increases in cell adhesion in all treatment groups and to all section classifications with the 1.5 μg interleukin-1 pre-treated group showing the largest increases (Table 12 expt 2). The third repetition of this experiment, illustrating reproducibility, showed the same trends, with the 1.5 μg dose of interleukin-1 eliciting the greatest increase in cancer cell adhesion in all categories (Table 12; expt 3).

4.4.4 Modulation of Cancer Cell Adhesion using RGD Peptides

To determine if the increase in adhesion observed following pre-treatment of the mice with 1.5 μg of interleukin-1 could be blocked by peptides that compete for integrin binding sites, adhesion assays were done in the presence of GRGDS peptides. These experiments showed a significant decrease in the adhesion of B16F1 cells to liver sections from interleukin-1 pre-treated mice

when the sections were treated with 50 or 100 μM concentrations of GRGDS peptides 30 seconds before the cells were introduced. Three of four experiments showed inhibition of adhesion in all compartments to the same level as to control sections or lower (Table 13). The first experiment showed a reduction of approximately 68% in both the 50 and 100 μM GRGDS treatment groups. All groups were reduced to their lowest levels at a concentration of 50 μM of GRGDS peptide with no further reduction at 100 μM.

To ensure that the reduction in adhesion was due to the blocking of integrin sites and not a non-specific effect of the peptide concentration, the experiment was reproduced using the GRGES peptide which does not block cancer cell adhesion (Humphries *et al.*, 1988). At a concentration of 50 μM the GRGES peptide did not reduce the elevated adhesion produced by the effects of interleukin-1. This was observed for all compartments of the liver. A concentration of 100 μM GRGES peptides significantly reduced the total number of cells adhered per high power field in comparison to interleukin-1 treatment but the value remained significantly above control levels. Similar results for the number of cells adhered to sinusoids were also seen. The number of cells adhered to hepatocytes returned to control levels in response to 100 μM GRGES treatment (Table 14; expt 3). In experiment 2 the total number of cells per high power field, was closer to interleukin-1 values than to control in response to 100 μM GRGES treatment (Table 14). This was also true for the sinusoids and large vessels, with the hepatocyte values falling directly between

the interleukin-1 and control values. A similar trend was noticed in Table 14 experiment 1 with values being reduced to control levels. Although the experiments were not perfectly reproducible, the trend that appeared was that 50 μM concentrations of GRGES peptide inhibited adhesion slightly or not at all when compared to the interleukin-1 treated group. Treatment with 100 μM peptide resulted in a further decrease in adhesion which may or may not have inhibited adhesion to control levels.

FIGURE 14. Effects of cell number on the attachment of B16F1 melanoma cells to frozen section of murine liver. Four aliquots of B16F1 cells were added to control liver sections mounted on Thermanox™ discs and allowed to incubate for 30 minutes. Non-adherent cells were removed by washing, stained using H&E, and examined microscopically to determine the number of cells adhered per high power field.

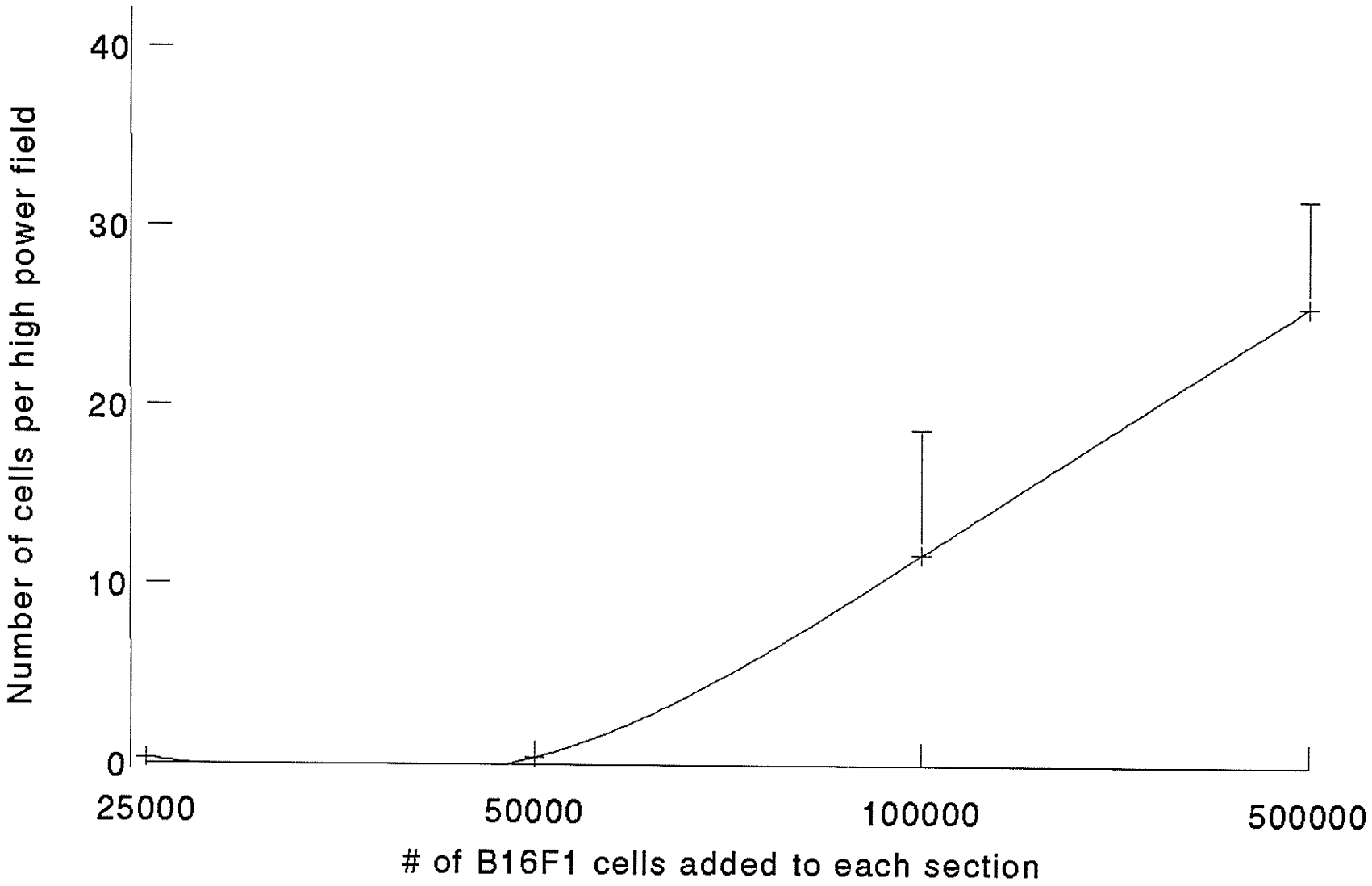
40
30
20
10
0
Number of cells per high power field
25000
50000
100000
500000
# of B16F1 cells added to each section

FIGURE 15. Effect of incubation time on B16F1 cell attachment to frozen sections of murine liver. $5x10^4$ cells were incubated on control liver sections mounted on Thermanox™ discs for varying periods of time. Non-adherent cells were removed by washing, the sections were stained with Haematoxylin and Eosin and the number of cells present per high power field was determined microscopically. (n = 6)

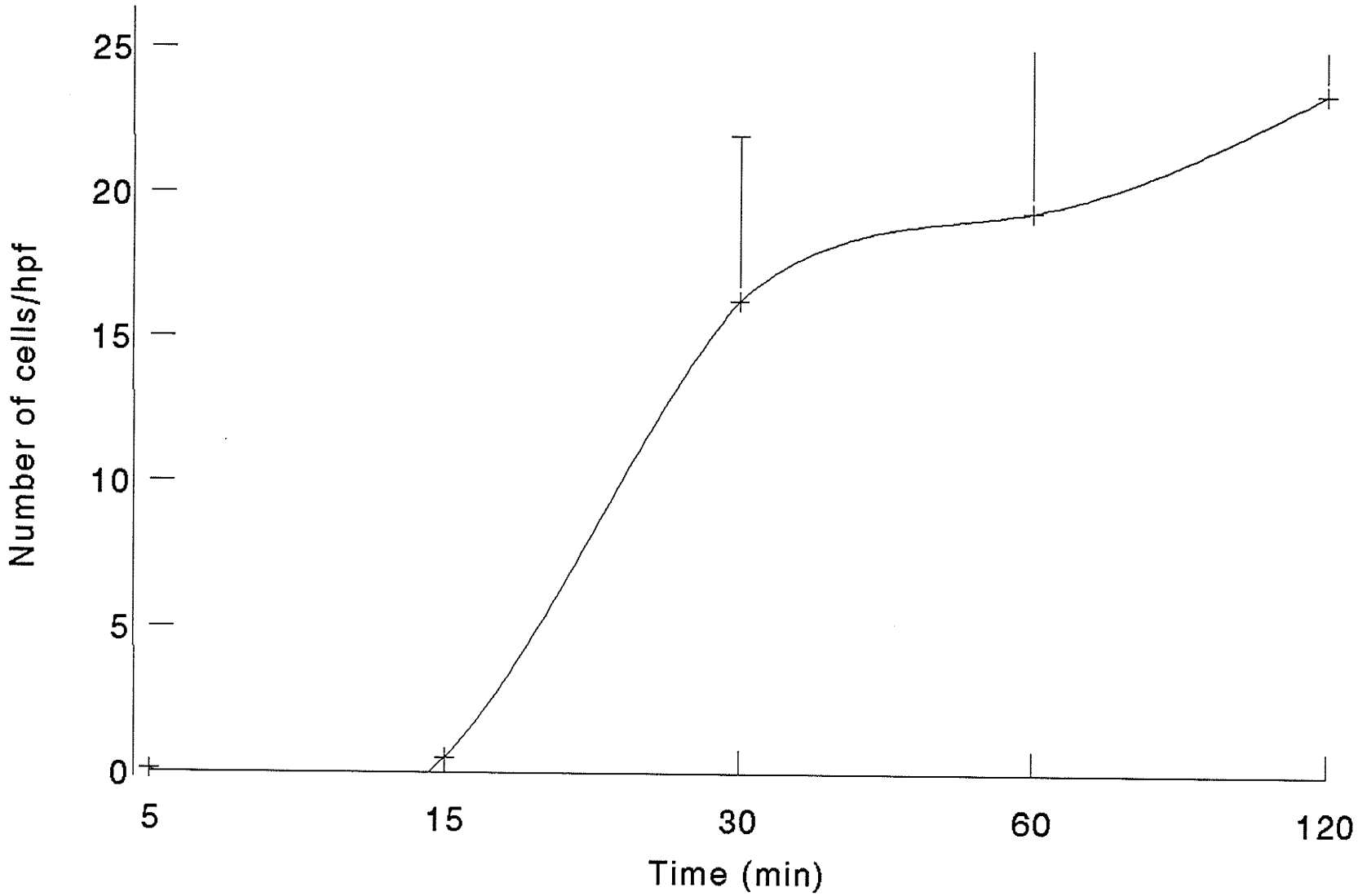
Number of cells/hpf
25
20
15
10
5
0
5
15
30
60
120
Time (min)

Table 12. Distribution of B16F1 melanoma cells on frozen liver sections from control or interleukin-1α treated C57bl/6 mice.*

	TREATMENT GROUPS			
	Control	IL-1 1 μg	IL-1 1.5 μg	IL-1 2 μg
Experiment #1				
Total cells/hpf	10.0±4	27.0±10$^{+\ddagger}$	37.0±10$^{+\ddagger}$	19.0±14
cells on hepatocytes/hpf	6.0±2	17.0±6$^{+\ddagger}$	23.0±7$^{+\ddagger}$	12.0±8
cells on sinusoids/hpf	3.0±2	9.0±4^{+}	12.0±3$^{+\ddagger}$	7.0±5
cells on large vessels/hpf	0.2±.1	0.8±.7	0.4±.6$^{+\ddagger}$	0.8±.4^{+}
Experiment #2				
Total cells/hpf	8.0±4	20.0±7$^{+\ddagger}$	30.0±5$^{+\ddagger}$	24.0±7$^{+\ddagger}$
cells on hepatocytes/hpf	7.0±4	12.0±4^{+}	16.0±3$^{+\ddagger}$	12.0±3^{+}
cells on sinusoids/hpf	1.0±.5	7.0±3^{+}	14.0±4$^{+\ddagger}$	12.0±5$^{+\ddagger}$
cells on large vessels/hpf	0.2±.1	0.4±.7$^{+\ddagger}$	0.7±.1$^{+\ddagger}$	0.5±.2$^{+\ddagger}$
Experiment #3				
Total cells/hpf	11.0±4	24.0±10^{+}	35.0±24^{+}	21.0±8^{+}
cells on hepatocytes/hpf	8.0±4	14.0±5	21.0±3^{+}	12.0±5
cells on sinusoids/hpf	2.0±.8	9.0±5^{+}	11.0±8^{+}	8.0±4^{+}
cells on large vessels/hpf	0.4±.2	1.0±.4	3.7±2$^{+\ddagger}$	0.7±.3

Table 12. Female C57bl/6 mice were injected intraperitoneally with either saline, 1μg, 1.5μg or 2μg IL-1 4 h before harvesting the livers . The livers were dissected into lobes, mounted onto cork with OCT compound and snap frozen in methyl butane cooled in liquid nitrogen. The tissue was stored at -80°C until used. 5 μm section of the tissue were cut on a cryostat and mounted on Thermanox™ discs and placed in 24 well plates. $5x10^4$ B16F1 cells were placed on each section and incubated for 15 minutes before non-adherent cells were removed by washing 3 times with HBSS. The sections were fixed in 70% ethanol, processed using haematoxylin and eosin and examined microscopically to determine the cell distribution. All conditions were done as replicates of 6. * values represent the mean and standard deviation

$^{+}$ values are statistically significant using Student's t-test ($p<.05$).

‡ values are statistically significant using Anova ($p<.05$)

Table 13. Inhibition of adhesion of B16F1 melanoma cells on frozen liver sections from Interleukin-1α treated C57bl/6 mice.*

	TREATMENT GROUPS			
	Control	IL-1 1.5μg	IL-1 50μMGRGDS	IL-1 100μMGRGDS
Experiment #1				
Total cells/hpf	18.0±8	35.0±7$^{+\diamond}$	25.0±7$^{\ddagger\nabla}$	26.0±2$^{\ddagger\nabla}$
cells on hepatocytes/hpf	12.0±6	24.0±5$^{+\diamond}$	18.0±3‡	17.0±2‡
cells on sinusoids/hpf	5.0±3	11.0±2$^{\diamond}$	7.0±1$^{\nabla}$	7.0±.5$^{\ddagger\nabla}$
cells on large vessels/hpf	0	0.5±.5	0	0.3±.5
Experiment #2				
Total cells/hpf	13.0±5	24.0±7$^{+\diamond}$	12.0±7$^{\ddagger\nabla}$	12.0±3$^{\ddagger\nabla}$
cells on hepatocytes/hpf	9.0±4	17.0±4$^{+\diamond}$	8.0±2$^{\ddagger\nabla}$	8.0±2$^{\ddagger\nabla}$
cells on sinusoids/hpf	4.0±1	7.0±2^{+}	4.0±2$^{\ddagger\nabla}$	4.0±1$^{\nabla\ddagger}$
cells on large vessels/hpf	0	0	0	0
Experiment #3				
Total cells/hpf	6.0±3	11.0±5^{+}	5.0±1‡	ND
cells on hepatocytes/hpf	4.0±2	7.0±3^{+}	4.0±1	ND
cells on sinusoids/hpf	2.0±.8	4.0±1$^{+\diamond}$	1.0±.8$^{\ddagger\nabla}$	ND
cells on large vessels/hpf	0.1±.1	0.4±.3^{+}	0.2±.2	ND
Experiment #4				
Total cells/hpf	16.0±5	33.0±6$^{+\diamond}$	14.0±4$^{\ddagger\nabla}$	14.0±9$^{\ddagger\nabla}$
cells on hepatocytes/hpf	12.0±5	23.0±4$^{+\diamond}$	10.0±3$^{\ddagger\nabla}$	9.0±7$^{\ddagger\nabla}$
cells on sinusoids/hpf	4.0±1	8.0±1$^{+\diamond}$	4.0±2$^{\ddagger\nabla}$	4.0±2$^{\ddagger\nabla}$
cells on large vessels/hpf	0.2±.4	0.8±.4$^{+\diamond}$	0$^{\ddagger\nabla}$	0$^{\ddagger\nabla}$

Table 13. Female C57bl/6 mice were injected intraperitoneally with either saline or 1.5μg IL-1 4 h before harvesting of livers . The livers were dissected into lobes, mounted onto cork with OCT compound and snap frozen in methyl butane cooled in liquid nitrogen. The tissue was stored at -80°C until used. 5 μm section of the tissue were cut on a cryostat and mounted on Thermanox™ discs and placed in 24 well plates. The appropriate concentration of GRGES peptides were added to each section 30 sec before $5x10^4$ B16F1 cells were added and incubated for 15 minutes before non-adherent cells were removed by washing 3 times in HBSS. The sections were fixed in 70% ethanol, processed using haematoxylin and eosin and examined microscopically to determine the cell distribution. All conditions were done as replicates of 6.

* values represent the mean and standard deviation

$^{+}$ values are statistically significant compared to control using Student's t-test ($p<0.05$). ‡ represents values significant compared to IL-1 ($p<.05$).

$^{\diamond}$ values are statistically significant compared to control using Anova ($p<0.05$) $^{\nabla}$ represents values significant compared to IL-1 ($p<.05$).

Table 14. Inhibition of adhesion of B16F1 melanoma cells on frozen liver sections from interleukin-1α treated C57bl/6 mice.*

	TREATMENT GROUPS			
	Control	IL-1 1.5μg	IL-1 50μMGRGES	IL-1 100μMGRGES
Experiment #1				
Total cells/hpf	23.0±9	36.0±11^{+}	26.0±7	20.0±5$^{\ddagger\nabla}$
cells on hepatocytes/hpf	17.0±7	27.0±8$^{+\diamond}$	19.0±4	15.0±4$^{\ddagger\nabla}$
cells on sinusoids/hpf	6.0±2	8.0±3	7.0±1	5.0±1‡
cells on large vessels/hpf	6.0±.2	0.6±.3	0.7±.2	0.7 ±.1
Experiment #2				
Total cells/hpf	15.0±7	27.0±10$^{+\diamond}$	25.0±13	21.0±7
cells on hepatocytes/hpf	11.0±5	17.0±6$^{\diamond}$	15.0±8	14.0±5
cells on sinusoids/hpf	4.0±2	8.0±3$^{+\diamond}$	9.0±5	7.0±2^{+}
cells on large vessels/hpf	0.2±.1	0.5±.1^{+}	0.7±.5	0.6±2^{+}
Experiment #3				
Total cells/hpf	14.0±4	29.0±6^{+}	30.0±6^{+}	20.0±5$^{+\ddagger}$
cells on hepatocyte/hpf	10.0±3	17.0±4^{+}	19.0±4^{+}	13.0±3‡
cells on sinusoids/hpf	4.0±1	8.0±3^{+}	9.0±2^{+}	7.0±2$^{+\ddagger}$
cells on large vessels/hpf	0.4±.2	1.0±.5^{+}	0.7±.4	0.8±.3^{+}

Table 14. Female C57bl/6 mice were injected intraperitoneally with either saline or 1.5 μg interleukin-1 4 h before harvesting of livers. The livers were dissected into lobes, mounted onto cork with OCT compound and snap frozen in methyl butane cooled in liquid nitrogen. The tissue was stored at -80°C until used. 5μm section of the tissue were cut on a cryostat and mounted on Thermanox™ discs and placed in 24 well plates. The appropriate concentration of GRGES peptides were added to each section 30 sec before $5x10^4$ B16F1 cells were added and incubated for 15 minutes before non-adherent cells were removed by washing 3 times in HBSS. The sections were fixed in 70% ethanol, processed using haematoxylin and eosin and examined microscopically to determine the cell distribution. All conditions were done as replicates of 6.

* values represent the mean and standard deviation

$^{+}$ values are statistically significant compared to control using Student's t-test ($p<.05$). ‡ represents values that are statistically significant compared to interleukin-1 using Student's t-test ($p<.05$).

$^{\diamond}$ values are statistically significant compared to control using Anova ($p<.05$). $^{\triangledown}$ represents values that are statistically significant compared to interleukin-1 using Anova ($p<.05$).

4.5 EFFECTS OF RGD PEPTIDES ON METASTASIS

4.5.1 Rationale

I postulate that if the phenomenon of increased tumour burden, modulated by interleukin-1, is due to the effect of an integrin as suggested by the *in vitro* frozen section assays, injection of GRGDS peptides should block this phenomenon.

4.5.2 Modulation of Experimental Metastasis by RGD Peptides

B16F1 cells were co-injected with 3 mg of either GRGDS or GRGES peptides as described previously in section 3.4.1. The doses of RGD peptides were based on values published previously by Humphries *et al.* (1988). Animals were examined by histology 7 days after injection as described. Table 15 shows that the peptides enhanced tumour growth. In control animals injected with peptides the tumour burden increased from 3% to 6% with the addition of GRGES peptides and increased to 9% with the addition of GRGDS peptides. The interleukin-1 pre-treated group showed the same trend with interleukin-1 alone giving 15% tumour by area and this value was increased to approximately 24% with the addition of GRGDS and GRGES peptides. The amount of necrotic tissue increased 10 fold in interleukin-1 pre-treated animals treated with peptides compared to animals treated with interleukin-1 alone.

Table 15. Effects of GRGDS and GRGES peptides on B16F1 Melanoma Metastasis. Percentage Normal, Tumour, and Other areas seen in liver sections of Interleukin-1 treated mice versus Control *

	% Normal	% Tumour	% Necrotic
Control	97(89-99)	3(0-10)	0.1(0-1)
Control + GRGES	94(92-100)	6(0-8)	0.3(0-.5)
Control + GRGDS	91(94-96)	9(4-16)	0.3(.2-.5)
IL-1	82(76-89)$^{+}$	15(2-22)	0.3(0-1.8)
IL-1 + GRGES	72(66-94)$^{+}$	23(5-31)$^{+}$	3.9(2-9)$^{+}$
IL-1 + GRGDS	73(67-85)$^{+}$	24(14-28)$^{+}$	3.1(1-7)$^{+}$

Female C57bl/6 mice were pre-treated with 1.5 μg interleukin-1α intraperitoneally 4 h before surgery. $3x10^5$ B16F1 cells were co-injected with 3 mg GRGDS or GRGES peptides. The animals were euthanized after 7 days, autopsies performed, and histology done on formalin fixed sections. The percent area occupied by each classification was determined using a Mertz graticule. Each experimental group represents 5 animals.

* Values are expressed as median and range

$^{+}$ values are statistically significant compared to control ($p<.05$)

5.0 DISCUSSION

5.1 METASTASIS ASSAY

5.1.1 Rationale

The purpose of establishing an animal model of metastasis was to elucidate the mechanisms of cancer cell arrest in the microvasculature by intravital microscopy. Mechanical trapping has been postulated to be the mechanism of cancer cell arrest in the vasculature, but adhesive interactions between surface molecules on cancer cells and endothelial cells have also been implicated in the arrest process. Before an attempt to investigate the arrest process could be made an appropriate animal model had to be established. Such a model would allow for the easy and reproducible injection of cancer cells into the circulation, be adaptable to modulation of the tumour burden and arrest patterns, and be amenable to analysis, by a single person, on the intravital microscope. With all these parameters in mind, a model of liver metastasis was established in C57bl/6 mice using a mesenteric vein injection of B16F1 melanoma cells (Morris *et al.*, 1993) and using interleukin-1α as the modulating agent.

5.1.2 Animal Model

It was established that B16F1 melanoma cells do form metastasis in the liver as well as other organs when injected into the portal venous circulation of C57bl/6 mice. The tumour burden was quantitated (as seen in Table 3) by counting discrete nodules on the surface of the organs and by changes in organ

weight. From this data, a cell concentration of $3x10^5$ was established and used throughout all following experiments. A time course was used to determine that a 7 day survival time after injection was optimal for quantisation of the nodules. This time period gave discrete nodules with few areas of confluence, showed no visible metastasis to other organs, and allowed for either an increase or decrease in tumour burden that would be measurable. The 14 and 21 day time points were deficient in one or more of these criteria (Table 4).

5.1.3 Modulation with Interleukin-1

In the first experiment using a 4 h pre-treatment with 1.5 μg interleukin-1 by intraperitoneal injection, three methods of quantification were used, counting of visible nodules, weighing of organs and histomorphometric analysis. Analysis by counting of nodules and histomorphometry showed an increase in tumour burden of 7 and 26 fold respectively, in animals that had been pre-treated with interleukin-1. In contrast the weights of the organs between the saline-treated control animals and the interleukin-1 treated animals were not different, but were significantly greater than the untreated controls. As this untreated control group was established from a different group of mice, the differences seen could be superficial and due to the size of the animals. Taking this into consideration and with the observation that no weight differences were seen, even when obvious differences in tumour burden were present this method of quantisation was discontinued due to lack of sensitivity. Further experimentation showed that the increase in tumour burden elicited in response

to the injection of interleukin-1 was consistently reproducible over three experiments. The magnitude of the increase in tumour burden ranged from 3-7 fold when nodules were counted and from 14-26 fold when the area occupied by tumour was assessed. It was also noted that there seemed to be a specific anatomical localization of early tumour growth around the portal triad region with little growth seen in the mid-zonal or central vein regions (Figure 5). Support for this observation is given by Barbera-Guillem *et* al (1993) who found that 90% of cancer cells injected into the liver via the spleen arrest in the periportal region. There were several possible hypothesis to explain this increase in tumour burden and differences in localization seen in animals pre-treated with interleukin-1. First was the possibility the interleukin-1 pre-treatment up-regulated adhesion molecules on the surface of the liver microvascular endothelium and resulted in a greater number of cancer cells adhering, extravasating and surviving to form metastasis. Second, is the possibility that interleukin-1 pre-treatment resulted in the production of specific growth factors that were beneficial to the growth of the cancer cells. This would cause a quicker advancement of the cells in animals pre-treated with interleukin-1 but assumes that the control animals would eventually show the same level of growth. Thirdly, it could be possible that interleukin-1 altered the hepatic blood flow of the animals in a way that caused fewer cells to be destroyed or more cells to be retained in the microvasculature. As the central hypothesis of this project was that adhesion molecules are responsible for the

arrest of cancer cells, the next experiments attempted to provide indirect evidence for an adhesive role.

5.2 ARREST OF RADIOACTIVELY-LABELLED CANCER CELLS

To determine if the increase in metastasis seen in the above experiments might be related to an early phenomenon (between the initial time of injection and 24 hours) or to a later event, B16F1 cells were labelled with [^{125}I]-UdR and injected via a mesenteric vein. [^{125}I]-UdR was used as the label since it is taken up in the nucleus and after this treatment the cells are unable to divide (Fidler, 1970). This eliminates the problem of the cells dividing during the 24 hour period of the assay. The animals were euthanized at times ranging from immediately after injection to 24 h later, their organs fixed, and counted in a gamma counter to assess the amount of radioactivity retained. An initial study involving 4 mice per group showed an increase in the retention of cells in the livers of animals pre-treated with interleukin-1 at 2 and 8 h later but the differences were not significant. We were unable to detect metastasis to the brain, lungs, spleen, kidney, adrenal gland, or ovary as the radioactivity associated with these organs was negligible. The radioactivity associated with the intestinal area was higher than other organs. This is not surprising as the mesentery was used as the site of injection and some residual cells would be expected there. However, the majority of the radioactivity present at all time points was in the liver. In a second more rigorous experiment a more distinct trend was observed. Immediately after injection there were twice as many cells

present in the livers of mice pre-treated with interleukin-1 as controls. After 2 h, both the control and interleukin-1 groups showed a steep decrease in the number of cells present but, whereas the number of cells in control animals continued to decline over the 24 h period the number of cells in the animals pre-treated with interleukin-1 reached a plateau. The final difference between the two groups at 24 hours was 7 fold. Since the cells are unable to divide, this would appear to discount the hypothesis that a growth factor was the sole reason behind the observed phenomenon. It would suggest that animals with an inflammatory response give the cancer cells an advantage and result in an more aggressive disease. It may be hypothesized that the cancer cells localize in a manner similar to leukocytes. In the process of inflammation leukocytes interact with adhesion molecules on the endothelial surface to facilitate their arrest and extravasation. As cancer cells possess many of the same adhesion molecules as leukocytes (Table 1) it may be possible that they are using a similar mechanism to facilitate extravasation. If the pre-treatment of the mice with interleukin-1 results in an active inflammatory response, as a consequence the adhesion molecules on the endothelial surface would be up-regulated. Theoretically, the cancer cells injected into animals undergoing an active inflammatory response would then be able to arrest and extravasate more quickly due to the increased probability of interacting with endothelial adhesion molecules. Cancer cells that are extravasated avoid the haemodynamic stresses of the blood and the circulating leukocytes which form the body's first

line of defense against foreign invaders. Thus, extravasated cancer cells would be expected to be destroyed at a lower frequency and could contribute to the slower decline in cancer cell numbers seen in interleukin-1 treated animals. If interleukin-1 treatment also resulted in a decrease in the hepatic flow rate, it is possible that the cancer cells would more quickly marginate making contact with the endothelium. A decreased flow rate would also protect the cells from haemodynamic destruction due to shear stress in the liver microvasculature. Other investigators have suggested that all cancer cells injected into the hepatic circulation, regardless of their metastatic ability, extravasate equally well (Koop *et al.*, 1994; Morris *et al.*, 1994). This may be true in animals not pre-treated with interleukin-1. The evidence presented here suggests that there is a distinct difference in retention, which correlates to increased metastasis at 7 days. My experiments show that the number of cancer cells in the liver of both control and interleukin-1 pre-treated mice decrease over 24 hours and is consistent with other data (Fidler, 1970; Weiss *et al.*, 1992). This decrease would suggest that the cells are being cleared from the system and the plateau in retention of cells injected into the interleukin-1 pre-treated animals would suggest these cells were protected from continual clearing. I would suggest that pre-treatment of the animals with interleukin-1 gives the cancer cells injected into this system a selective advantage over the cells injected into control animals. This advantage may be the result of an increased retention and/or ability to extravasate due to a greater probability of interaction with

adhesion molecules on the endothelial surface.

5.3 INTRAVITAL MICROSCOPY OF CANCER CELL TRANSIT

5.3.1 Rationale

As I have shown that the increase in metastasis seen at 7 days can be correlated with an immediate increase in retention of B16F1 cells in the liver, it was decided to investigate the immediate differences in cancer cell arrest in control versus interleukin-1 pre-treated mice by intravital microscopy. This technique allowed me to observe real time quantitatable images of the interactions of cancer cells with the quiescent and perturbed liver microvasculature.

5.3.2 Cell labelling

The use of an appropriate fluorescent label was imperative in developing the technique of intravital microscopy. The ideal label would not compromise the viability of the cells, would only label living cells, and would be remain strongly fluorescent over a long period of time. In assessing the suitability of three fluorescent labels (latex microbeads (Morris *et al.*, 1993), fluorescein isothiocyanate (Butcher *et al.*, 1980), and calcein AM (Morris *et al.*, 1993)) several observations were made.

I noted that in labelling B16F1 cells with .05μm fluorescently labelled latex microbeads there was a decrease in viability of the cells in all labelling conditions compared with control. No condition examined produced the desired 95% viability assessed by trypan blue. The passage of cells through either a

20 gauge needle to create single cell suspensions or the 30 gauge canula did not further decrease the viability of the cells. Since the mechanism of uptake or the final destination within the cells was unknown, electron microscopy was undertaken. It appeared that immediately after labelling, the beads were found in vacuoles in the cytoplasm of the B16F1 cells (Figure 9). The presence of numerous bead-containing vacuoles in the cytoplasm could possibly result in an increased fragility of the cell and lead to the higher incidence of death in the harvesting protocol. It was also found that the cells were removed easily from the tissue culture flask using 1% trypsin digestion but did not lift following incubation with 5 mM EGTA. If the cells were allowed to continue in culture in either medium supplemented with 10% fetal bovine serum for 4 h or 1% fetal bovine serum overnight, the cells removed easily following incubation with 5 mM EGTA and the viability increased to levels similar to untreated cells. It would seem that the introduction of microbeads resulted in an increased adherence of the cells to the plastic of the culture flasks. There are two simple explanations for this behaviour. First, the uptake of the beads might cause the activation of the cancer cells, resulting in an up-regulation of the adhesion molecules on their surface and causing them to be more firmly adhered to the plastic of the culture flask. In this way incubating with serum for a period of time would allow the cells to deactivate and to be harvested according to the protocol stated for work involving adhesion assays. Second, it is possible that a charge on the beads that are unable to be removed from the flask with

washing served to result in the firm adhesion of the cells (personal communication Dr. Jordon, Polyscience). The addition of serum would mask these charges and allow the cells to be removed with EGTA. The increase in viability after incubation with serum is likely due to the dead cells lifting from the flask and being aspirated with the media. This would leave only the viable cells to be harvested and hence give the appearance of increased viability. In assessing the percent of viable cells that were fluorescent when labelled with microbeads it was found that approximately 60% of the cells exhibited fluorescence and that the fluorescence was not evenly distributed between cells or within cells. It would appear that not all cells were equally able to take up beads and as a consequence the identification and outline of individual cells would be difficult using intravital microscopy. It was also noted that some cells that stained with trypan blue still contained beads and so differentiation between living and dead cells could not be ensured.

In examining the use of fluorescein isothiocyanate label it was found that all viable cells were strongly fluorescent, except for cells labelled with 140 mg/ml for 20 min, and remained strongly fluorescent for more than 30 minutes. It must be noted though that the viability of the cells in all labelling groups was decreased below the optimal level of 95%. The shorter the labelling period the greater the viability, but even with moderate levels of FITC for short time periods the viability was not acceptable (Table 10).

The last fluorescent label examined proved to be the most promising.

Calcein AM, a vital cell dye, did not affect the viability of cells and consistently labelled almost all viable cells as assessed by trypan blue exclusion. Calcein AM appeared to fluorescently label all viable cells. Calcein AM can differentiate living cells from dead cells by using cellular mechanisms to cleave the calcein, resulting in fluorescence, thus it would seem to be more accurate method of assessing viability than trypan blue exclusion which only measures membrane integrity. The duration of the fluorescence of this label is limited to less than 10 minutes under constant ultra-violet excitation. I decided that the initial intravital experiments would focus on the immediate interactions of the cancer cells with the hepatic vasculature and so the lifetime of fluorescence would not be an issue.

5.3.3 Patterns of Arrest

In comparing the arrest pattern of cancer cells in saline treated animals to interleukin-1 treated animals, striking differences were found. In saline treated animals, cancer cells arrested in vessels approximately 16 μm in diameter, or sinusoidal vessels. In animals pre-treated with interleukin-1, cancer cells arrested in vessels of 34 μm in diameter. From the size distribution of B16F1 cells (Figure 8) it is obvious that most cells in control animals are arresting in vessels the same size as the majority of the B16F1 cells. Therefore, this arrest is most likely due to mechanical trapping. In animals pre-treated with interleukin-1 the B16F1 cells arrested in vessels significantly larger than the size of the largest B16F1 cells in the size distribution. The arrest of these cells was

often associated with the wall of the portal tract capillaries but on occasion the cells seem to become arrested in the middle of the diameter of a vessel (Figure 10 and 11). As an extension of this data it was found that cells injected into animals pre-treated with interleukin-1 did not enter the sinusoids whereas cells injected into saline treated animals travelled a median distance of 32 μm into sinusoids. As stated above this did not appear to relate to the size of the cancer cells. It appears that cells injected into animals pre-treated with interleukin-1 preferentially arrest in the portal tract capillaries whereas cells injected into control animals become mechanically trapped in the sinusoids. Other investigators have shown distinct differences in the expression of adhesion molecules between hepatic sinusoidal lining cells and portal tract capillaries (Table 2). In view of the differences in arrest patterns, it seems possible that an increase in the expression of specific adhesion molecules on the portal tract capillaries may be responsible for the arrest of the cells in this location. In the discussion of the metastasis assay it was observed that early tumours seemed to localize around the portal tract capillaries in both control and interleukin-1 pre-treated animals. It is possible that this increase in the number of cells arresting in the portal tract capillaries also correlated with the increase in metastasis. That is, that the larger vessels allow the preferential growth of cancer cells, whereas agents in the sinsuoids act to quickly eliminate the cells that arrest there. Since the greatest proportion of Kupffer cells are present in the perivenous segment of the sinusoids it could be postulated that

the cancer cells reaching the sinusoids are destroyed by Kupffer cells. Indeed, Barbera Guillem *et al.* (1993) have shown the vast majority of injected cancer cells die in this perivenous area. Therefore, if interleukin-1 treatment of the vasculature causes cells to be arrested in the portal tract capillaries, not allowing them to reach the sinusoids, where mechanisms to destroy them exist it, is possible that there is an increase in cancer cell survival and extravasation and therefore an increase in metastasis.

5.3.4 Velocity Profile

A velocity profile of cells in both saline treated and interleukin-1 treated animals was determined. The positioning of individual fluorescently labelled cancer cells was followed frame by frame and marked on the traced image of the vessel system. The distances travelled in each frame was measured and then divided by the elapsed time taken for the movement. A velocity profile was established for each cell. These individual profiles were then compiled to create an overall average velocity profile for B16F1 cells injected into saline-treated control animals and interleukin-1 treated animals. These profiles showed that the entry velocity of cells into the field of view as well and the maximum velocity attained was significantly lower in animals pre-treated with interleukin-1. There are at least two possible explanations for this data. The first is that pre-treatment of the animals with interleukin-1 results in the increase in expression of adhesion molecules on the endothelial surfaces. This increase in expression could result in more cancer cell/endothelial cell interactions leading

to slower velocities and arrest in the larger vessels. The second hypothesis is that pre-treatment of the animals with interleukin-1 causes inherent changes in the liver or in the hepatic circulation, apart from adhesion molecule expression, that would result in a decrease in overall hepatic blood flow rate and cancer cell velocity. Interleukin-1 is known to cause a systemic increase in blood pressure but the effect on hepatic venous circulation does not appear to have been investigated. To address this point, the rate of hepatic venous circulation was investigated by determining the velocities of indigenous red blood cells and of fluorescently labelled 6 μm latex microbeads in both saline treated and interleukin-1 treated animals. I found that a significant decrease in the velocity of latex microbeads in the hepatic circulation of interleukin-1 treated mice and a decrease (although not significant) in the velocity of rbc's in animals pre-treated with interleukin-1. The velocity of the red blood cells was an approximation made by tracing the flow of these cells in video recordings of animals injected with cancer cells and is not expected to be as reliable as the velocities obtained from the injected microbeads. However, the observation that the microbeads are charged particles which can interact with the vessel walls (personal communication Dr.Jordon, Polysciences) suggest their velocity is not a true measure of the fluid flow in the liver but represent only the distinct velocity of the microbeads within the liver. Even though both situations were not ideal, the results still show a difference in the hepatic venous flow rate in animals pre-treated with interleukin-1 and are consistent with the observation

that interleukin-1 treatment results in a shunting of blood away from the mesentery and hepatic circulation to more essential organs. To determine the actual rate of hepatic circulation an experiment in which fluorescently labelled murine red blood cells are injected into the hepatic circulation and traced would be optimal. The fluorescent label would also allow the accurate tracking of individual cells and the use of murine red blood cells would prevent any abnormal adhesive interactions with the vessel wall. This information could explain the differences in the velocities of cancer cells between interleukin-1 treated and saline- treated animals but could not likely explain all the differences in arrest patterns. It can be hypothesized that in a condition of inflammation and decreased hepatic flow that the slower rate of travel of the cells afford them a greater chance to marginate and contact the up-regulated adhesion molecules on the endothelial surface, resulting in the arrest of cells in the portal tract capillaries instead of continuing into the sinusoids and becoming mechanically trapped. Cancer cells are known to secrete cytokines that can activate endothelial cells and cause an up-regulation in surface adhesion molecule expression (Mattei *et al.*, 1994; Takeda *et al.*, 1991). In this way it is also possible that the cancer cells themselves, by secreting inflammatory mediators, could cause the decrease in hepatic flow rates and the increase in expression adhesion molecules which may result in a more efficient arrest and extravasation process. Although the decrease in hepatic flow rate after treatment with interleukin-1 may be seen as a draw back to the model system,

I would submit that it is not. I would suggest that this system may more accurately simulate the role of inflammatory mediators, either endogenous or exogenously supplied by cancer cells, in liver metastasis.

5.4 FROZEN SECTION ASSAY

5.4.1 Rationale

My observations using intravital microscopy showed distinct differences in the arrest patterns of cancer cells injected into animals pre-treated with interleukin-1 compared to control animals. I postulated that these differences were due to the upregulation of adhesion molecules on endothelial surfaces in the liver microvasculature. In an attempt to relate this observation to the expression of an adhesion molecule, I examined the attachment of B16F1 cells to cryostat sections of liver from interleukin-1 treated and control animal groups. I found increased adhesion of B16F1 cells to frozen liver sections from mice pre-treated with interleukin-1.

5.4.2 Interleukin-1 Modulation

Interleukin-1 pre-treatment of mice resulted in a dose- dependent increase in adhesion of B16F1 cells to frozen liver sections from these mice. Treating the mice with a dose of 1 μg of interleukin-1 for 4 h before the livers were harvested resulted in a 3 fold increase in adhesion of cancer cells to the frozen sections. Increasing the dose of interleukin-1 to increased the number of cells adhered to 4 times that of control, but a increase in dose to 2 μg did not cause any further increase in adhesion. The 1.5 μg dose resulted in the a

maximal level of adhesion of B16F1 cells to all compartments of the liver tissue. It is known that hepatocytes as well as endothelial cells can respond to perturbation and express inducible adhesion molecules on their surfaces (Kemperman *et al.*, 1995). Since this system deals with cut tissue surfaces the cancer cells are able to interact with all geographic and cellular compartments and so any surface with an increase in adhesion molecules could result in an increase in total adhesion to the section. The adhesive abilities of the cells did not increase at high doses of interleukin-1 and treatment with 2 μg caused a decrease from maximum stimulation. It is known that interleukin-1 has the ability to damage endothelial cells, causing their retraction and death (Lafrenie *et al.*, 1992b; Honn *et al.*, 1994a). Perhaps the same effect can be seen in hepatocytes. If the cells have been damaged by the interleukin-1 treatment they would not be expected to express maximal levels of adhesion molecules on their surfaces and the total number of adherent cancer cells along with the number of adherent cancer cells in the specifically affected compartments would decrease.

5.4.3 Modulation Using RGD Peptides

The addition of 50 and 100 μM of GRGDS peptides to the adhesion assay reduced the attachment of B16F1 cells to interleukin-1 stimulated livers to control levels in 3 of 4 experiments. GRGES peptides caused no significant reduction in adhesion at a concentration of 50 μM but 100 μM of peptide caused a decrease in the number of cells adhered to levels between interleukin-

1 and control. Since the control peptides did not block adhesion at 50 μM the reduction caused by the GRGDS peptides can be considered "real" and not simply a non-specific phenomenon produced through the addition of peptides to the system. The GRGDS peptides are known to compete for integrin binding sites, so this observation would appear to implicate an integrin in the adhesive process. Just as adhesion of B16F1 cells to liver section was increased on endothelial cells, sinusoidal lining cells and hepatocytes, the reduction of adhesion in response to GRGDS addition was seen in all compartments. Since the concentrations of GRGDS peptides used completely inhibited the interleukin-1 effect a dose curve to determine the IC 50 would be an important extension of this data. Along with this, scanning electron microscopy of the liver section with adherent cancer cells might show the exact location of adhesion and confirm that the classification scheme developed differentiating sinusoids from hepatocytes is accurate at the level of light microscopy.

5.5 METASTASIS ASSAY USING RGD PEPTIDES

5.5.1 Rationale

In summary, GRGDS peptides inhibited the adhesion of cancer cells *in vitro* whereas GRGES peptides did not. To assess if this phenomenon could also be observed *in vivo*, GRGDS and GRGES peptides were co-injected with cancer cells in an experimental metastasis assay.

5.5.2 Modulation using RGD peptides

Co-injection of GRGDS and GRGES peptides did not reduce the rates of

liver metastases in C57bl/6 mice. Contrary to expectation, the area of tumour in the livers of mice treated with either GRGDS or GRGES peptides was increased. This was true for both the control group and the interleukin-1 pre-treatment group. The area of necrotic tissue was also increased in both groups but was increased by more than 10 times in the interleukin-1 treated animals. It is possible that the dose of peptides resulted in damage of the endothelial cells in this model. However, 3mg, has been used previously by others (Humphries *et al.*, 1988; Humphries *et al.*, 1986) as an effective dose for *in vivo* tumour reduction. This could be addressed through an electron microscopic study of the liver tissue from these animals looking specifically for damage to endothelial cells. The destruction or retraction of endothelial cells would allow the cancer cells an easier passage into the surrounding tissue resulting in a greater tumour burden than that seen even with pre-treatment with interleukin-1. In the *in vitro* model, the system is static allowing the cancer cells to adhere to any liver compartment and the tissue frozen and cut so no damage is possible. *In vivo*, the cancer cells must first interact with the endothelial cells, so this compartment is the only one susceptible to blocking. Because the system is living, damage to the tissue is also possible. In examining the data on large vessels in the frozen section tables it can be seen that, although there was an increase in the number of adherent cells, the number of cells involved is relatively small in comparison to the other compartments and the decreases in response to peptide treatment are less

dramatic. Since the exact distribution and expression of adhesion molecules in the different compartments of murine liver is unknown, perhaps the effect of the GRGDS peptide is more effective in the mid-zone regions and on hepatocytes. *In vivo*, the mid zonal region is reached with reduced efficiency, especially in animals pre-treated with interleukin-1, as I have shown through intravital microscopy. The hepatocytes would not be in contact until after the cells have extravasated. If the endothelium of the portal tract capillaries were damaged, increasing the opportunity for cells to extravasate, it might be expected that an increased rate of metastasis would result. In extension, if the sinusoidal lining cells (endothelial cells and Kupffer cells) were damaged as well, the cells entering this mid-zone region might be able to grow instead of being eliminated by the defenses there. It is also worthy of note that the animals injected with peptides needed more care in the form of external heat and stimulation to survive the surgical procedure. Animals treated only with interleukin-1 or saline did not experience these same difficulties. This lends credence to the theory that the peptides had detrimental effects on the systemic vasculature. Attempts made at injecting peptides into interleukin-1 pre-treated animals on the intravital microscope were not successful. After the injection was started the blood flow became extremely sluggish, the cells did not appear and the mice quickly died. In light of the final results of the metastasis assay, further attempts at characterizing the arrest patterns of cancer cells in the presence of GRGDS peptides were abandoned.

5.6 CONCLUSION: A ROLE FOR CANCER CELL ARREST BY NON-MECHANICAL MEANS

It is well accepted that the haematogenous spread of cancer is the most important route leading to the formation of metastasis, but there has been much argument as to how cancer cells become arrested within the vasculature. The results of these studies show an increase in hepatic metastasis in animals that have been pre-treated with interleukin-1 which correlates to an increased retention of radiolabelled cancer cells at short time periods. Intravital microscopy has shown that there is a difference in the anatomical arrest position of cancer cells injected into animals pre-treated with interleukin-1 compared to animals treated with saline. The cells injected into animals pre-treated with interleukin-1 arrested in large portal tract capillaries where size restrictions did not appear to play a role. The vast majority of cells injected into control animals became mechanically trapped in the sinusoids. This suggests a role for adhesion molecules on the endothelial surfaces of portal tract capillaries in this process of arrest *In vitro* studies to attempt identification of an adhesion molecule responsible for this arrest showed inhibition of adhesion through the use of GRGDS peptides and pointed to a role for integrins. *In vivo* studies indirectly supported the involvement of adhesion molecules in metastasis but these studies were not able to define a role for RGD-dependent integrin adhesion molecules in this process. The next step in confirming a role for adhesion molecules in cancer cell arrest is to examine a panel of antibodies

against specific adhesion molecules, known to be present on the portal tract capillaries, using the *in vitro* technique developed here. These studies should promote a more specific means of inhibition than the peptides and should provide the potential for fewer non-specific side effects. It would be of special interest to utilize the technique of intravital microscopy to see how these antibodies affected the arrest pattern of cancer cells *in vivo*.

REFERENCES

Abbassi, O., Kishimoto, T.K., McIntire, L.V., Anderson, D.C., and Smith, C.W. (1993). E-selectin supports neutrophil rolling in vitro under conditions of flow. J Clin Invest *92*, 2719-2730.

Arndt, H., Palitzsch, K.D., Anderson, D.C., Rusche, J., Grisham, .M.B., and Granger, D.N. (1995). Leucocyte-endothelial cell adhesion in a model of intestinal inflammation. Gut *37 #3*, 374-379.

Auerbach, R., Lu, W.C., Pardon, E., Gumkowski, F., Kaminski, G., and Kaminski, M. (1987). Specificity of adhesion between murine tumor cells and capillary endothelium: an in vitro correlate of preferential metastasis in vivo. Cancer Res *47*, 1492-1496.

Barbera-Guillem, E., Smith, I., and Weiss, L. (1993). Cancer-cell traffic in the liver. II. Arrest, transit and death of B16F1 and M5076 cells in the sinusoids. Int J Cancer *53*, 298-301.

Bauer, C., Marzi, I., Bauer, M., Fellger, H., and Larsen, R. (1995). Interleukin-1 receptor antagonist attenuates leukocyte-endothelial interactions in the liver after hemorrhagic shock in the rat. Crit. Care Med. *23 #6*, 1099-1105.

Bereta, M., Bereta, J., Cohen, S., Zaifert, D., and Cohen, M.C. (1991). Effect of inflammatory cytokines on the adherence of tumor cells to endothelium in a murine model. Cell Imm *136*, 263-277.

Bertomeu, M.C., Gallo, S., Lauri, D., Haas, T.A., Orr, F.W., Bastida, E., and Buchanan, M.R. (1993). Interleukin 1-induced cancer cell/endothelial cell adhesion in vitro and its relationship to metastasis in vivo: role of vessel wall 13-HODE synthesis and integrin expression. Clin Expl Metastasis *11*, 243-250.

Biancone, L., Araki, M., Araki, K., Vassalli, P., and Stamenkovic, I. (1996). Redirection of tumor metastasis by expression of E-selectin in vivo. J Exp Med *183*, 581-587.

Bremer, C., Bradford, B.U., Hunt, K.J., Knecht, K.T., Connor, H.D., Mason, R.P., and Thurman, R.G. (1994). Role of Kupffer cells in the pathogenesis of hepatic reperfusion injury. Am. J. Physiol *267*, G630-G636.

Bresalier, R.S., Schwartz, B., Kim, Y.S., Duh, Q.Y., Kleinmann, H.K., and Sullam, P.M. (1995). The laminin alpha1 chain Ile-Lys-Val-Ala-Val (IKVAV)-containing peptide promotes liver colonization by human colon cancer cells. Cancer Res *55*, 2476-2480.

Brodt, P., Fallavolitta, L., Norton, C.R., and Wolitzky, B.A. (1994). E selectin mediated adhesion of carcinoma cells to the liver endothelium and liver metastasis. Proc Am Ass Cancer Res *35 (abstract 311)*,

Brouwer, A., Wisse, E., and Knook, D.L. (1988). Sinusoidal endothelial cells and perisinusoidal fat-storing cells. In The liver: Biology and pathobiology. I.M. Arias, W.B. Jakoby, H. Popper, D. Schachter, and D.A. Shafritz, eds. (New York: Raven Press Ltd.), pp. 665-682.

Burchill, S.A., Bradbury, M.F., Pittman, K., Southgate, J., Smith, B., and Selby, P. (1995). Detection of epithelial cancer cells in peripheral blood by reverse transcriptase-polymerase chain reaction. Br. J. Cancer *71*, 278-281.

Butcher, E.C., Scollay, R.G., and Weissman, I.L. (1980). Direct fluorescent labeling of cells with fluorescein or rhodamine isothiocyanate. II. Potential application to studies of lymphocyte migration and maturation. J Immunol Methods *37*, 109-121.

Butcher, E.C. and Weissman, I.L. (1980). Direct fluorescent labeling of cells with fluorescein or rhodamine isothiocyanate. 1. Technical aspects. J Immunol Methods *37*, 97-108.

Chambers, A.F., Schmidt, E.E., MacDonald, I.C., Morris, V.L., and Groom, A.C. (1992). Early steps in hematogenous metastasis of B16F1 melanoma cells in chick embryos studied by high-resolution intravital videomicroscopy. J Nat Cancer Inst *10*, 797-803.

Chambers, A.F., MacDonald, I.C., Schmidt, E.E., Koop, S., Morris, V.L., Khokha, R., and Groom, A.C. (1995). Steps in tumor metastasis: new concepts from intravital videomicroscopy. Cancer and Metastasis Reviews *14*, 279-301.

Chirivi, R.G.S., Garofalo, A., Martin-Padura, I., Mantovani, A., and Giavazzi, R. (1993). Interleukin 1 receptor antagonist inhibits the augmentation of metastasis induced by interleukin 1 or lipopolysaccharide in a human melanoma/nude mouse system. Cancer Res *53*, 5051-5054.

Couvelard, A., Scoazec, J.Y., and Feldmann, G. (1993). Expression of cell-cell and cell-matrix adhesion proteins by sinusoidal endothelial cells in the normal and cirrhotic human liver. Am J Path *143 #3*, 738-752.

Crissman, J.D., Hatfield, J., Schaldenbrand, M., Sloane, B.F., and Honn, K.V. (1985). Arrest and Extravasation of B16 Amelanotic Melanoma in Murine Lungs: A Light and Electron Microscopic Study. Lab Invest *53 #4*, 470-478.

Crissman, J.D., Hatfield, J.S., Menter, D.G., Sloane, B.F., and Honn, K.V. (1988). Morphological study of the interaction of intravascular tumor cells with endothelial cells and subendothelial matrix. Cancer Res *48*, 4065-4072.

Deaciuc, I.V., Bagby, G.J., Neisman, M.R., Skrepnik, N., and Spitzer, J.J. (1994). Modulation of hepatic sinusoidal endothelial cell function of Kupffer cells: an example of intercellular communication in the liver. Hepatology *19*, 464-470.

Decker, K. (1990). Biologically active products of stimulated liver macrophages (Kupffer cells). Eur. J. Biochem. *192*, 245-261.

Dejana, E., Bertocchi, F., Bortloami, M.C., Regonesi, A., Tonta, A., Breviario, F., and Giavazzi, R. (1988). Interleukin 1 promotes tumor cell adhesion to cultured human endothelial cells. J Clin Invest *82*, 1466-1470.

Denhardt, D.T. and Chambers, A.F. (1994). Overcoming obstacles to metastasis - defenses against host defenses: osteopontin (OPN) as a shield against attack by cytotoxic host cells. J Cell Biochem *56*, 48-51.
Dore, M., Korthuis, R.J., Granger, N., Entman, M.L., and Smith, C.W. (1993). P-selectin mediates spontaneous leukocyte rolling in vivo. Blood *82 #4*, 1308-1316.

Elices, M.J., Osborn, L., Takada, Y., Crouse, C., Luhowdkyl, S., Hemler, M.E., and Lobb, R.R. (1990). VCAM-1 on activated endothelium interacts with the leukocyte integrin VLA-4 at a site distinct from the VLA-1/fibronectin binding site. Cell *60*, 577-584.

Essani, N.A, Fisher, M.A., Farhood, A., Manning, A.M., Smith, C.W., and Jaeschke, H. (1995). Cytokine-induced upregulation of hepatic intercellular adhesion molecule-1 messenger RNA expression and its role in the pathophysiology of murine endotoxin shock and acute liver failure. Hepatology *21*, 1632-1639.

Feder, L.S., Todaro, J.A., and Laskin, D.L. (1993). Characterization of interleukin-1 and interleukin-6 production by hepatic endothelial cells and macrophages. J Leukoc Biol *53*, 126-132.

Fidler, I.J. (1970). Metastasis: quantitative analysis of distribution and fate of tumor emboli labeled with 125I-5-Iodo-2'deoxyuridine. J Nat Cancer Inst *45*, 773-782.

Fidler, I.J. (1991). The biology of human cancer metastasis. Acta Oncologica *30 #6*, 669-675.

Friedrichs, K., Ruiz, P., Franke, F., Gille, I., Terpe, H.J., and Imhof, B.A. (1995). High expression level of alpha6 integrin in human breast carcinoma is correlated with reduced survival. Cancer Res *55*, 901-906.

Garofalo, A., Chirivi, R.G., Foglieni, C., Piggot, R., Mortarini, R., Martin-Padura, I., Anichini, A., Gearing, A.J., Sanchez Madrid, F., and Dejana, E. (1995). Involvement of the very late antigen 4 integrin on melanoma in interleukin 1-augmented experimental metastases. Cancer Res *55*, 414-419.

Gauthier, T.W., Scalia, R., Murohara, T., Guo, J.P., and Lefer, A.M. (1995). Nitric oxide protects against leukocyte-endothelium interactions in the early stages of hypercholesterolemia. Arterioscler-Thromb-Vasc-Biol. *15 #10*, 1652-1659.

Gerhard, M., Juhl, H., Kalthoff, H., Schreiber, H.W., Wagener, C., and Neumaier, M. (1994). Specific detection of carcinoembryonic antigen-expressing tumor cells in bone marrow aspirates by polymerase chain reaction. J. Clin. Oncol. *12*, 725-729.

Giavazzi, R., Foppolo, M., Dossi, R., and Remuzzi, A. (1993). Rolling and adhesion of human tumor cells on vascular endothelium under physiological flow conditions. J Clin Invest *92*, 3038-3044.

Goetz, D.J., El-Sabban, M.E., Hammer, D.A., and Pauli, B.U. (1996). Lu-ECAM-1-mediated adhesion of melanoma cells to endothelium under conditions of flow. Int J Cancer *65*, 192-199.

Granert, C., Raud, J., Xie, X., Lindquist, L., and Lindbom, L. (1994). Inhibition of leukocyte rolling with polysaccharide fucoidin prevents pleocytosis in experimental meningitis in the rabbit. J Clin Invest *93*, 929-936.

Hamada, J., Cavanaugh, P.G., Miki, K., and Nicolson, G.L. (1993). A paracrine migration-stimulating factor for metastatic tumor cells secreted by mouse hepatic sinusoidal endothelial cells: Identification as complement component C3b. Cancer Res *53*, 4418-4423.

Hardan, I., Weiss, L., Hershkoviz, R., Greenspoon, N., Alon, R., Cahalon, L., Reich, S., Slavin, S., and Lider, O. (1993). Inhibition of metastatic cell colonization in murine lungs and tumor-induced morbidity by non-peptidic arg-gly-asp mimetics. Int J Cancer *55*, 1023-1028.

Heuff, G., Van Der Ende, M.B., Boutkan, H., Prevoo, W., Bayon, L.G., Fleuren, G.J., Beelen, R.H.J., Meijer, S., and Dijkstra, C.D. (1993). Macrophage populations in different stages of induced hepatic metastases in rats: an immunohistochemical analysis. Scand J Immunol *38*, 10-16.

Honn, K.V., Tang, D.G., Grossi, I., Duniec, Z.M., Timar, J., Renaud, C., Leithauser, M., Blair, I., Johnson, C.R., and Diglio, C.A. (1994a). Tumor cell-derived 12(S)-hydroxyeiconsatetraenoic acid induces microvascular endothelial cell retraction. Cancer Res *54*, 565-574.

Honn, K.V., Tang, D.G., Grossi, I.M., Renaud, C., Duniec, Z.M., Johnson, C.R., and Diglio, C.A. (1994b). Enhanced endothelial cell retraction mediated by 12(S)-HETE: a proposed mechanism for the role of platelets in tumor cell metastasis. Expt Cell Res. *210*, 1-9.

Humphries, M.J., Olden, K., and Yamada, K.M. (1986). A synthetic peptide from fibronectin inhibits experimental metastasis of murine melanoma cells. Science *233*, 467-470.

Humphries, M.J., Yamada, K.M., and Olden, K. (1988). Investigation of the biological effects of anti-cell adhesive synthetic peptides that inhibit experimental metastasis of B16-F10 murine melanoma cells. J Clin Invest *81*, 782-790.

Imamura, H., Sutto, F., Brault, A., and Huet, P.M. (1995). Role of Kupffer cells in cold ischemia/reperfusion injury of rat liver. Gastroenterology *109*, 189-197.

Incardona, F., Lewalle, J.M., Morandi, V., Lambert, S., Legrand, Y., Foidart, J.M., and Legrand, C. (1995). Thrombospondin modulates human breast adenocarcinoma cell adhesion to human vascular endothelial cells. Cancer Res *55*, 166-173.

Inoue, S., Nakao, A., Kasai, Y., Harada, A., Nonami, T., and Takagi, H. (1995). Detection of hepatic micrometastasis in pancreatic adenocarcinoma patients by two-stage polymerase chain reaction/restriction fragment length polymorphism analysis. Jpn. J. Cancer Res. *86*, 626-630.

Ishii, S., Mizoi, T., Kawano, K., Cay, O., Thomas, P., Nachman, A., Ford, R., Shoji, Y., Kruskal, J.B., Steele, G., and Jessup, J.M. (1996). Implantation of human colorectal carcinoma cells in the liver studied by in vivo fluorescence videomicroscopy. Clin Expl Metastasis *14*, 153-164.

Iwai, K., Ishikura, H., Kaji, M., Sugiura, H., Ishizu, A., Takahashi, C., Kato, H., Tanabe, T., and Yoshiki, T. (1993). Importance of E-selectin (ELAM-1) and sialyl Lewis(a) in the adhesion of pancreatic carcinoma cells to activated endothelium. Int J Cancer *54*, 972-977.

Johnson, R.C., Mayadas, T.N., Frenette, P.S., Mebius, R.E., Subramaniam, M., Lacasce, A., Hynes, R.O., and Wagner, D.D. (1995). Blood cell dynamics in P-selectin-deficient mice. Blood *86 #3*, 1106-1114.

Kawaguchi, S., Kikuchi, K., Ishii, S., Takada, Y., Kobayashi, S., and Uede, T. (1992). VLA-4 molecules on tumor cells initiate an adhesive interaction with VCAM-1 molecules on endothelial cell surface. Jpn. J. Cancer Res. *83*, 1304-1316.

Kayano, K., Sakaida, I., Kubota, M., Yasunaga, M., and Okita, K. (1995). Functional differences between activated and normal rat liver macrophages: LPS uptake capacity by flow cytometric analysis in contrast with TNF-alpha release. Liver *15*, 253-259.

Kemperman, H., Driessens, M., La Riviere, G., Meijne, A., and Roos, E. (1994). The role of integrins and integrin activation in liver metastasis. Invasion and Metastasis *95;14*, 98-108.

Kemperman, H., Driessens, M.H.E., La Riviere, G., Meijne, A.M.L., and Roos, E. (1995). Adhesion mechanisms in liver metastasis formation. Canc Surv *24*, 67-79.

Koop, S., Khokha, R., Schmidt, E.E., MacDonald, I.C., Morris, V.L., Chambers, A.F., and Groom, A.C. (1994). Overexpression of metalloproteinase inhibitor in B16F10 cells does not affect extravasation but reduces tumor growth. Cancer Res *54*, 4791-4697.

Kubes, P., Jutila, M., and Payne, D. (1995). Therapeutic potential of inhibiting leukocyte rolling in ischemia/reperfusion. J Clin Invest *95 #6*, 2510-2519.

Lafrenie, R.M., Podor, T.J., Buchanan, M.R., and Orr, F.W. (1992a). Up-regulated biosynthesis and expression of endothelial cell vitronectin receptor enhances cancer cell adhesion. Cancer Res *52*, 2202-2208.

Lafrenie, R.M., Shaughnessy, S.G., and Orr, F.W. (1992b). Cancer cell interactions with injured or activated endothelium. Cancer and Metastasis Reviews *11*, 377-388.

Lafrenie, R.M., Gallo, S., Podor, T.J., Buchanan, M.R., and Orr, F.W. (1994). The relative roles of vitronectin receptor, E-selectin and alpha4B1 in cancer cell adhesion to interleukin-1-treated endothelial cells. Eur J Cancer *30A;14*, 2151-2158.

Lauri, D., Bertomeu, M.C., Orr, F.W., Bastida, E., Sauder, D., and Buchanan, M.R. (1990). Interleukin 1 increases tumor cell adhesion to endothelial cells through an RGD dependent mechanism: in vitro and in vivo studies. Clin Expl Metastasis *8 #1*, 27-32.

Lawrence, M.B. and Springer, T.A. (1991). Leukocytes roll on a selectin at physiologic flow rates: distinction from and prerequisite for adhesion through integrins. Cell *65*, 859-873.

Lehr, H.A., Olofsson, A.M., Carew, T.E,, Vajkoczy, P., von Andrian, U.H., Hubner, C., Berndt, M.C., Steinberg, D., Messmer, K., and Arfors, K.E. (1994). P-selectin mediates the interaction of circulating leukocytes with platelets and microvascular endothelium in response to oxidized lipoprotein in vivo. Lab Invest *71 #3*, 380-386.

Lehr, H.A., Krombach, F., Munzing, S., Bodlaj, R., Glaubitt, S.I., Seiffge, D., Hubner, C., von Andrian, U.H., and Messmer, K. (1995). In vitro effects of oxidized low density lipoprotein of CD11/CD18 and L-selectin presentation on neutrophils and monocytes with relevance for the in vivo situation. Am J Path *146 #1*, 218-227.

Ley, K., Linnermann, G., Meinen, M., Stoolman, L.M., and Gaehtgens, P. (1993). Fucoidin, but not yeast polyphosphomannan PPME, inhibits leukocyte rolling in venules of the rat mesentery. Blood *81;1*, 177-185.

Ley, K., Bullard, D.C., Arbones, M.L., Bosse, R., Vestweber, D., Tedder, T.F., and Beaudet, A.L. (1995). Sequential contribution of L- and P-selectin of leukocyte rolling in vivo. J Exp Med *181*, 669-675.

Luster, M.I., Germolec, D.R., Yoshida, T., Kayama, F., and Thompson, M. (1994). Endotoxin-induced cytokine gene expression and excretion in the liver. Hepatology *19*, 480-488.

Majuri, M.L., Hakkarainin, M., Paavonen, T., and Renkonen, R. (1994). Carcinoembryonic antigen is expressed on endothelial cells. A putative mediator of tumor cell extravasation and metastasis. APMIS *102*, 432-438.

Mancuso, F., Flower, R.J., and Perritti, M. (1995). Leukocyte transmigration, but not rolling or adhesion, is selectively inhibited by dexamethasone in the hamster post-capillary venule. Involvement of endogenous lipocortin 1. J Immunol *155 #1*, 377-386.

Martin-Padura, I., Mortarini, R., Lauri, D., Bernasconi, S., Sanchez-Madrid, F., Parmiani, G., Mantovani, A., Anichini, A., and Dejana, E. (1991). Heterogeneity in human melanoma cell adhesion to cytokine activated endothelial cells correlates with VLA-4 expression. Cancer Res *51*, 2239-2241.

Marzi, I., Bauer, M., Secchi, A., Bahrami, S., Redi, H., and Schlag, G. (1995). Effect of anti-tumor necrosis factor alpha on leukocyte adhesion in the liver after hemorrhagic shock: an intravital microscopic study in the rat. Shock *3 #1*, 27-33.

Mattei, S., Colombo, M.P., Melani, C., Silvani, A., Parmiani, G., and Herlyn, M. (1994). Expression of cytokine/growth factors and their receptors in human melanoma and melanocytes. Int J Cancer *56*, 853-857.

Mayadas, T.N., Johnson, R.C., Rayburn, H., Hynes, R.O., and Wagner, D.D. (1993). Leukocyte rolling and extravasation are severely compromised in p selectin-deficient mice. Cell *74*, 541-554.

Mayer, B., Lorenz, C., Babic, R., Jauch, K.W., Schildberg, F.W., Funke, I., and Johnson, J.P. (1995). Expression of leukocyte cell adhesion molecules on gastric carcinomas: Possible involvement of LFA-3 expression in the development of distant metastases. Int J Cancer *64*, 415-423.

McCarthy, S.A., Kuzu, I., Gatter, K.C., and Bicknell, R. (1991). Heterogeneity of the endothelial cell and its role in organ preference of tumour metastasis. Trends Pharmacol Sci *12*, 462-467.

McCartney, A.C. (1995). Pathology of ocular melanomas. Br. Med. Bull. *51 #3*, 678-693.

McCuskey, P.A., Kan, Z., and Wallace, S. (1994). An electron microscopy study of Kupffer cells in livers of mice having Friend erythroleukemia hepatic metastases. Clin Expl Metastasis *12*, 416-426.

Meijer, S., Peretz, T., Gaynor, J.J., Tan, C., Hajdu, S.I., and Brennan, M.F. (1990). Primary colorectal sarcoma. A retrospective review and prognostic factor study of 50 consecutive patients. Arch. Surg. *125 #9*, 1163-1168.

Meterissian, S.H., Toth, C.A., Steele, G., and Thomas, P. (1994). Kupffer cell/tumor cell interactions and hepatic metastasis in colorectal cancer. Cancer Letters *81*, 5-12.

Minnicozzi, M., Ramirez, M.M., Egan, R.W., Gleich, G.J., Kobayashi, I., Kim, D., and Duran, W.N. (1995). Polyarginine and eosinophil-derived major basic protein increase microvascular permeability independently of histamine of nitric oxide release. Microvascular Research *50 #1*, 56-70.

Morris, V.L., MacDonald, I.C., Koop, S., Schmidt, E.E., Chambers, A.F., and Groom, A.C. (1993). Early interactions of cancer cells with the microvasculature in mouse liver and muscle during hematogenous metastasis: videomicroscopic analysis. Clin Expl Metastasis *11 #1*,

Morris, V.L., Koop, S., MacDonald, I.C., Schmidt, E.E., Grattan, M., Percy, D., Chambers, A.F., and Groom, A.C. (1994). Mammary carcinoma cell lines of high and low metastatic potential differ not in extravasation but in subsequent migration and growth. Clin Expl Metastasis *12*, 357-367.

Neirodzik, M.L., Kajumo, F., and Karpatkin, S. (1992). Effect of thrombin treatment of tumor cells on adhesion of tumour cells to platelets in vitro and tumor metastasis in vivo. Cancer Res *52*, 3267-3272.

Nicolson, G.L. (1988). Cancer metastasis: tumor cell and host organ properties important in metastasis to specific secondary sites. Biochim Biophys Acta *948*, 175-224.

Nourshargh, S., Larkin, S.W., Das, A., and Williams, T.J. (1995). Interleukin-1-induced leukocyte extravasation across rat mesenteric microvessels is mediated by platelet-activating factor. Blood *85 #9*, 2553-2558.

Okahara, H., Yagita, H., Miyake, K., and Okumura, K. (1994). Involvement of very late activation antigen (VLA-4) and vascular cell adhesion molecule 1 (VCAM-1) in tumor necrosis factor alpha enhancement of experimental metastasis. Cancer Res *54*, 3233-3236.

Orosz, P., Kruger, A., Hubbe, M., Ruschoff, J., Von Hoegen, P., and Mannel, D.M. (1995). Promotion of experimental liver metastasis by tumour necrosis factor. Int J Cancer *60*, 867-871.

Orr, F.W. (1994). Cancer cell chemotaxis: Mechanisms and influence on site-specific tumor metastasis. Adv Mol Cell Bio *9*, 153-189.

Paavonen, T., Tiisala, S., Majuri, M.L., Bohling, T., and Renkonen, R. (1994). In vivo evidence of the role of alpha4B1-VCAM-1 interaction in sarcoma, but not in carcinoma extravasation. Int J Cancer *58*, 298-302.

Pauli, B.U., Augustin-Voss, H.G., El-Sabban, M.E., Johnson, R.C., and Hammer, D.A. (1990). Organ-preference of metastasis. The role of endothelial cell adhesion molecules. Cancer and Metastasis Reviews *9*, 175-189.

Piali, L., Hammel, P., Uherek, C., Bachmann, G., Gisler, R.H., Dunon, D., and Imhof, B.A. (1995). CD31/PECAM-1 is a ligand for alpha v beta 3 integrin involved in adhesion of leukocytes to endothelium. J Cell Bio *130*, 451-460.

Price, E.A., Coombe, D.R., and Murray, J.C. (1996). Endothelial CD44H mediates adhesion of a melanoma cell line to quiescent human endothelial cells in vitro. Int J Cancer *65*, 513-518.

Rak, J.W., St.Croix, B.D., and Kerbel, R.S. (1995). Consequences of angiogenesis for tumor progression, metastasis and cancer therapy. Anticancer Drugs *6*, 3-18.

Rappaport, A.M. and Wanless, I.R. (1993). Physioanatomic considerations. In Diseases of the liver. L. Schiff and E.R. Schiff, eds. (Philadelphia: Lippincott Company), pp. 1-33.

Rice, G.E., Gimbrone, M.A., and Bevilacqua, M.P. (1988). Tumor cell-endothelial interactions increased adhesion of human melanoma cells to activated vascular endothelium. Am J Path *133 #2*, 204-210.

Rice, G.E., Munro, J.M., Corliss, C., and Bevilacqua, M.P. (1991). Vascular and nonvascular expression of INCAM-110. Am J Path *138*, 385-393.

Rice, G.E. and Bevilacqua, M.P. (1989). An inducible endothelial cell surface glycoprotein mediates melanoma adhesion. Science *246*, 1303-1306.

Rocha, M., Kruger, A., Van-Rooijen, N., Schirrmacher, V., and Umansky, V. (1995). Liver endothelial cells participate in T-cell-dependent host resistance to lymphoma metastasis by production of nitric oxide in vivo. Int J Cancer *63 #3*, 405-411.

Roskams, T., Moshage, H., De Vos, R., Guido, D., Yap, P., and Desmet, V. (1995). Heparin sulfate proteoglycan expression in normal human liver. Hepatology *21*, 950-958.

Ruiz, P., Dunon, D., Sonnenberg, A., and Imhof, B.A. (1993). Suppression of mouse melanoma metastasis by EA-1, a monoclonal antibody specific for alpha 6 integrins. Cell Adhes. Commun. *1*, 67-81.

Rusciano, D. and Burger, M.M (1992). Why do cancer cells metastasize into particular organs? BioEssays *14 #3*, 185-194.

Salmi, M. and Jalkanen, S. (1996). Human vascular adhesion protein 1 (VAP-1) is a unique sialoglycoprotein that mediates carbohydrate-dependant binding of lymphocytes to endothelial cells. J Exp Med *183*, 569-579.

Schadendorf, D., Heidel, J., Gawlik, C., Suter, L., and Czarnetzki, B.M. (1995). Association with clinical outcome of expression of VLA-4 in primary cutaneous malignant melanoma as well as P-selectin and E-selectin on intratumoral vessels. J Nat Cancer Inst *87 #5*, 366-371.

Scoazec, J.Y., Racine, L., Couvelard, A., Flejou, J.F., and Feldmann, G. (1994). Endothelial cell heterogeneity in the normal human liver acinus: in situ immunohistochemical demonstration. Liver *14*, 113-123.

Scoazec, J.Y. and Feldmann, G. (1991). In situ immunophenotyping study of endothelial cells of the human hepatic sinusoid: results and functional implications. Hepatology *14*, 789-797.

Scoazec, J.Y. and Feldmann, G. (1994). The cell adhesion molecules of hepatic sinusoidal endothelial cells. J Hepatol *20*, 296-300.

Sers, C., Reithmuller, G., and Johnson, J.P. (1994). MUC18, a melanoma-progression associated molecule, and its potential role in tumor vascularization and hematogenous spread. Cancer Res *54*, 5689-5694.

Shih, I.M., Elder, D.E., Speicher, D., Johnson, J.P., and Herlyn, M. (1994). Isolation and functional characterization of the A32 melanoma-associated antigen. Cancer Res *54*, 2514-2520.

Smedsrod, B., Pertoft, H., Eriksson, S., Fraser, J.R.E., and Laurent, T.C. (1984). Studies in vitro on the uptake and degradation of sodium hyaluronate in rat liver endothelial cells. Biochem J. *223*, 617-626.

Smedsrod, B., Kjellen, L., and Pertoft, H. (1985). Endocytosis and degradation of chondriotin sulphate by liver endothelial cells. Biochem J. *229*, 63-71.

Smedsrod, B., DeBleser, P.J., Lovisetti, P., Vanderkerken, K., Wisse, E., and Geerts, A. (1994). Cell biology of liver endothelial and kupffer cells. Gut *35*, 1509-1516.

Steinhoff, G., Behrend, M., Schrader, B., Duijvestijn, A.M., and Wonigeit, K. (1993). Expression patterns of leukocyte adhesion ligand molecules on human liver endothelia. Am J Path *142*, 481-488.

Swain, M.G., Tjandra, K., Kanwar, S., and Kubes, P. (1995). Neutrophil adhesion is impaired in rat model of cholestasis. Gastroenterology *109 #3*, 923-932.

Takeda, K., Fujii, N., Nitta, Y., Sakihara, H., Nakayama, K., Rikiishi, H., and Kumagai, K. (1991). Murine tumor cells metastasizing selectively in the liver: ability to produce hepatocyte-activating cytokines interleukin-1 and/or -6. Jpn. J. Cancer Res. *82*, 1299-1308.

Tamaki, M., Aoyagi, M., Morita, I., Hirakawa, K., and Murota, S. (1995). Cell adhesion molecules acting between C6 glioma and endothelial cells. J. Neurooncol. *24*, 181-188.

Tang, D.G., Diglio, C.A., and Honn, K.V. (1994). Activation of microvascular endothelium by eiconsanoid 12 (S)-Hydroxyeicosatetraenoic acid leads to enhanced tumor cell adhesion via up-regulation of surface expression of abB3 Integrin: A posttranscriptional protein kinase C- and cytoskeleton-dependent process. Cancer Res *54*, 1119-1129.

Tobal, K., Sherman, L.S., Foss, A.J., and Lightman, S.L. (1993). Detection of melanocytes from uveal melanoma in peripheral blood using the polymerase chain reaction. Invest. Ophthalmol. Vis. Sci. *34 #9*, 2622-2625.

Tomita, Y., Saito, T., Saito, K., Oite, T., Shimizu, F., and Sato, S. (1995). Possible significance of VLA-4 (alpha 4 beta 1) for hematogenous metastasis of renal-cell cancer. Int J Cancer *60*, 753-758.

Tozeren, A., Kleinman, H.K., Grant, D.S., Morales, D., and Mercurio, A.M. (1995). E-selectin-mediated dynamic interactions of breast and colon-cancer cells with endothelial cell monolayers. Int J Cancer *60*, 426-431.

Tressler, R.J., Updyke, T.V., Yeatman, T., and Nicolson, G.L. (1993). Extracellular annexin II is associated with divalent cation-dependent tumor cell-endothelial cell adhesion of metastatic RAW117 large-cell lymphoma. J Cell Biochem *53*, 265-276.

Tressler, R.J., Yeatman, T., and Nicolson, G.L. (1994). Extracellular annexin VI expression is associated with divalent cation-dependent endothelial cell adhesion of metastatic RAW117 large-cell lymphoma cells. Expt Cell Res. *215*, 395-400.

Verschraegen, C.F., Giovanella, B.C., Mendoza, J.T., Kozielski, A.J., and Stehlin, J.S. (1991). Specific organ metastases of human melanoma cells injected into the arterial circulation of nude mice. Anticancer Research *11*, 529-536.

Vidal, M.J., Zocchi, M.R., Poggi, A., Pellegatta, F., and Chierchic, S.L. (1992). Involvement of nitric oxide in tumor cell adhesion to cytokine-activated endothelial cells. J Cardio Pharmacol *20 suppl.12*, S155-S159.

Vidal-Vanaclocha, F., Rocha, M., Asumendi, A., and Barbera-Guillem, E. (1993). Isolation and enrichment of two sublobular compartment-specific endothelial cell subpopulations from liver sinusoids. Hepatology *18*, 328-339.

Vidal-Vanaclocha, F., Amezaga, C., Asumendi, A., Kaplanski, G., and Dinarello, C.A. (1994). Interleukin-1 receptor blockade reduces the number and size of murine B16 melanoma hepatic metastasis. Cancer Res *54*, 2667-2672.

Volpes, R., Van Den Oord, J.J., and Desmet, V.J. (1991). Distribution of the VLA family of integrins in normal and pathological human liver tissue. Gastroenterology *101*, 200-206.

Volpes, R., Van Den Oord, J.J., and Desmet, V.J. (1992). Vascular adhesion molecules in acute and chronic liver inflammation. Hepatology *15*, 269-275.

Warren, B.A. (1982). Ultrastructural aspects of the invasion of liver by cancer cells. In Liver Metastasis. L. Weiss and H.A. Gilbert, eds. (Boston: G.K. Hall Medical Publishers), pp. 40-50.

Weiss, L., Ward, P.M., Harlos, J.P., and Holmes, J.C. (1984). Target organ patterns of tumors in mice following the arterial dissemination of B16 melanoma cells. Int J Cancer *33*, 825-830.

Weiss, L. (1990). Metastatic inefficiency. Adv Cancer Res *54*, 159-211.

Weiss, L. (1992). Comments on hematogenous metastatic patterns in humans as revealed by autopsy. Clin Expl Metastasis *10*, 191-199.

Weiss, L., Nannmark, U., Johansson, B.R., and Bagge, U. (1992). Lethal deformation of cancer cells in the microcirculation: a potential rate regulator of hematogenous metastasis. Int J Cancer *50*, 103-107.

Weiss, L. and Ward, P.M. (1982). Arrest and retention of circulating cancer cells in the lungs of animals with defined metastatic status. Cancer Res *42*, 1998-1903.

Werner Wasik, M., von Muenchhausen, W., Nolan, J.P., and Cohen, S.A. (1989). Endogenous interferon alpha/beta produced by murine Kupffer cells augments liver-associated natural killing activity. Cancer Immunol. Immunother *28*, 107-115.

Wiezorek, J.S., Brown, D.H., Kupperman, D.E., and Brass, C.A. (1994). Rapid conversion to high xanthine oxidase activity in viable Kupffer cells during hypoxia. J Clin Invest *94*, 2224-2230.

Wojtukiewicz, M.Z., Tang, D.G., Nelson, K.K., Walz, D.A., Diglio, C.A., and Honn, K.V. (1992). Thrombin enhances tumor cell adhesive and metastatic properties via increased alphaIIbB3 expression on the cell surface. Thrombosis research *68*, 233-245.

Wojtukiewicz, M.Z., Tang, D.G., Ciarelli, J.J., Nelson, K.K., Walz, D.A., Diglio, C.A., Mammen, E.F., and Honn, K.V. (1993). Thrombin increases the metastatic potential of tumor cells. Int J Cancer *54*, 793-806.

Wood, S. (1958). Pathogenesis of metastasis formation observed in vivo in the rabbit ear chamber. Arch Pathol *66*, 550-568.

Ye, C., Kiriyama, K., Mistouoka, C., Kannagi, R., Ito, K., Watanabe, T., Kondo, K., Akiyama, S., and Takagi, H. (1995). Expression of E-selectin on endothelial cells of small veins in human colorectal cancer. Int J Cancer *61*, 455-460.

Zavadsky, K.E. and Lee, Y.T.M. (1994). Liver metastases from colorectal carcinoma: Incidence, resectability, and survival results. Am Surg *60 #12*, 929-933.

Zetter, B.R. (1990). The cellular basis of site-specific tumor metastasis. New Eng J Med *322 #9*, 605-612.

Zhang, J.X., Bauer, M., and Clemens, M.G. (1995). Vessel and target cell-specific actions of endothelin-1 and endothelin-3 in rat liver. Am. J. Physiol *269 2 Pt 1*, G269-G277.

Zhu, D., Cheng, C.F., and Pauli, B.U. (1991). Mediation of lung metastasis of murine melanomas by a lung-specific endothelial cell adhesion molecule. Proc Natl Acad Sci USA *88*, 9568-9572.

Zocchi, M.R., Vidal, M., and Poggi, A. (1993). Involvement of CD56/N-CAM molecule in the adhesion of human solid tumor cell lines to endothelial cells. Expt Cell Res. *204*, 130-135.